Electronic Supplementary Information

Functional group engineering in naphthalimides: a conceptual insight to fine-tune the supramolecular self-assembly and condensed state luminescence

Niranjan Meher,[a] *and Parameswar Krishnan Iyer**[a,b]

[a]Department of Chemistry, [b]Center for Nanotechnology, Indian Institute of Technology Guwahati, Guwahati-781039, Assam, India

*AUTHOR INFORMATION (P. K. Iyer)

E-mail: pki@iitg.ac.in;

Fax: +91 361 258 2349

Experimental Methods

Materials and Instrumentations: All starting materials and reagents (viz: 1,8-naphthalic anhydride, 4-bromo-1,8-naphthalic anhydride, hexylamine and phenylboronic acid derivatives) were purchased from Sigma Aldrich (INDIA) and were of reagent grade. HPLC grade solvents used in this study were purchased from Fisher Scientific Ltd. and RANKEM. NMR (^{1}H, ^{13}C) spectra were recorded with a Bruker Avance 600 MHz spectrometer. All solutions for ^{1}H and ^{13}C spectra were obtained taking residual solvent signal as internal reference. Electro spray ionization mass spectrometry (ESI-MS) was recorded on a Waters (Micro mass MS-Technologies) Q-Tof MS Analyzer spectrometer. Microbalance (± 0.1mg) and volumetric glassware were used for the preparation of solutions. UV/vis and PL spectra were recorded on a Perkin-Elmer Model Lambda-750 spectrophotometer and a Horiba Fluoromax-4 spectrofluorometer respectively using 4 mm quartz cuvettes at 298 K. Life-time measurements were performed using a time-correlated single photon counting set up from Horiba. The laser diode 375 (DeltaDiode-375) was used as a source with excitation wavelength of 375 nm. Malvern Zetasizer instrument was used to measure the hydrodynamic diameter of the compounds. Field emission scanning electron microscopy (FESEM) images were obtained on Sigma Carl ZEISS field emission scanning electron microscope. X-ray diffraction (XRD) measurements were performed using Bruker D2 PHASER X-ray diffractometer (10 mA, 30 kV) equipped with Ni-filtered Cu Kα radiation, at a wavelength of 0.154 nm. The samples were scanned in the 2θ range of 5–50^{o} at a scan rate of 1.2^{o} min^{-1}. Single crystal data were obtained with a Bruker SMART APEX diffractometer equipped with a CCD area detector.

Preparation of the Test Solution: Stock solutions of probes **1-15** and **HNI** (1×10^{-5} M) was prepared in DMF, while stock solutions of various test species (1×10^{-5} M) were prepared by dissolving an appropriate amount of the testing species in methanol. The test solutions of the probes (10 μM) were prepared at different water fraction in DMF for aggregation study. The probe (10 μM) nanoaggregate suspension in 99.9% water was prepared for the titration study with various analytes. The resulting solution was shaken well at room temperature before recording the spectra.

Preparation of FESEM samples: The morphological analysis of the supramolecular self-assembly was carried out by FE-SEM. As pictured in Figure 5q, simple methodology was

performed to prepare the samples. The dilute suspension of the naphthalimide congeners (10 μM) in 99.9% water-0.1% DMF were drop casted on aluminium foil coated glass surface and were dried in room temperature overnight before analysis.

Theoretical Studies: To investigate the non-fluorescent nature of **15** in both solution and condensed state, the electronic properties of all the congeners along with various other small molecules were calculated using density functional theory (DFT). The ground state and excited state optimized geometries along with HOMO/LUMO electron density and energy were calculated using B3LYP hybrid functional incorporated in the Gaussian 09 package.[1,2] The 6-31G(d) basis set for all the atoms has been used in all calculations, which offers high quality outcomes at a reasonable time.

Quantum Yield Calculations: Fluorescence quantum yields (Φ_s) of the naphthalimides were calculated by taking quinine sulfate (Φ_r = 0.57 in 0.1 M H_2SO_4) as standard and using the equation shown below:

$$\Phi_s = \Phi_r (A_r F_s / A_s F_r) (\eta s^2 / \eta r^2)$$

Where, s and r represent sample and reference, Φ signifies the quantum yield, A denotes absorbance, F signifies relative integrated fluorescence intensity, and η represents the refractive index of the medium.

Synthetic route

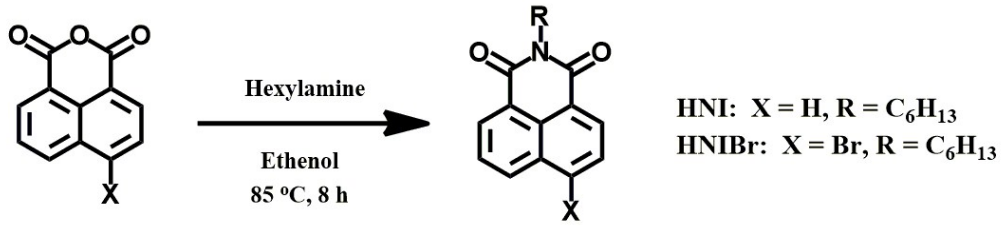

Scheme S1. The synthetic procedure used to prepare probe **HNI** and **HNIBr**.

Synthetic Procedure for HNI and HNIBr: 1,8-naphthalic anhydride (5 m.mol) was taken in ethanol (20 mL) and hexylamine (5.2 m.mol) was added to it drop wise at room temperature. The suspension was heated at 85 ^{o}C with vigorous stirring for 12h. Then the mixture was cooled to room temperature and then kept at 5 ^{o}C for 1 h to recrystallize **HNI**. The solvent was filtered out and the HNI residue was washed with ethanol to get the pure light brown crystalline solid of HNI (84% yield). Similar synthetic procedure was followed for **HNIBr** (4-bromo-1,8-naphthalic anhydride was taken in place 1,8-naphthalic anhydride) yielding a light green color solid with 81% yield.

Characterization data of HNI: ^{1}H NMR (600 MHz, $CDCl_3$, δ ppm) 0.91 (t, 3H), 1.35 (m, 4H), 1.44 (m, 2H), 1.75 (m, 2H), 4.19 (t, 2H), 7.77 (t, 2H), 8.22 (d, 2H), 8.61 (d, 2H). ^{13}C NMR (150.00 MHz, $CDCl_3$, δ ppm) 14.22, 22.71, 26.94, 28.20, 31.70, 40.63, 122.85, 127.04, 128.24, 131.29, 131.67, 133.96, 164.32. HRMS (+ESI): Calculated for $C_{18}H_{19}NO_2$ 281.1416 $[M]^+$, Found 282.1371 $[M+1]^+$.

Characterization data of HNIBr: ^{1}H NMR (600 MHz, $CDCl_3$, δ ppm) 0.87 (t, 3H), 1.32 (m, 6H), 1.70 (m, 2H), 4.12 (t, 2H) 7.77 (t, 1H), 7.95 (d, 1H), 8.32 (d, 1H), 8.46 (d, 1H), 8.57 (d, 1H). ^{13}C NMR (150.00 MHz, $CDCl_3$, δ ppm) 14.18, 22.68, 26.89, 28.11, 31.64, 40.71, 122.28, 123.14, 128.09, 128.91, 130.17, 130.54, 131.09, 131.18, 131.99, 133.15, 163.54, 163.56. HRMS (+ESI): Calculated for $C_{18}H_{18}BrNO_2$ 359.0521 $[M]^+$, 361.0500$[M+2]^+$, Found 360.0600 $[M+H]^+$, 362.0581 $[M+H+2]^+$.

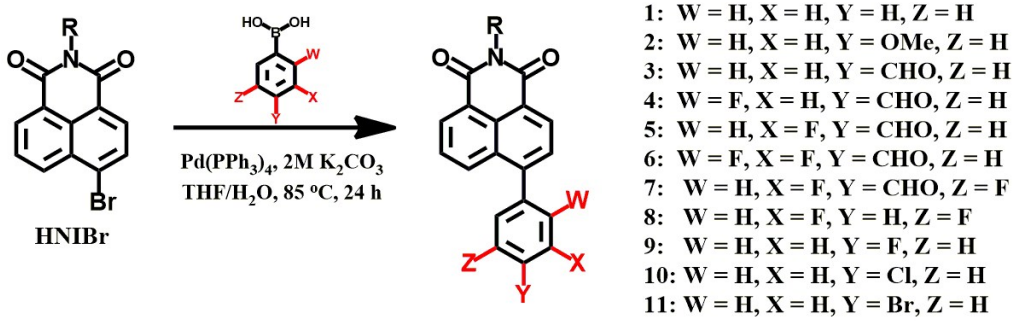

Scheme S2. The synthetic procedure used to prepare probe **1** to **11**.

Synthetic Procedure for 1 to 11: Compound **HNIBr** (0.5 m.mol) and the respective boronic acid (1 m.mol) were dissolved into 6 mL of THF in 50 ml round bottom flask, and then 2 mL of 2.0 M potassium carbonate solution was added to the flask. The mixture solutions was degassed with nitrogen for 15 min and then 5 mg of catalyst $Pd(PPh_3)_4$ was added to them. The mixtures were stirred at 85 °C under nitrogen atmosphere and the progress of reactions was monitored by taking TLC. After 15 h, the solutions were cooled and extracted with $CHCl_3$. The organic layers were dried over anhydrous sodium sulfate. The solvent was removed and were purified by column chromatography.

Characterization data for 1: ^{1}H NMR (600 MHz, $CDCl_3$, δ ppm) 0.90 (t, 3H), 1.34 (m, 4H), 1.45 (m, 2H), 1.75 (m, 2H), 4.20 (t, 2H) 7.53 (m, 5H), 7.70 (m, 2H), 8.26 (d, 1H), 8.64 (t, 2H). ^{13}C NMR (150.00 MHz, $CDCl_3$, δ ppm) 14.22, 22.72, 26.96, 28.23, 31.72, 40.67, 121.94, 123.06, 126.95, 127.97, 128.59, 128.79, 130.01, 130.18, 130.93, 131.28, 132.73, 138.97, 146.97, 164.27, 164.47. HRMS (+ESI): Calculated for $C_{24}H_{23}NO_2$ 357.1729 $[M]^+$, Found 358.1806 $[M+H]^+$.

Characterization data for 2: ^{1}H NMR (600 MHz, $CDCl_3$, δ ppm) 0.89 (t, 3H), 1.35 (m, 4H), 1.44 (m, 2H), 1.75 (m, 2H), 3.92 (s, 3H), 4.20 (t, 2H) 7.08 (d, 2H), 7.45 (d, 2H), 7.68 (m, 2H), 8.30 (d, 1H), 8.62 (d, 2H). ^{13}C NMR (150.00 MHz, $CDCl_3$, δ ppm) 14.22, 22.73, 26.96, 28.23, 31.72, 40.66, 55.59, 114.29, 114.92, 116.15, 121.54, 123.06, 126.82, 127.89, 130.30, 131.00, 131.27, 132.84, 146.80, 160.04, 164.33, 164.53. HRMS (+ESI): Calculated for $C_{25}H_{25}NO_3$ 387.1834 $[M]^+$, Found 388.1963 $[M+H]^+$.

Characterization data for 3: ^{1}H NMR (600 MHz, $CDCl_3$, δ ppm) 0.89 (t, 3H), 1.34 (m, 4H), 1.43 (m, 2H), 1.74 (m, 2H), 4.19 (t, 2H) 7.71 (m, 4H), 8.07 (d, 2H), 8.17 (d, 1H), 8.66 (t, 2H), 10.15 (s, 1H). ^{13}C NMR (150.00 MHz, $CDCl_3$, δ ppm) 14.10, 22.68, 26.91, 28.17, 31.66, 40.69, 122.71, 123.19, 127.37, 127.92, 128.71, 129.77, 129.97, 130.16, 130.60, 130.89, 131.32, 131.57, 132.09, 136.22, 145.04, 145.17, 163.97, 164.18, 191.76. HRMS (+ESI): Calculated for $C_{25}H_{23}NO_3$ 385.1678 $[M]^+$, Found 386.1839 $[M+H]^+$.

Characterization data for 4: ^{1}H NMR (600 MHz, $CDCl_3$, δ ppm) 0.89 (t, 3H), 1.35 (m, 4H), 1.42 (m, 2H), 1.74 (m, 2H), 4.20 (t, 2H) 7.63 (t, 1H), 7.74 (m, 2H), 7.76 (d, 1H), 7.79 (d, 1H), 7.87 (d, 1H), 8.67 (m, 2H), 10.11 (d, 1H). ^{13}C NMR (150.00 MHz, $CDCl_3$, δ ppm) 14.22, 22.72, 26.95, 28.22, 31.70, 40.76, 116.26, 116.41, 123.27, 127.58, 128.70, 130.62, 131.59, 131.76,

132.99, 138.70, 138.74, 139.01, 159.38, 161.04, 163.97, 164.17, 190.43. ^{19}F NMR (564.00 MHz, DMSO-d_6, δ ppm) -112.76. HRMS (+ESI): Calculated for $C_{25}H_{22}FNO_3$ 403.1584 $[M]^+$, Found 404.1640 $[M+H]^+$.

Characterization data for 5: ^{1}H NMR (600 MHz, $CDCl_3$, δ ppm) 0.88 (t, 3H), 1.32 (m, 4H), 1.41 (m, 2H), 1.74 (m, 2H), 4.19 (t, 2H) 7.36 (d, 1H), 7.43 (d, 1H), 7.70 (d, 1H), 7.74 (t, 1H), 8.06 (t, 1H), 8.17 (d, 1H), 8.66 (d, 2H), 10.48 (s, 1H). ^{13}C NMR (150.00 MHz, $CDCl_3$, δ ppm) 14.20, 22.71, 26.93, 28.20, 31.69, 40.77, 118.12, 118.26, 123.32, 127.68, 127.88, 129.18, 129.20, 129.54, 130.70, 131.62, 143.77, 147.33, 147.39, 163.71, 163.90, 164.13, 165.44, 186.70, 186.74. ^{19}F NMR (564.00 MHz, DMSO-d_6, δ ppm) -120.07. HRMS (+ESI): Calculated for $C_{25}H_{22}FNO_3$ 403.1584 $[M]^+$, Found 404.1649 $[M+H]^+$.

Characterization data for 6: ^{1}H NMR (600 MHz, $CDCl_3$, δ ppm) 0.90 (t, 3H), 1.33 (m, 4H), 1.43 (m, 2H), 1.75 (m, 2H), 4.20 (t, 2H) 7.34 (t, 1H), 7.75 (m, 2H), 7.77 (t, 1H), 7.96 (d, 1H), 8.68 (m, 2H), 10.47 (s, 1H). ^{13}C NMR (150.00 MHz, $CDCl_3$, δ ppm) 14.22, 22.72, 26.95, 28.22, 31.70, 40.80, 123.34, 123.37, 123.83, 125.96, 126.00, 126.97, 126.99, 127.83, 128.58, 128.72, 129.76, 130.56, 131.72, 134.51, 137.68, 163.85, 164.07, 185.70. ^{19}F NMR (564.00 MHz, DMSO-d_6, δ ppm) -144.83 (d), -138.63 (d). HRMS (+ESI): Calculated for $C_{25}H_{21}F_2NO_3$ 421.1489 $[M]^+$, Found 422.1563 $[M+H]^+$.

Characterization data for 7: ^{1}H NMR (600 MHz, $CDCl_3$, δ ppm) 0.89 (t, 3H), 1.34 (m, 4H), 1.44 (m, 2H), 1.74 (m, 2H), 4.19 (t, 2H) 7.18 (d, 2H), 7.70 (d, 1H), 7.78 (d, 1H), 8.17 (d, 1H), 8.67 (t, 2H), 10.45 (s, 1H). ^{13}C NMR (150.00 MHz, $CDCl_3$, δ ppm) 14.21, 22.71, 26.93, 28.20, 31.69, 40.82, 114.21, 114.24, 114.35, 114.38, 123.44, 123.61, 127.81, 127.97, 128.74, 129.27, 13.63, 131.20131.76142.54, 147.51, 163.78, 164.03, 184.12. ^{19}F NMR (564.00 MHz, DMSO-d_6, δ ppm) -144.85. (d). HRMS (+ESI): Calculated for $C_{25}H_{21}F_2NO_3$ 421.1489 $[M]^+$, Found 422.5724 $[M+H]^+$.

Characterization data for 8: ^{1}H NMR (600 MHz, $CDCl_3$, δ ppm) 0.89 (t, 3H), 1.34 (m, 4H), 1.44 (m, 2H), 1.74 (m, 2H), 4.19 (t, 2H), 6.98 (t, 1H) 7.04 (d, 2H), 7.68 (d, 1H), 7.75 (t, 1H), 8.20 (d, 1H), 8.65 (t, 2H). ^{13}C NMR (150.00 MHz, $CDCl_3$, δ ppm) 14.22, 22.73, 26.95, 28.22, 31.71, 40.76, 104.20 (d), 113.18 (dd), 122.88, 123.27, 127.52, 127.87, 128.74, 129.74, 130.75, 131.55, 131.85, 142.07, 144.11, 162.34, 164.01, 164.24. ^{19}F NMR (564.00 MHz, DMSO-d_6, δ

ppm) -109.10. HRMS (+ESI): Calculated for $C_{24}H_{21}F_2NO_2$ 393.1540 $[M]^+$, Found 394.1611 $[M+H]^+$.

Characterization data for 9: ^{1}H NMR (600 MHz, $CDCl_3$, δ ppm) 0.90 (t, 3H), 1.34 (m, 4H), 1.44 (m, 2H), 1.75 (m, 2H), 4.20 (t, 2H), 7013 (t, 1H) 7.25 (m, 2H), 7.48 (t, 1H), 7.67 (d, 1H), 7.71 (t, 1H), 8.21 (d, 1H), 8.64 (t, 2H). ^{13}C NMR (150.00 MHz, $CDCl_3$, δ ppm) 14.22, 22.73, 26.96, 28.24, 31.73, 40.70, 114.21, 115.75, 115.84, 115.89, 115.98, 123.17, 127.12, 128.05, 130.89, 131.36, 131.67, 131.72, 132.40, 139.43, 145.79, 164.20, 164.40. ^{19}F NMR (564.00 MHz, DMSO-d_6, δ ppm) -113.48. HRMS (+ESI): Calculated for $C_{24}H_{22}FNO_2$ 375.1635 $[M]^+$, Found 376.1726 $[M+H]^+$.

Characterization data for 10: ^{1}H NMR (600 MHz, $CDCl_3$, δ ppm) 0.90 (t, 3H), 1.34 (m, 4H), 1.44 (m, 2H), 1.75 (m, 2H), 4.20 (t, 2H), 7.44 (d, 2H) 7.53 (d, 2H), 7.67 (d, 1H), 7.71 (t, 1H), 8.20 (dd, 1H), 8.64 (d, 2H). ^{13}C NMR (150.00 MHz, $CDCl_3$, δ ppm) 14.22, 22.73, 26.96, 28.23, 31.72, 40.72, 122.31, 123.19, 127.20, 127.95, 129.10, 130.06, 130.88, 131.29, 131.41, 132.28, 134.92, 137.37, 145.54, 164.16, 164.37. HRMS (+ESI): Calculated for $C_{24}H_{22}ClNO_2$ 391.1339 $[M]^+$, Found 391.1594 $[M+H]^+$.

Characterization data for 11: ^{1}H NMR (600 MHz, $CDCl_3$, δ ppm) 0.89 (t, 3H), 1.34 (m, 4H), 1.44 (m, 2H), 1.74 (m, 2H), 4.19 (t, 2H), 7.38 (d, 2H) 7.68 (m, 2H), 8.19 (d, 1H), 8.63 (d, 2H). ^{13}C NMR (150.00 MHz, $CDCl_3$, δ ppm) 14.22, 22.72, 26.95, 28.22, 31.72, 40.71, 114.21, 123.08, 127.20, 127.88, 128.80, 129.97, 13087, 131.41, 131.57, 132.04, 132.26, 137.84, 145.53, 164.15, 164.35. HRMS (+ESI): Calculated for $C_{24}H_{22}BrNO_2$ 435.0834 $[M]^+$, Found 436.0912 $[M+H]^+$.

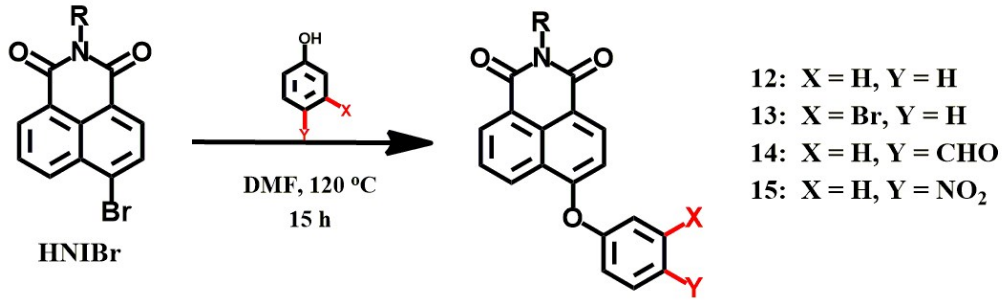

Scheme S3. The synthetic procedure used to prepare probe **12** to **15**.

Synthetic Procedure for 12 to 15: To a solution of **HNIBr** (0.5 mmol) in DMF (10 mL), 0.7 mmol of the respective phenol derivative and K_2CO_3 (300 mg) were added and the mixture was vigorous stirred and heated at 130 ^oC for 15 hours. The solvent was evaporated under vacuum and residue extracted with chloroform (40×5 mL). The organic layer was washed with H_2O several times followed by brine, dried over anhydrous Na_2SO_4 and concentrated under reduced pressure to get crude product that was purified by silica gel column chromatography increasing the polarity slowly using mixture of hexane and chloroform to get the pure the products.

Characterization data for 12: ^1H NMR (600 MHz, $CDCl_3$, δ ppm) 0.89 (t, 3H), 1.34 (m, 4H), 1.44 (m, 2H), 1.74 (m, 2H), 4.17 (t, 2H), 6.91 (d, 1H), 7.19 (d, 2H), 7.31 (t, 1H), 7.48 (t, 2H), 7.78 (dd, 1H), 8.45 (d, 1H), 8.68 (m, 2H),. ^{13}C NMR (150.00 MHz, $CDCl_3$, δ ppm) 14.22, 22.72, 26.96, 28.25, 31.72, 40.58, 110.76, 116.81, 120.91, 122.83, 124.09, 125.71, 126.63, 128.67, 129.83, 130.54, 132.00, 132.91, 155.00, 159.97, 163.92, 164.54. HRMS (+ESI): Calculated for $C_{24}H_{23}NO_3$ 373.1678 $[M]^+$, Found 394.1768 $[M+H]^+$.

Characterization data for 13: ^1H NMR (600 MHz, $CDCl_3$, δ ppm) 0.89 (t, 3H), 1.34 (m, 4H), 1.44 (m, 2H), 1.74 (m, 2H), 4.17 (t, 2H), 6.98 (d, 1H), 7.12 (d, 1H), 7.34 (m, 2H), 7.42 (d, 1H), 7.79 (t, 1H), 8.49 (d, 1H), 8.62 (d, 1H), 8.66 (d, 1H). ^{13}C NMR (150.00 MHz, $CDCl_3$, δ ppm) 14.22, 22.72, 26.95, 28.24, 31.72, 40.62, 111.63, 117.61, 119.29, 122.94, 123.51, 123.98, 124.15, 126.91, 128.42, 128.70, 129.84, 131.58, 132.12, 132.73, 156.01, 158.99, 163.78, 164.43. HRMS (+ESI): Calculated for $C_{24}H_{22}BrNO_3$ 451.0783 $[M]^+$, Found 452.0861 $[M+H]^+$.

Characterization data for 14: ^1H NMR (600 MHz, $CDCl_3$, δ ppm) 0.89 (t, 3H), 1.34 (m, 4H), 1.44 (m, 2H), 1.74 (m, 2H), 4.18 (t, 2H), 7.13 (d, 1H), 7.27 (m, 2H), 7.79 (t, 1H), 7.98 (d, 2H), 8.55 (m, 2H), 8.67 (d, 1H), 10.01 (s, 1H). ^{13}C NMR (150.00 MHz, $CDCl_3$, δ ppm) 14.22, 22.73, 26.95, 28.24, 31.71, 40.68, 113.65, 118.61, 119.92, 123.10, 124.63, 127.20, 128.32, 129.95, 132.23, 132.39, 132.53, 133.23, 157.69, 161.04, 163.68, 164.29, 190.70. HRMS (+ESI): Calculated for $C_{24}H_{23}NO_4$ 401.1627 $[M]^+$, Found 402.1759 $[M+H]^+$.

Characterization data for 15: ^1H NMR (600 MHz, $CDCl_3$, δ ppm) 0.89 (t, 3H), 1.34 (m, 4H), 1.44 (m, 2H), 1.74 (m, 2H), 4.18 (t, 2H), 7.19 (d, 1H), 7.23 (d, 2H), 7.80 (dd, 1H), 8.32 (d, 2H), 8.49 (d, 1H), 8.56 (d, 1H), 8.68 (t, 1H). ^{13}C NMR (150.00 MHz, $CDCl_3$, δ ppm) 14.21, 22.72, 26.94, 28.23, 32.07, 40.71, 114.34, 119.38, 123.19, 124.66, 126.48, 127.44, 128.08, 129.97, 132.32, 132.40, 139.43, 144.38, 156.97, 161.37, 163.55, 164. HRMS (+ESI): Calculated for $C_{24}H_{22}BrNO_3$ 418.1529 $[M]^+$, Found 419.1665 $[M+H]^+$.

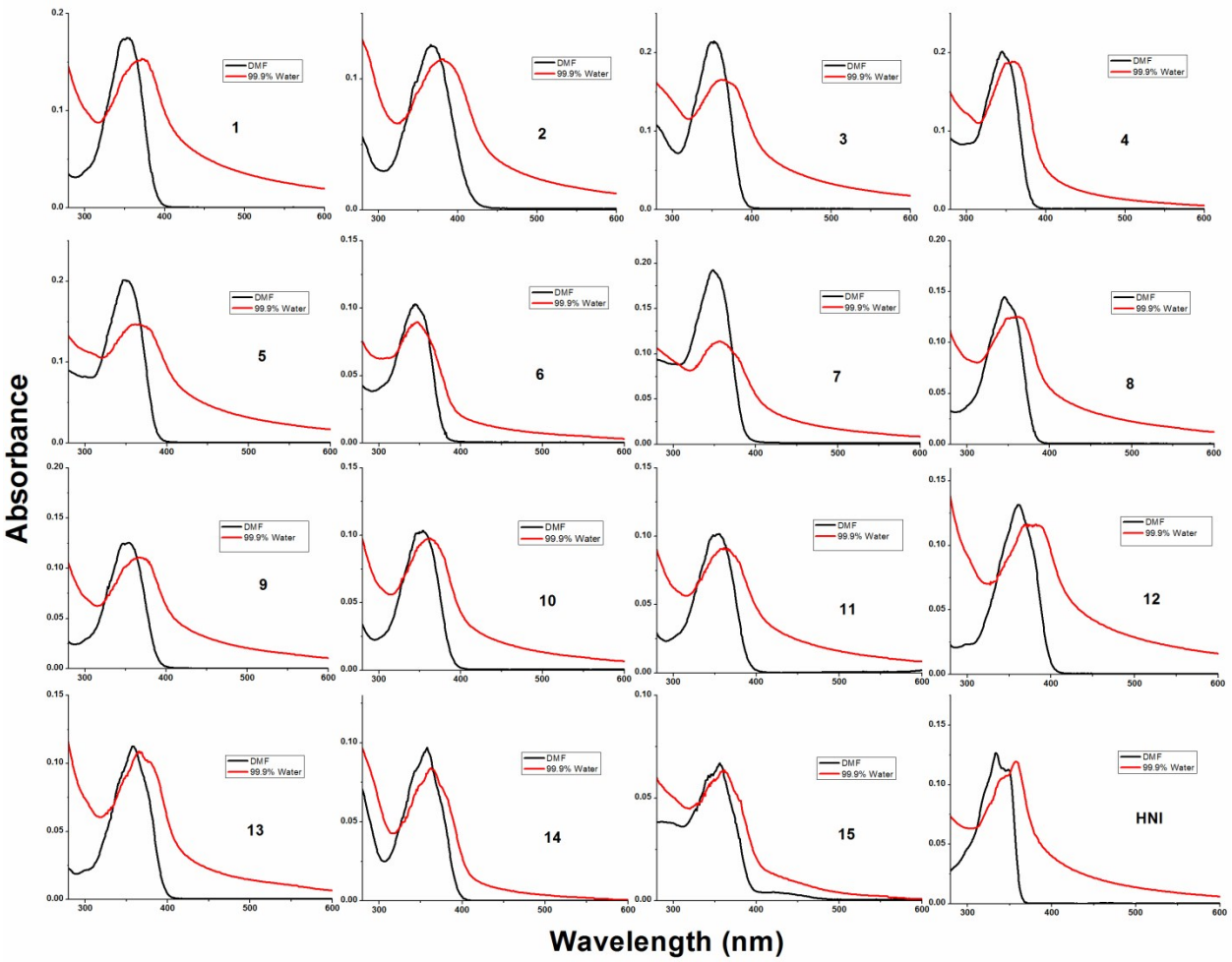

Figure S1. Absorption spectra of **1-15** and **HNI** in DMF and at 99.9% water fraction in DMF (at 25 ^{o}C, 10 μM).

Table S1. Photophysical data for the naphthalimide congeners (**1-15** and **HNI**)

Compound	Solvent[a]	$\lambda_{abs.max}$ (nm)	A	$\lambda_{em.max}$ (nm)	Φ_{FL}[b]
1	0%	353	0.17455	426	0.118
1	50%	359	0.18166	443	0.122
1	99.9%	372	0.15220	460	0.019
2	0%	368	0.11020	491	0.655
2	50%	374	0.13110	521	0.114
2	99.9%	381	0.11543	463	0.304
3	0%	350	0.21420	423	0.028
3	50%	354	0.21704	430	0.088
3	99.9%	362	0.16463	450	0.062
4	0%	347	0.20255	413	0.013
4	50%	352	0.20539	421	0.047
4	99.9%	362	0.18934	433	0.025
5	0%	348	0.20211	423	0.022
5	50%	352	0.20776	431	0.069
5	99.9%	361	0.14708	434	0.047
6	0%	347	0.10352	417	0.031
6	50%	345	0.10855	420	0.072
6	99.9%	347	0.08998	444	0.038
7	0%	349	0.19361	433	0.034
7	50%	350	0.19989	427	0.045
7	99.9%	356	0.11397	432	0.012
8	0%	347	0.14628	410	0.019
8	50%	348	0.14956	424	0.041
8	99.9%	366	0.12658	450	0.019
9	0%	354	0.12579	426	0.796
9	50%	358	0.13033	448	0.927
9	99.9%	366	0.11103	460	0.057
10	0%	354	0.10327	425	0.657
10	50%	354	0.10831	447	0.873
10	99.9%	364	0.09815	459	0.179
11	0%	354	0.10217	426	0.465
11	50%	355	0.10632	444	0.599
11	99.9%	364	0.09043	452	0.183
12	0%	357	0.13058	431	0.130
12	50%	362	0.13412	439	0.010
12	99.9%	385	0.11644	472	0.151
13	0%	356	0.11379	426	0.768
13	50%	359	0.11796	436	0.119
13	99.9%	365	0.10871	468	0.152

14	0%	356	0.09735	424	0.663
14	50%	358	0.09883	436	0.644
14	99.9%	361	0.08361	463	0.233
15	0%	354	0.06762	429	**0.007**
15	50%	354	0.06931	434	**0.005**
15	99.9%	361	0.06317	462	**0.004**
HNI	0%	334	0.12687	381	0.011
HNI	50%	334	0.12780	390	0.034
HNI	99.9%	357	0.12013	462	0.146

[a] Different fraction of water content in DMF. [b] Fluorescence quantum yields calculated using quinine sulfate as the standard (0.1 M H_2SO_4, λ_{ex}=350 nm, Φ_{FL} = 57.7%).

Table S2. CIE coordinates for the naphthalimide congeners (**1**-**15** and **HNI**) in solution and solid state.

Naphthalimidess	Solution		Solid	
	x	y	x	y
1	0.153	0.049	0.164	0.314
2	**0.175**	**0.366**	0.143	0.159
3	0.154	0.053	0.201	0.408
4	0.156	0.046	0.19	0.195
5	0.153	0.055	0.159	0.165
6	0.154	0.054	0.173	0.178
7	0.151	0.066	0.169	0.168
8	0.161	0.048	0.148	0.215
9	0.152	0.053	0.147	0.085
10	0.153	0.051	0.149	0.087
11	0.153	0.055	0.144	0.183
12	0.153	0.061	0.149	0.139
13	0.153	0.052	0.146	0.111
14	0.154	0.048	0.16	0.147
15	0.158	0.073	0.227	0.525
HNI	0.211	0.171	0.151	0.177

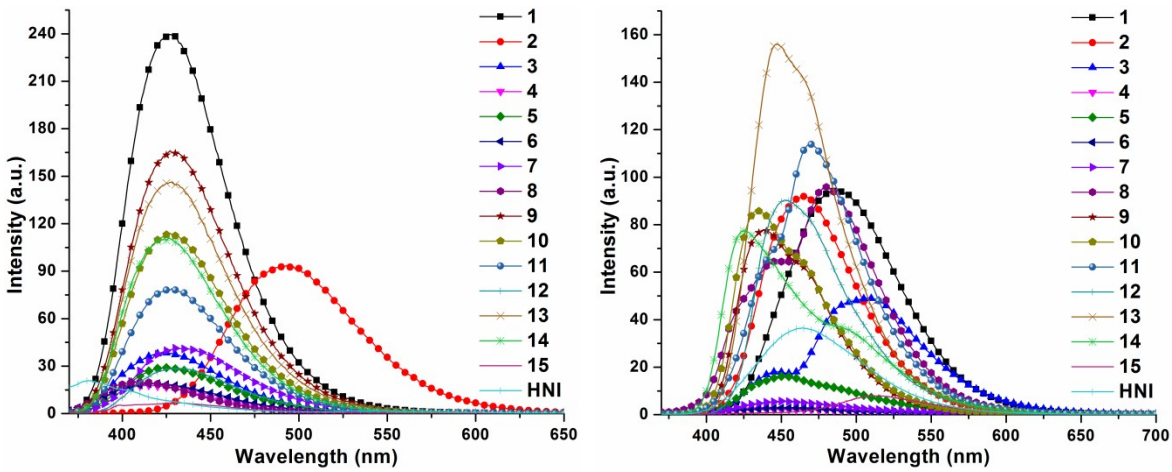

Figure S2. (left) Fluorescence spectra of all the congeners in their solution state (in DMF, 10 μM).(right) Solid-state fluorescence spectra of the luminogens. λ_{ex} = 355 nm

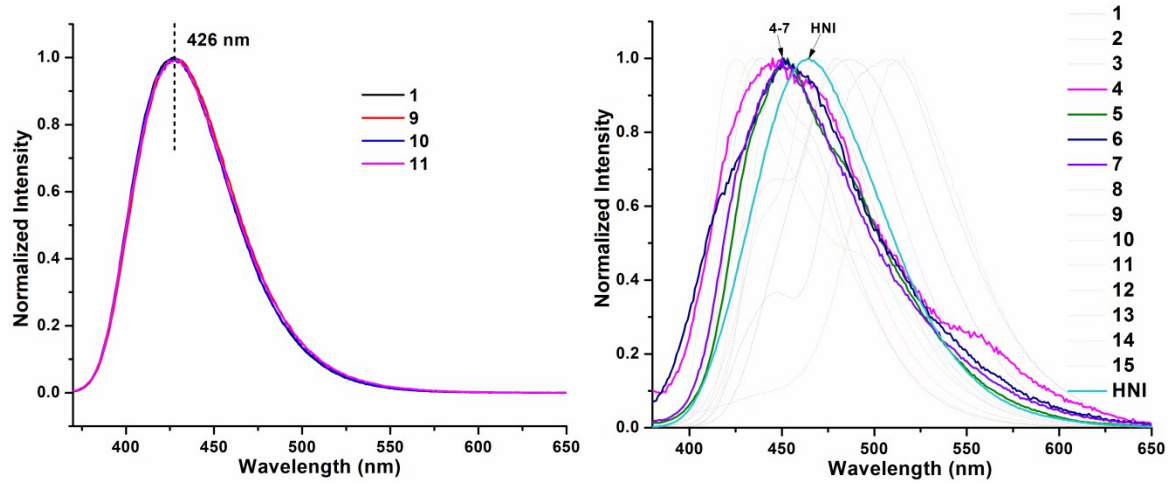

Figure S3. (Left) Fluorescence spectra of 1, 9, 10 and 11 in DMF (10 μM, λ_{ex} = 355 nm). (Right) Solid-state fluorescence spectra of the luminogens **1-15** and **HNI** (λ_{ex} = 355 nm).

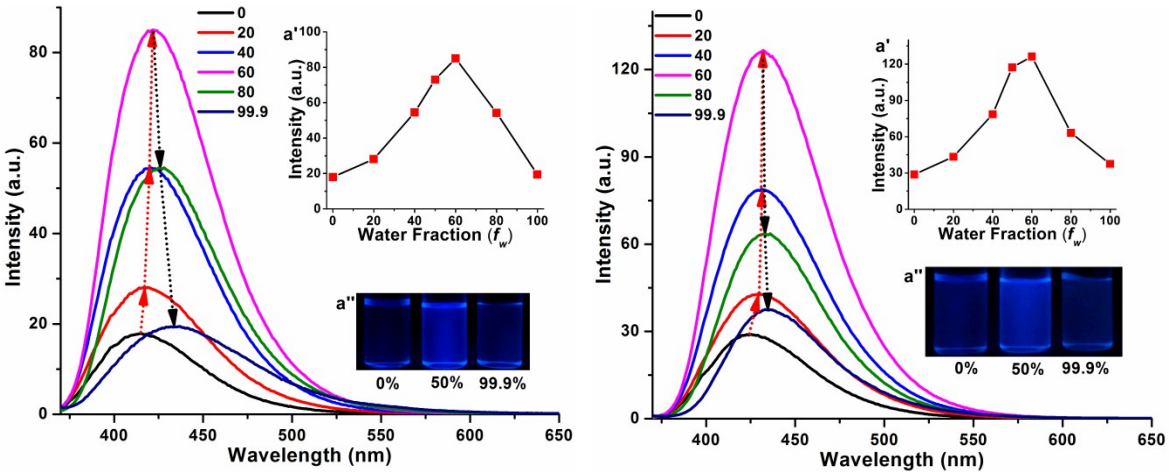

Figure S4. Emission spectra of (left) **4** and (right) **5** at different water fraction in DMF (at 25 ^{o}C, 10 μM, λ_{ex} = 355 nm). Insets: the respective (a') plot of $\lambda_{emi.max}$ Vs water fraction and (a'') digital photographs at different water fraction in DMF under UV irradiation at 365 nm.

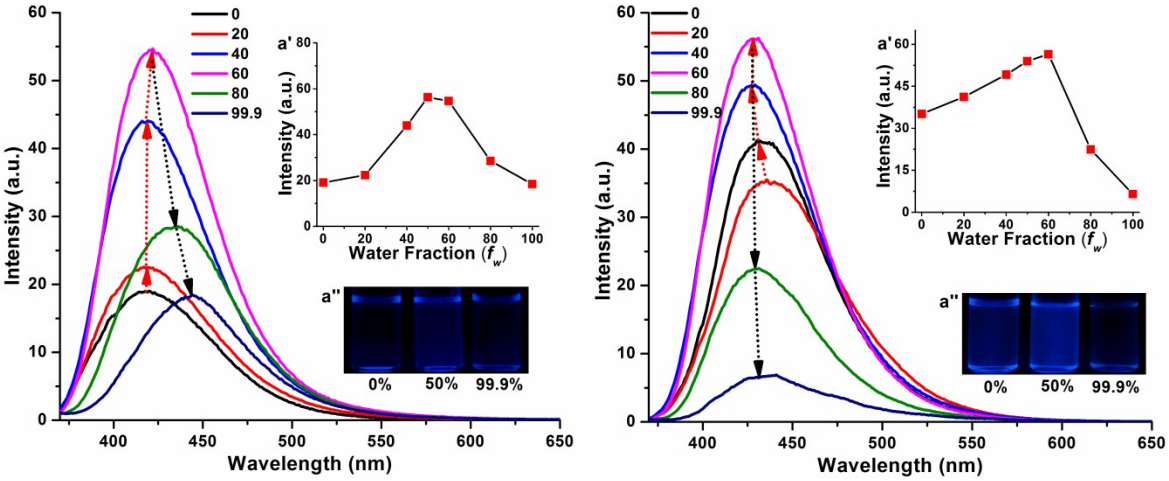

Figure S5. Emission spectra of (left) **6** and (right) **7** at different water fraction in DMF (at 25 ^{o}C, 10 μM, λ_{ex} = 355 nm). Insets: the respective (a') plot of $\lambda_{emi.max}$ Vs water fraction and (a") digital photographs at different water fraction in DMF under UV irradiation at 365 nm.

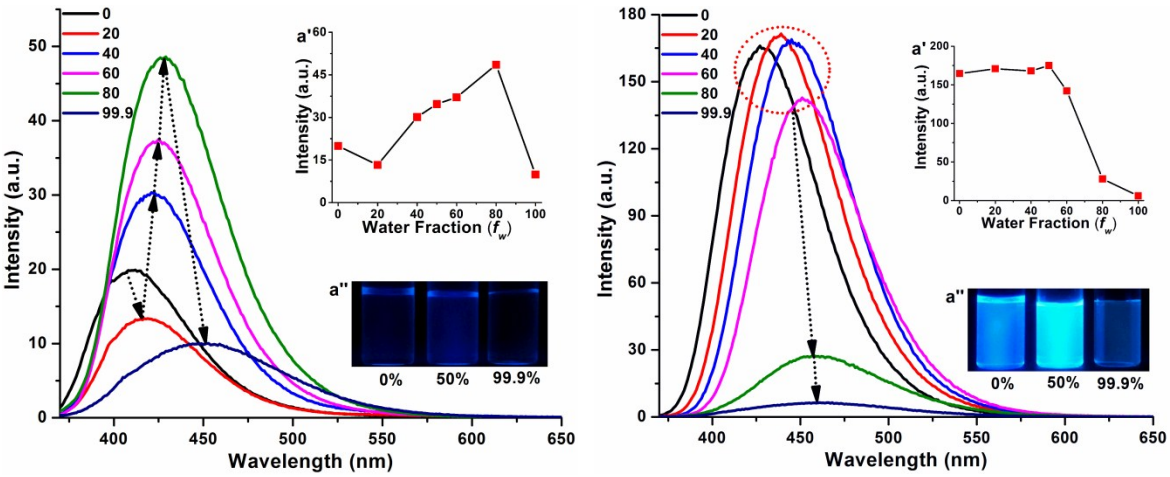

Figure S6. Emission spectra of (left) **8** and (right) **9** at different water fraction in DMF (at 25 ^{o}C, 10 μM, λ_{ex} = 355 nm). Insets: the respective (a') plot of $\lambda_{emi.max}$ Vs water fraction and (a") digital photographs at different water fraction in DMF under UV irradiation at 365 nm.

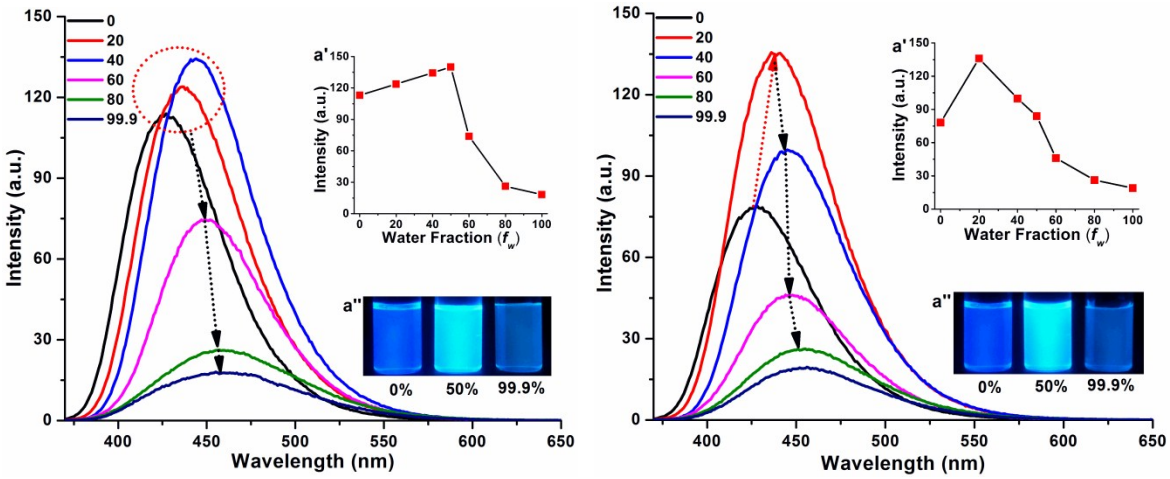

Figure S7. Emission spectra of (left) **10** and (right) **11** at different water fraction in DMF (at 25 ^{o}C, 10 μM, λ_{ex} = 355 nm). Insets: the respective (a') plot of $\lambda_{emi.max}$ Vs water fraction and (a") digital photographs at different water fraction in DMF under UV irradiation at 365 nm.

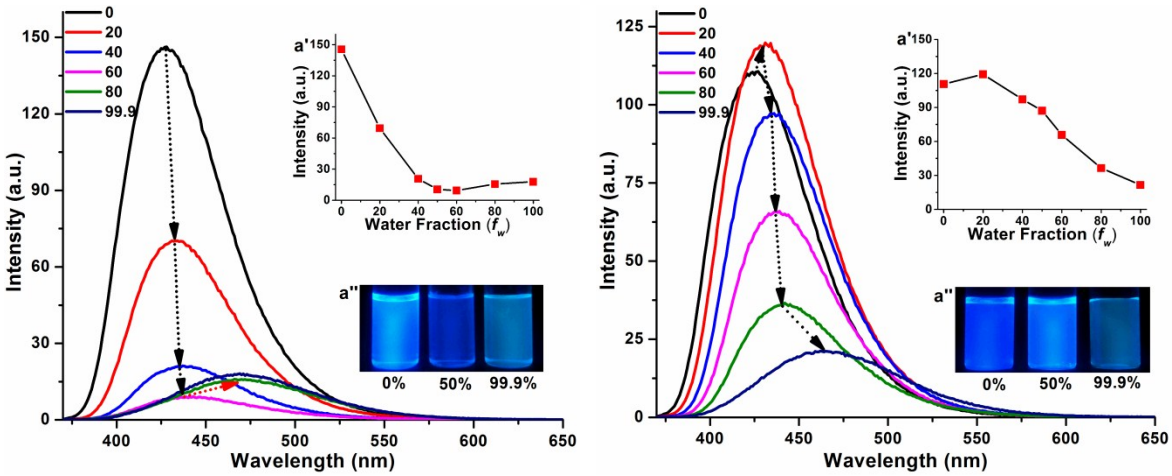

Figure S8. Emission spectra of (left) **13** and (right) **14** at different water fraction in DMF (at 25 ^{o}C, 10 μM, λ_{ex} = 355 nm). Insets: the respective (a') plot of $\lambda_{emi.max}$ Vs water fraction and (a") digital photographs at different water fraction in DMF under UV irradiation at 365 nm.

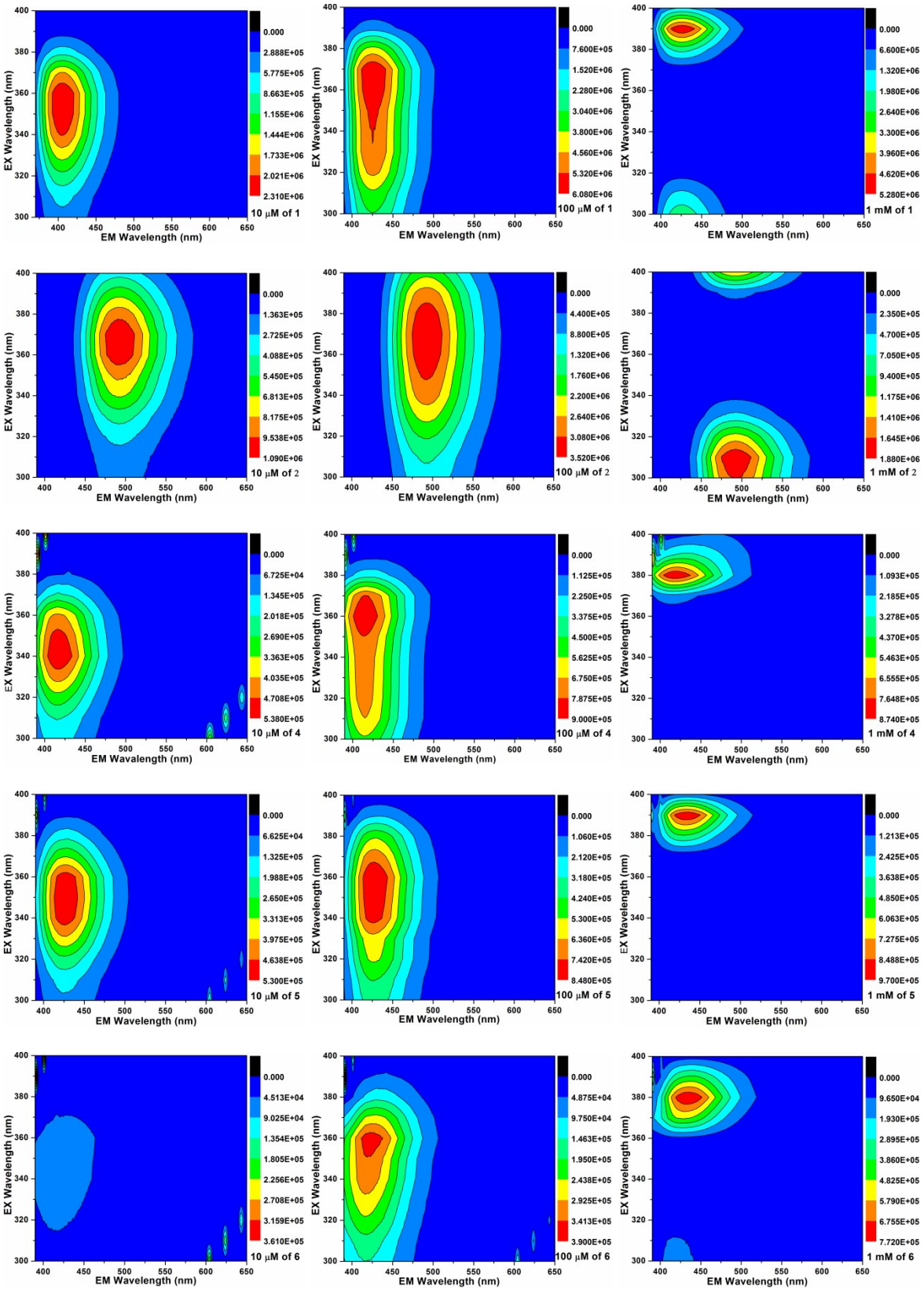
EX Wavelength (nm)
EM Wavelength (nm)
10 μM of 1
100 μM of 1
1 mM of 1
10 μM of 2
100 μM of 2
1 mM of 2
10 μM of 4
100 μM of 4
1 mM of 4
10 μM of 5
100 μM of 5
1 mM of 5
10 μM of 6
100 μM of 6
1 mM of 6

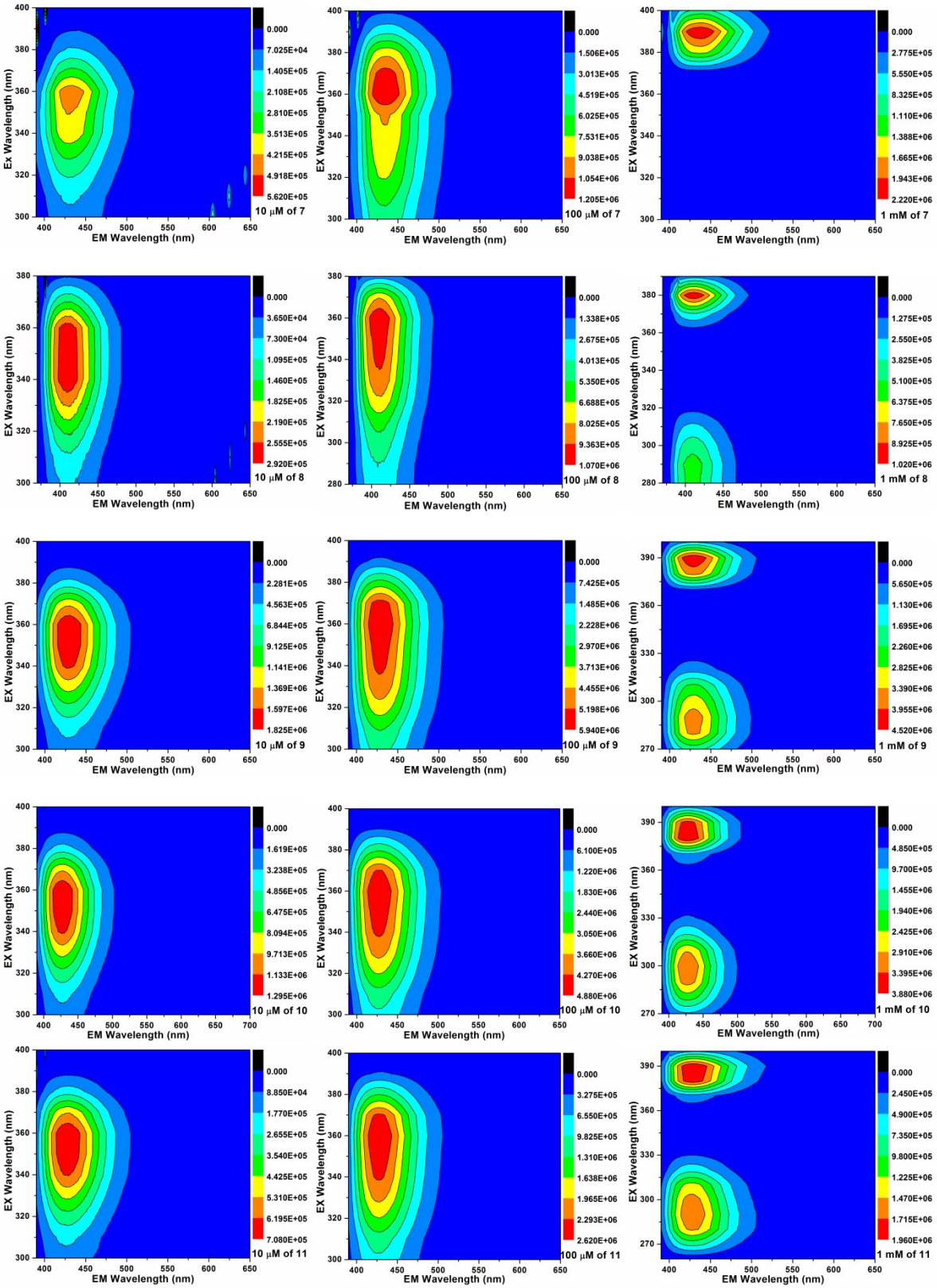
Ex Wavelength (nm)
EX Wavelength (nm)
EM Wavelength (nm)
10 μM of 7
100 μM of 7
1 mM of 7
10 μM of 8
100 μM of 8
1 mM of 8
10 μM of 9
100 μM of 9
1 mM of 9
10 μM of 10
100 μM of 10
1 mM of 10
10 μM of 11
100 μM of 11
1 mM of 11

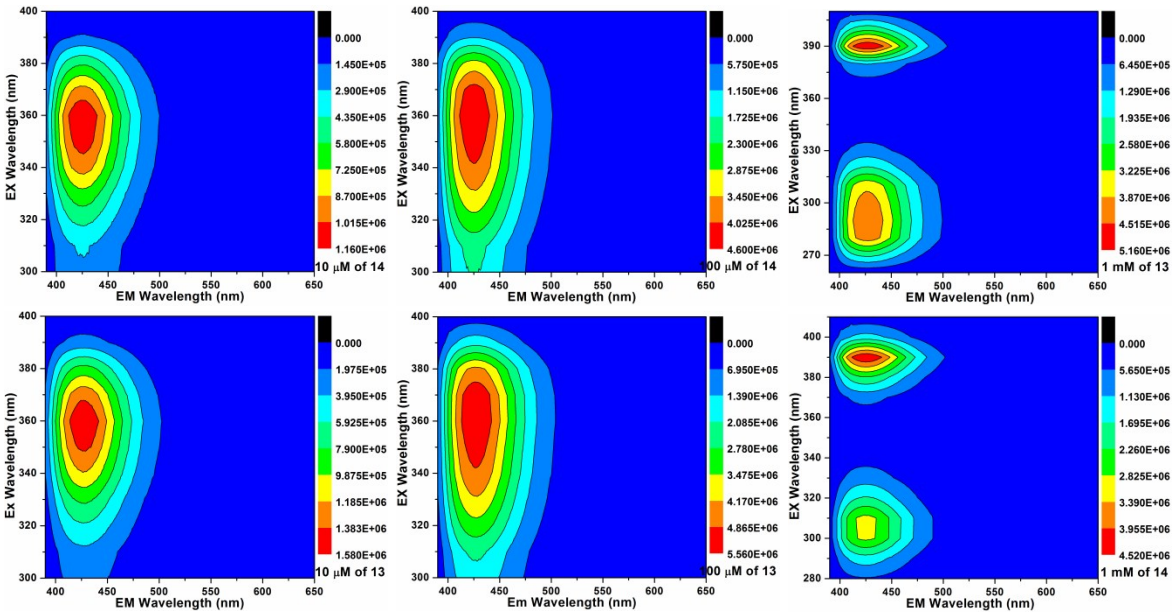

Figure S9. Excitation-emission matrix (EEM) spectra (2D contour projections) of **1**, **2**, **4-11**, **13** and **14** in DMF at different probe concentrations at 25 °C. Each row represents the EEM spectra of one congeners with increasing concentrations from left to right.

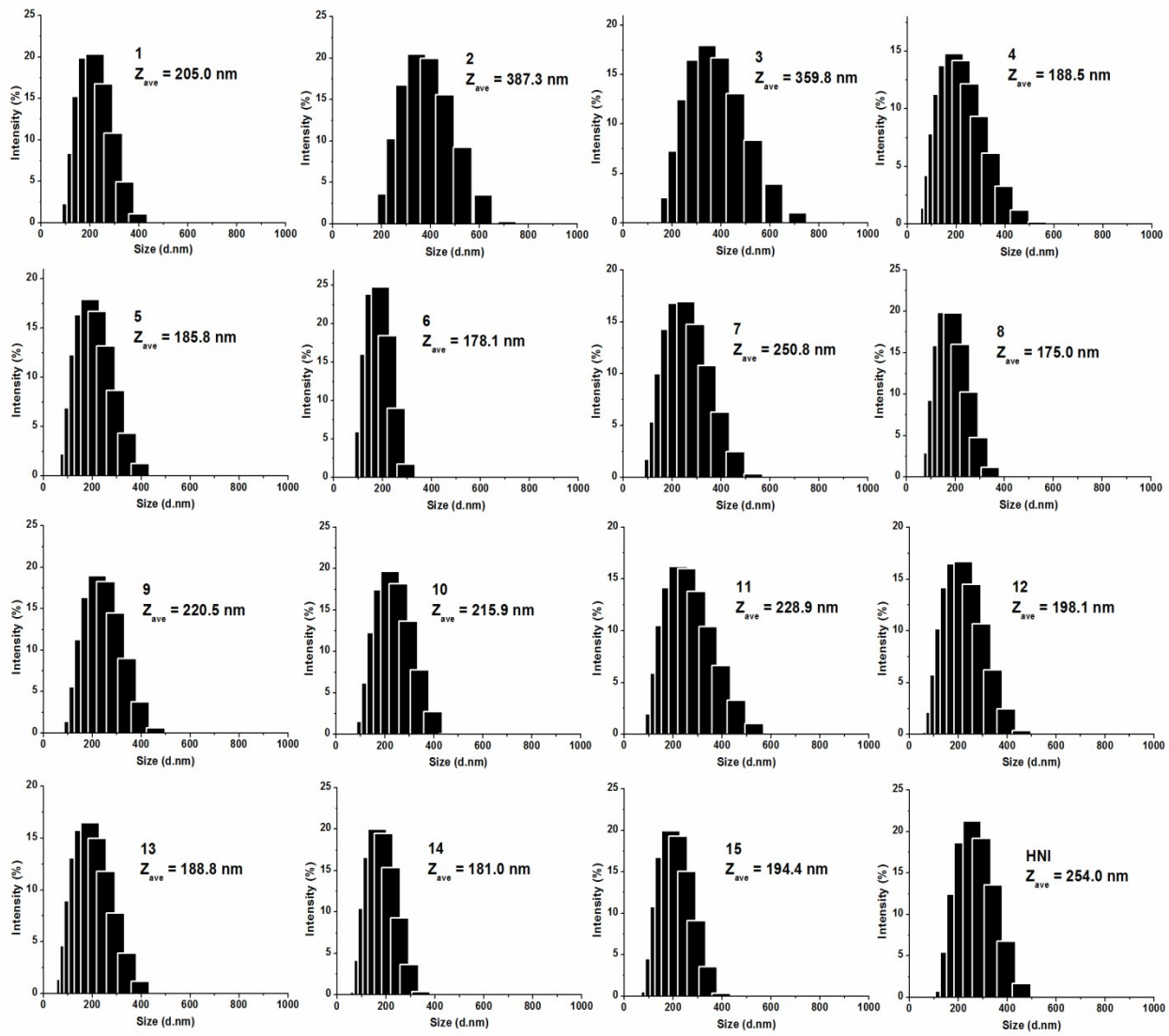

Figure S10. Size distribution of **1-15** and **HNI** nanoaggregates (10 μM) by DLS measurements in water at 25 ^{o}C.

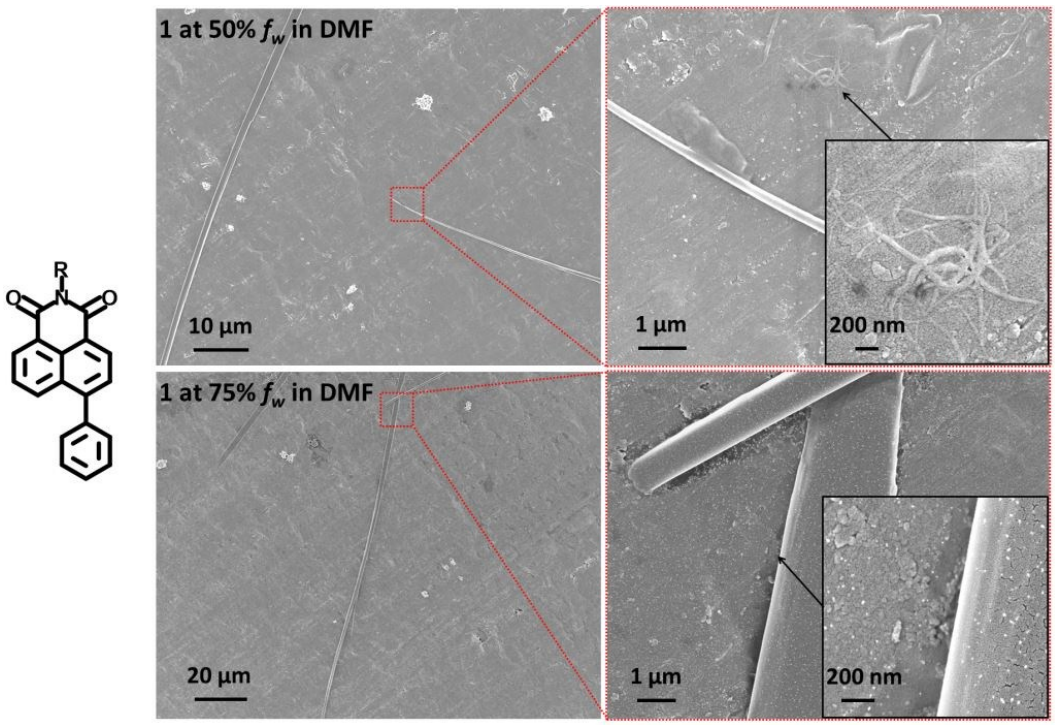

Figure S11. FESEM images of the homogeneously dispersed nano-assembly of **1** formed at different f_w in DMF along with its magnified image at selected area (10 μM). The FESEM images were obtained by simple drop-casting technique followed by room temperature drying of the dispersed solution of the luminogens as schematically presented in Figure 5q.

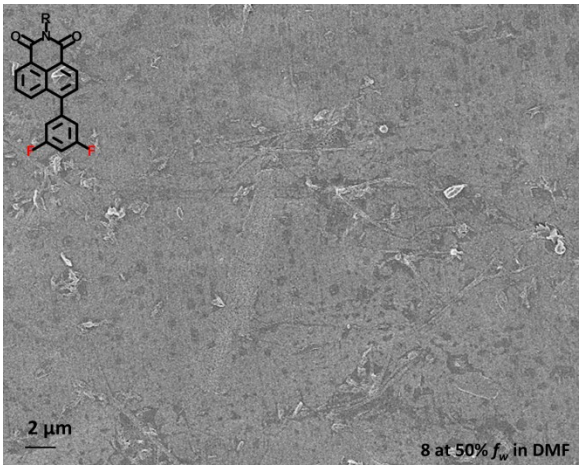

Figure S12. FESEM images of the homogeneously dispersed nano-assembly of **8** formed at 50% f_w in DMF by simple drop-casting technique followed by room temperature drying as schematically presented in Figure 5q (10 μM).

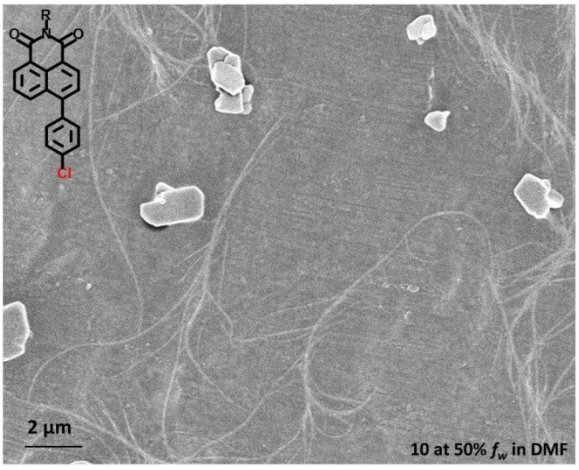

Figure S13. FESEM images of the homogeneously dispersed nano-assembly of **10** formed at 50% f_w in DMF by simple drop-casting technique followed by room temperature drying as schematically presented in Figure 5q (10 μM).

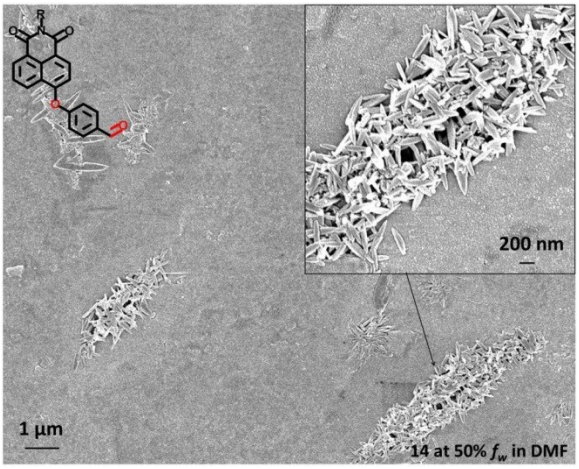

Figure S14. FESEM images of the homogeneously dispersed nano-assembly of **14** formed at 50% f_w in DMF by simple drop-casting technique followed by room temperature drying as schematically presented in Figure 5q (10 μM).

Crystallographic Details

Concentrated solutions of the congeners in DMF were prepared by heating at 60 ^{o}C and then were filtered off to leave behind the undissolved compound or any dust particles. After about 1-3 weeks, different shaped crystals for **2**, **8**, **9, 10** and **12** suitable for X-ray structure analysis were obtained. However, several attempts to obtain crystals for other congeners in various solvents and their mixture failed or very thin/small crystals were obtained that were not suitable for single crystal analysis. For the control study, the crystal data for HNI was obtained from Cambridge Crystallographic Data Centre where the crystals of HNI were generated by slow diffusion of n-hexane into a solution of dichloromethane containing HNI.[3] Nevertheless, we also obtained the HNI crystal in DMF and were found to have exactly the same intermolecular packing arrangement to that of the HNI single crystal obtained from CCDC which shows the non-polymorphic nature of HNI.

Table S3. SC-XRD Data and Parameters for **2**, **8**, **12** and **HNI** crystals**.**

Compound Code	**2**	**8**	**9**
CCDC	1830094	1830095	1855370
Empirical Formula	$C_{25}H_{25}N_1O_3$	$C_{24}H_{21}F_2N_1O_2$	$C_{24}H_{22}F_1N_1O_2$
Formula Weight	387.47	393.42	375.42
Temperature	298(2) K	298(2) K	298(2) K
Wavelength	0.71073 Å	0.71073 Å	0.71073 Å
Crystal System	monoclinic	monoclinic	triclinic
Space Group	C 12/c1	P 21/c	P -1
Unit Cell Dimension	a = 30.150(3) Å, α= 90^{o} b = 9.1044(5) Å, β = 103.266(3)^{o} c = 14.8046(14) Å, γ = 90^{o}	a = 14.4864(12) Å, α= 90^{o} b = 7.2999(5) Å, β = 92.947(8) ^{o} c = 19.0729(15) Å, γ = 90^{o}	a = 7.9798(6) Å, α= 75.043(7)^{o} b = 8.9908(8) Å, β = 80.201(7)^{o} c = 14.1265(12) Å, γ = 79.756(7)^{o}
Volume	4051.4(6) A^3	2014.3(3) A^3	955.29(14) A^3
Z	8	4	2
Absorption coefficient	0.083 mm^{-1}	0.091 mm^{-1}	0.089 mm^{-1}
F (000)	1648	856	396
Theta range for data collection	2.978 to 24.354^{o}	3.369 to 21.882^{o}	3.369 to 21.882^{o}
Index Range	-27<=h<=26, -6<=k<=10, -13<=l<=14	-17<=h<=19, -9<=k<=8, -23<=l<=23	-10<=h<=10, -11<=k<=11, -18<=l<=15
Reflections Collected/unique	2054/1456 (R_{int} = 0475)	4650/1590 (R_{int} = 0.0521)	4284/1881 (R_{int} = 0.0307)
Goodness-of-fit on F^2	1.085	1.147	1.079
Final R indices [I>2σ(I)]	R1 = 0.0579, ωR2 = 0.1521	R1 = 0.0799, ωR2 = 0.1520	R1 = 0.0667, ωR2 = 0.1396
R indices (all data)	R1 = 0.0786, ωR2 = 0.1740	R1 = 0.2098, ωR2 = 0.2074	R1 = 0.1494, ωR2 = 0.1935
Refinement method	SHELXL	SHELXL	SHELXL

Compound Code	10	12	HNI
CCDC	1882969	1830096	1014214
Empirical Formula	$C_{24}H_{22}Cl_1N_1O_2$	$C_{24}H_{23}N_1O_3$	$C_{18}H_{19}NO_2$
Formula Weight	391.89	373.44	281.34
Temperature	298(2) K	298(2) K	298(2) K
Wavelength	0.71073 Å	0.71073 Å	0.71073 Å
Crystal System	Triclinic	Triclinic	Monoclinic
Space Group	P -1	P -1	P 21/n
Unit Cell Dimension	a = 7.9984(11) Å, α= 76.640(4) ° b = 9.3801(12) Å, β = 80.682(4) ° c = 13.8330(18) Å, γ = 79.490(4)°	a = 7.7872(5) Å, α= 102.882(7) ° b = 8.7869(7) Å, β = 96.881(6) ° c = 15.0163(14) Å, γ = 92.192(6)°	a = 8.2418(14) Å, α= 90° b = 16.336(3) Å, β = 103.266(3)° c = 11.3610(19) Å, γ = 90°
Volume	985.0(2)	992.18(14) A^3	1488.8(4) A^3
Z	2	2	4
Absorption coefficient	0.204 mm^{-1}	0.080 mm^{-1}	0.082 mm^{-1}
F (000)	360	396	600
Theta range for data collection	3.171 to 28.517°	3.593 to 26.097°	2.22 to 25.99°
Index Range	-10<=h<=10, -12<=k<=12, -18<=l<=18	-10<=h<=9, -11<=k<=11, -18<=l<=19	-10<=h<=10, -20<=k<=20, -13<=l<=14
Reflections Collected/unique	4063/1721 (Rint = 0.0909)	4449/2485 (R_{int} = 0.0207)	11160/2930 (R_{int} = 0.0346)
Goodness-of-fit on F^2	0.889	1.035	1.036
Final R indices [I>2σ(I)]	R1 = 0.0509, ωR2 = 0.0950	R1 = 0.0776, ωR2 = 0.2024	R1 = 0.0569, ωR2 = 0.1592
R indices (all data)	R1 = 0.1312, ωR2 = 0.1099	R1 = 0.1252, ωR2 = 0.2433	R1 = 0.0689, ωR2 = 0.1744
Refinement method	SHELXL	SHELXL	SHELXL

The data integration and reduction were processed with SAINT.[4] SHELXL-97 was used for the structure solutions via direct method and refined by full-matrix least-squares on F^2.[5]

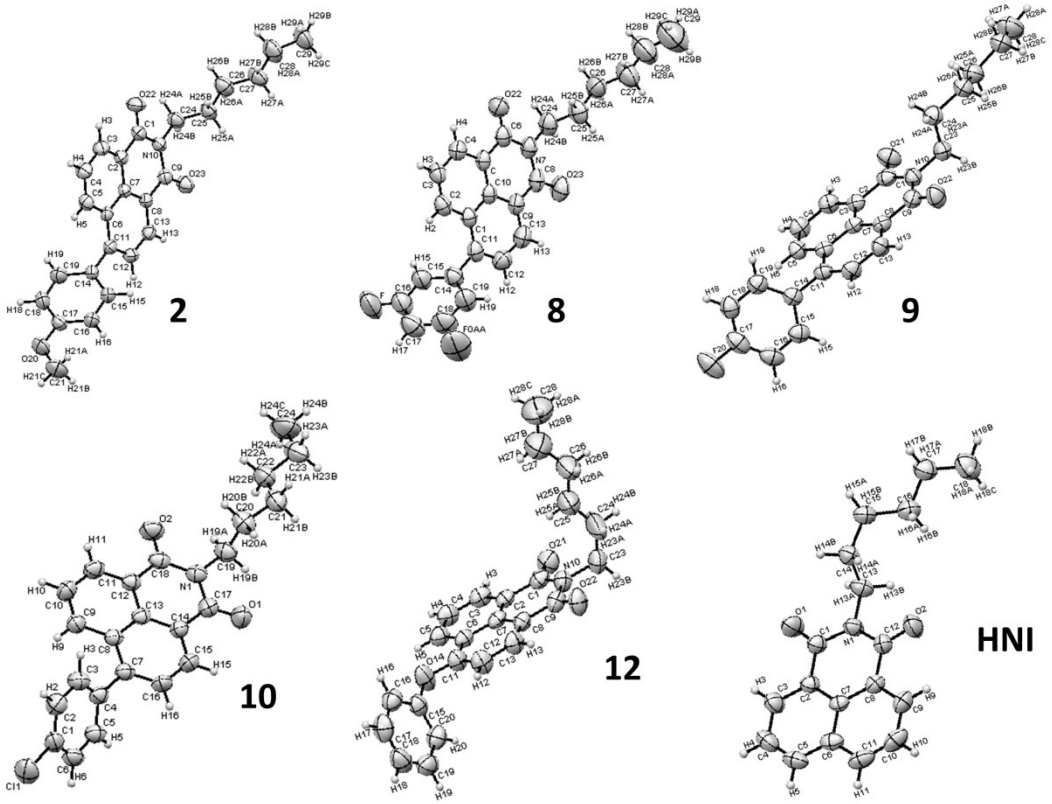

Figure S15. Oak Ridge Thermal Ellipsoid Plot (ORTEP) of compounds (**2, 8, 9, 10, 12** and **HNI**) with the thermal ellipsoids set at 50% probability.

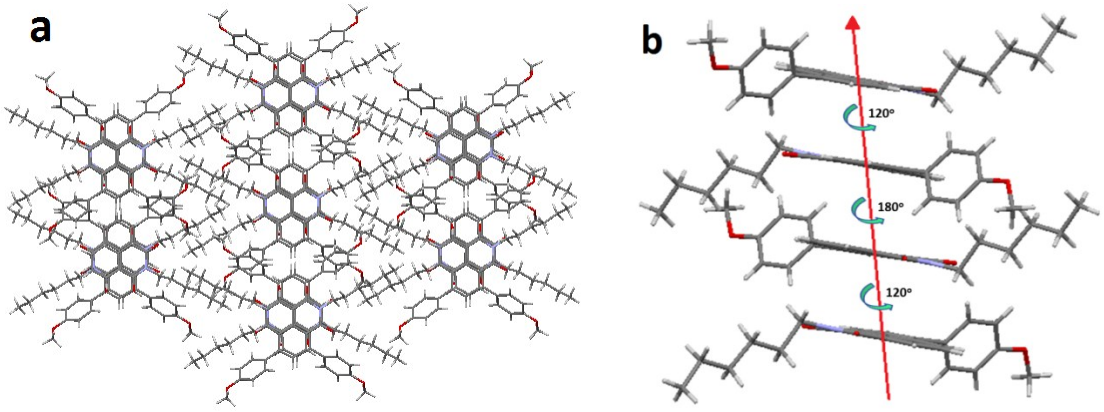

Figure S16. (a) Single crystal packing diagram of **2** as viewed down along crystallographic c axis. (b) Face-to-face packing in **2** showing the rotation angle considering the naphthalimide core.

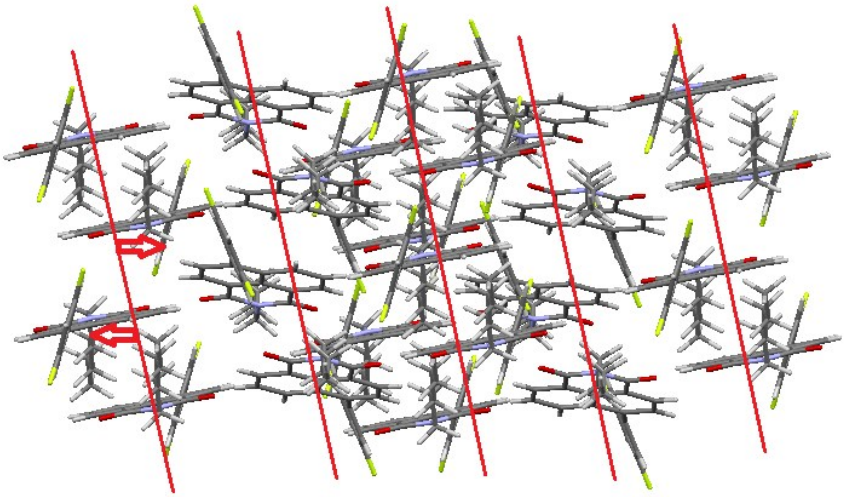

Figure S17. Single crystal packing diagram of **8**.

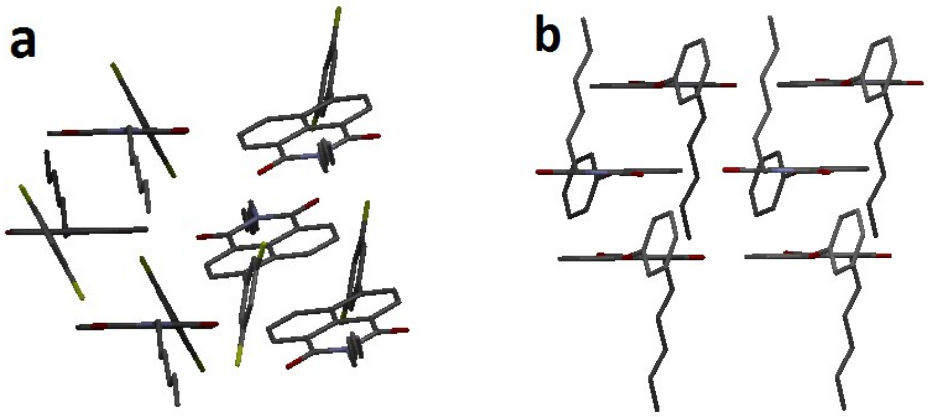

Figure S18. Single crystal packing diagram of (a) **8** and (b) **12** showing the arrangement perturbation in the naphthalimide congeners by simple structural modification.

Figure S19. Crystal structures of **2**, **8, 9** and **10** (left to right) showing the dihedral angle between naphthalimide and phenyl planes.

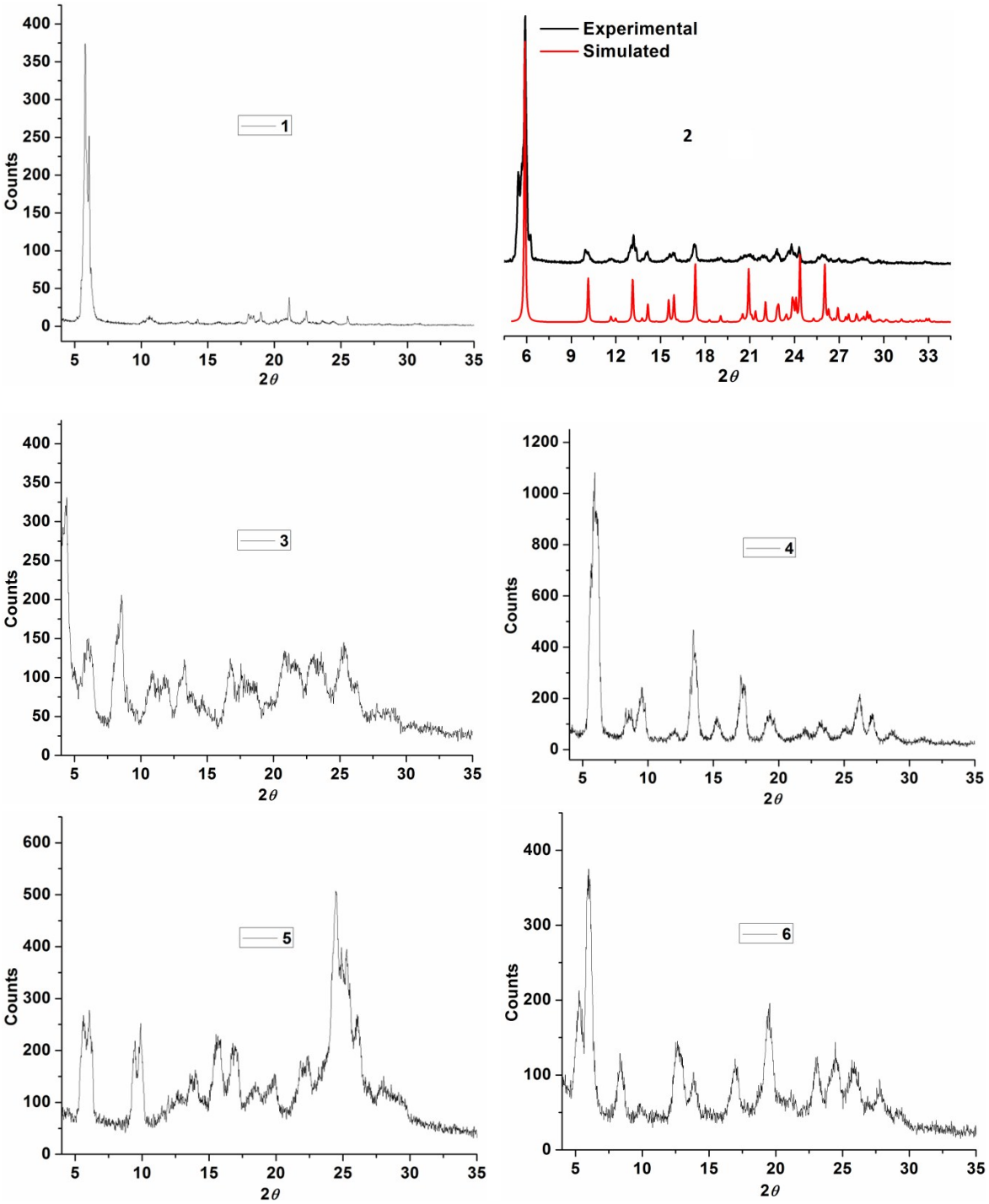
Counts
2θ
1
Experimental
Simulated
2
3
4
5
6

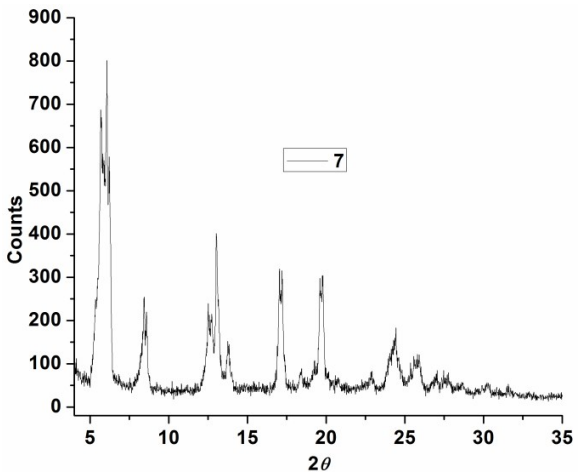
Counts
2θ
7

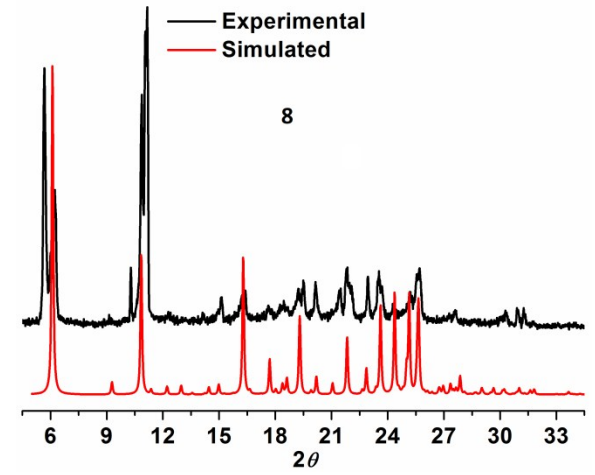
Experimental
Simulated
8
2θ

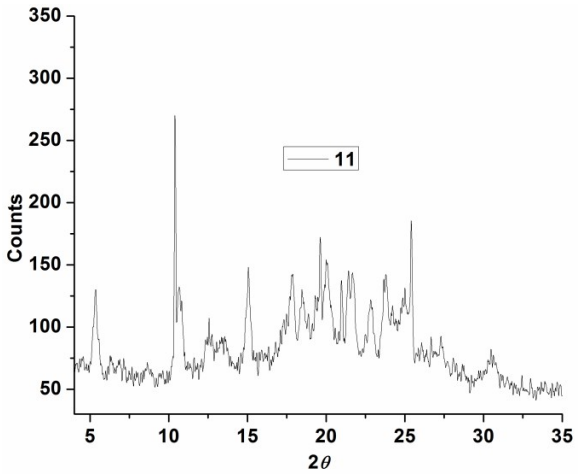
Counts
2θ
11

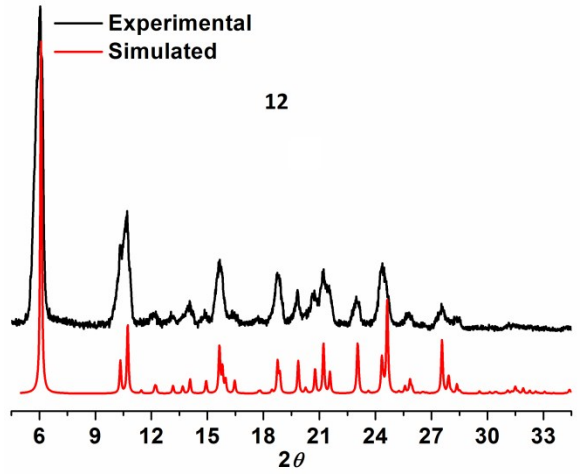
Experimental
Simulated
12
2θ

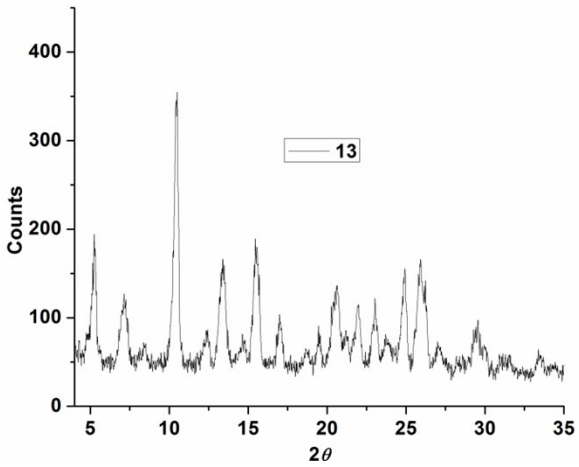
Counts
2θ
13

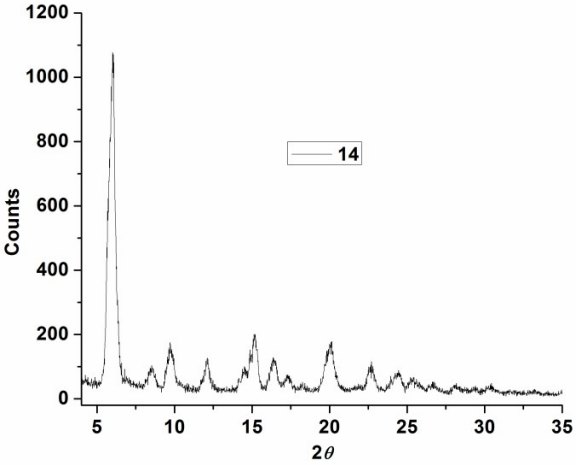
Counts
2θ
14

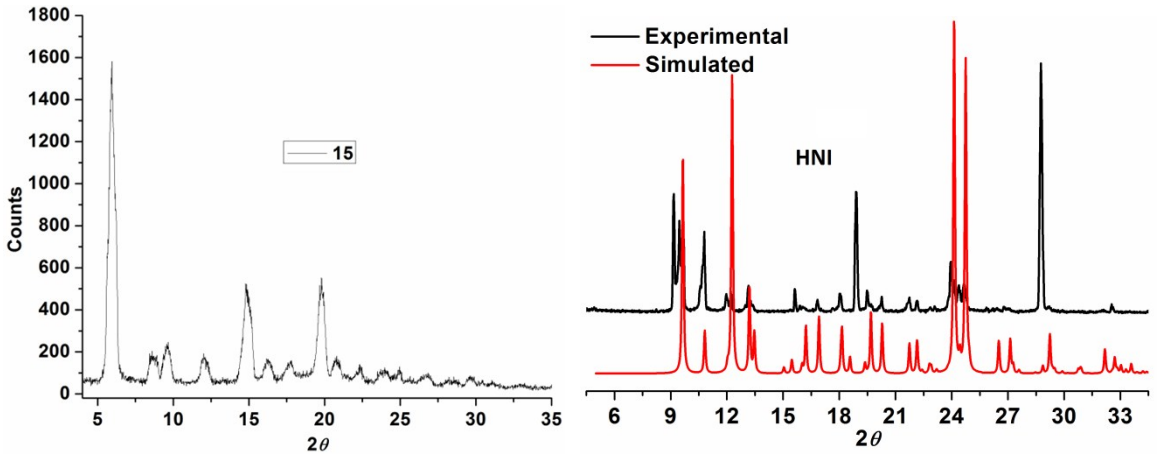

Figure S20. PXRD pattern of the congeners. For few compounds with single crystal XRD data, the simulated PXRD patterns have been compared with their respective experimental data.

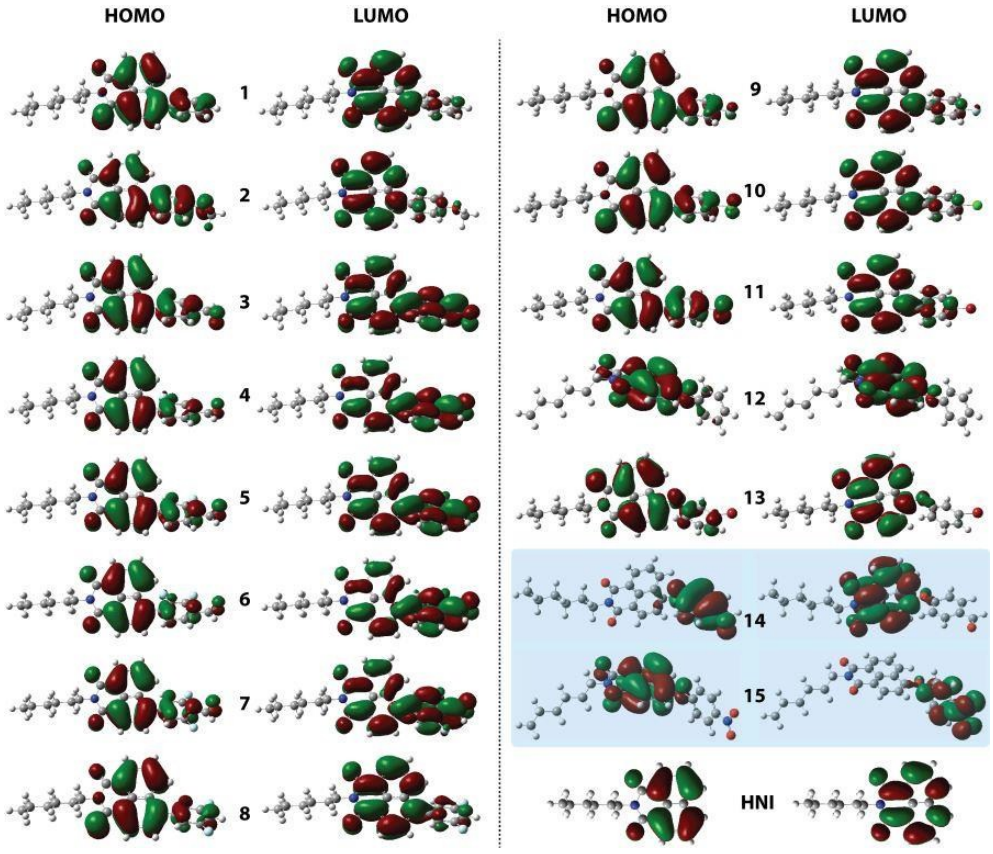

Figure S21. Optimized structures and HOMO/LUMO electron density of the congeners in the excited states. Computations were executed using time dependent density functional theory with the B3LYP exchange functional employing 6-31G* basis sets in the Gaussian 09 program.[1,2]

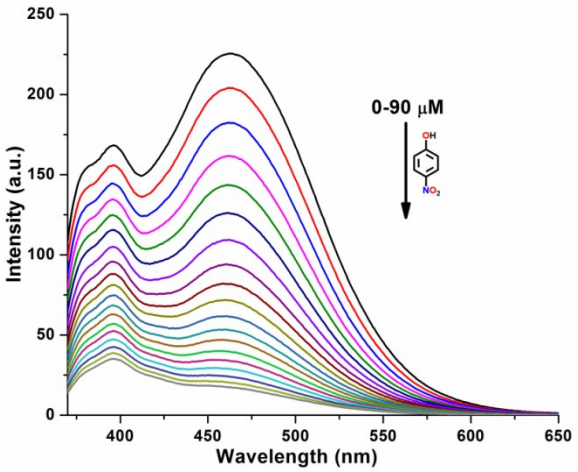

Figure S22. Fluorescence response of **HNI** toward p-nitrophenol in water at 25 °C.

Table S4. DFT calculated HOMO and LUMO energy levels of **HNI** and other small aromatic analytes.[1,2]

Molecules	**HOMO (eV)**	**LUMO (eV)**
HNI	-6.56638	-2.55488
p-nitrophenol	-7.13701	-2.76141
Phenol	-0.12109	5.20799
Bromobenzene	-6.68802	-0.36218
Chlorobenzene	-6.89482	-0.43212
Fluorobenzene	-6.84013	-0.34314
2-fluorobenzaldehyde	-7.01972	-2.08793
3-Bromophenol	-6.40203	-0.42776
3-Fluorobenzaldehyde	-7.28123	-2.22834
4-hydroxybenzaldehyde	-6.64775	-1.7116
1,3-Difluorobenzene	-7.12394	-0.64328
2,3-Difluorobenzaldehyde	-7.28531	-2.38045
2,6-Difluorobenzaldehyde	-7.12013	-2.32521
Benzaldehyde	-6.99306	-1.9018
Benzene	-6.75387	0.102043
PhOMe	-6.50706	-0.02122

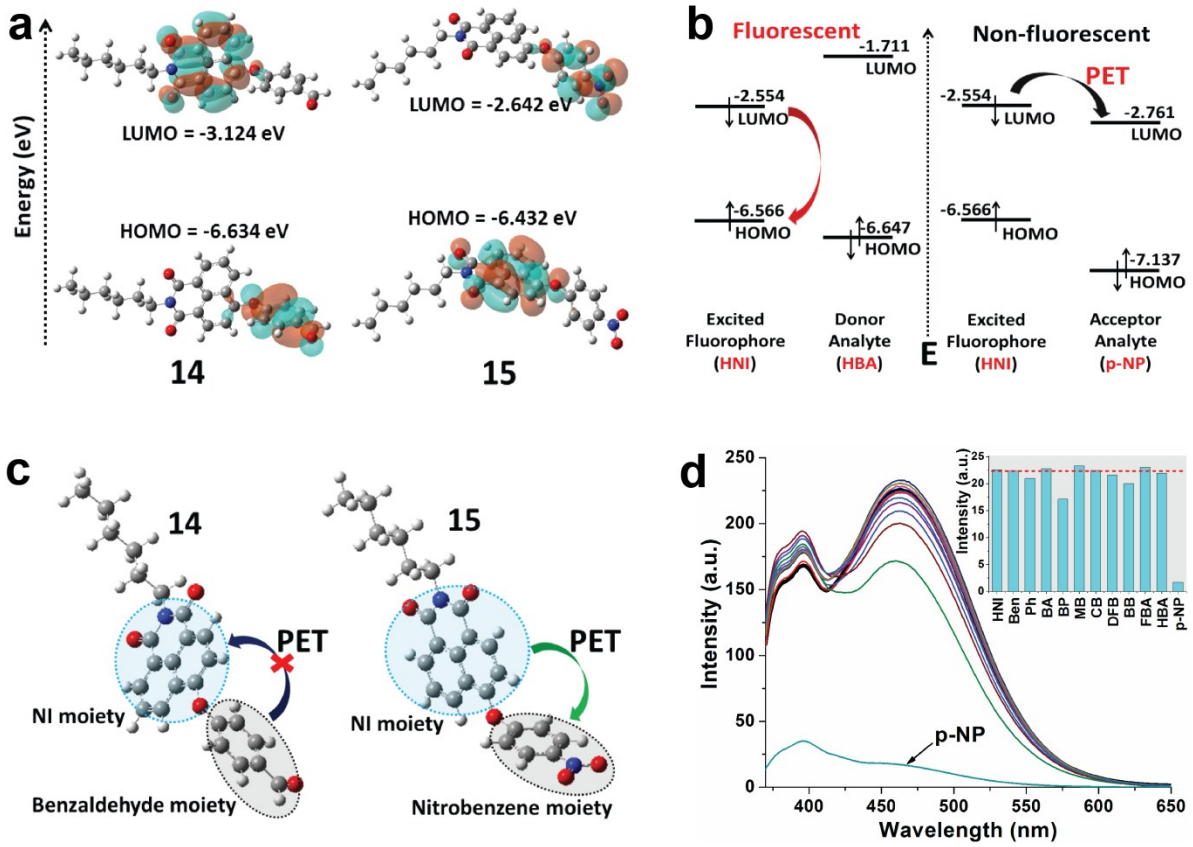

Figure S23 (a) HOMO/LUMO electron distribution in **14** and **15**. (b) Schematic molecular orbital diagram of the fluorescence on/off switch in HNI via PET process with p-hydroxybenzaldehyde and p-nitrophenol (values are in eV). (c) Optimized structure of **14** and **15** presenting the co-regulation of response emission by the PET mechanism. (d) Fluorescence emission spectra of HNI (10 μM) in presence of various small molecules (90 μM) in water. Inset: bar diagram showing the fluorescence intensity of HNI and HNI + small molecules at 470 nm; left to right: HNI only, benzene (Ben), phenol (Ph), benzaldehyde (BA), bromophenol (BP), methoxybenzene (MB), chlorobenzene (CB), difluorobenzene (DFB), bromobenzene (BB), fluorobenzaldehyde (FBA), p-hydroxybenzaldehyde (HBA), p-nitrophenol (p-NP).

^{1}H NMR Spectra

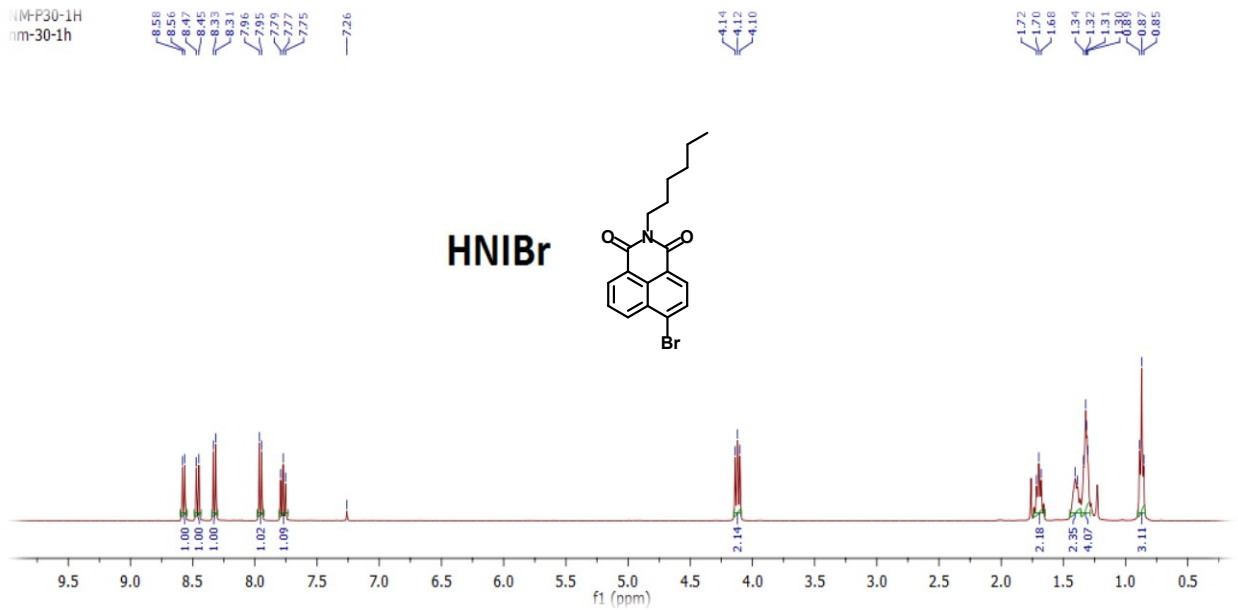

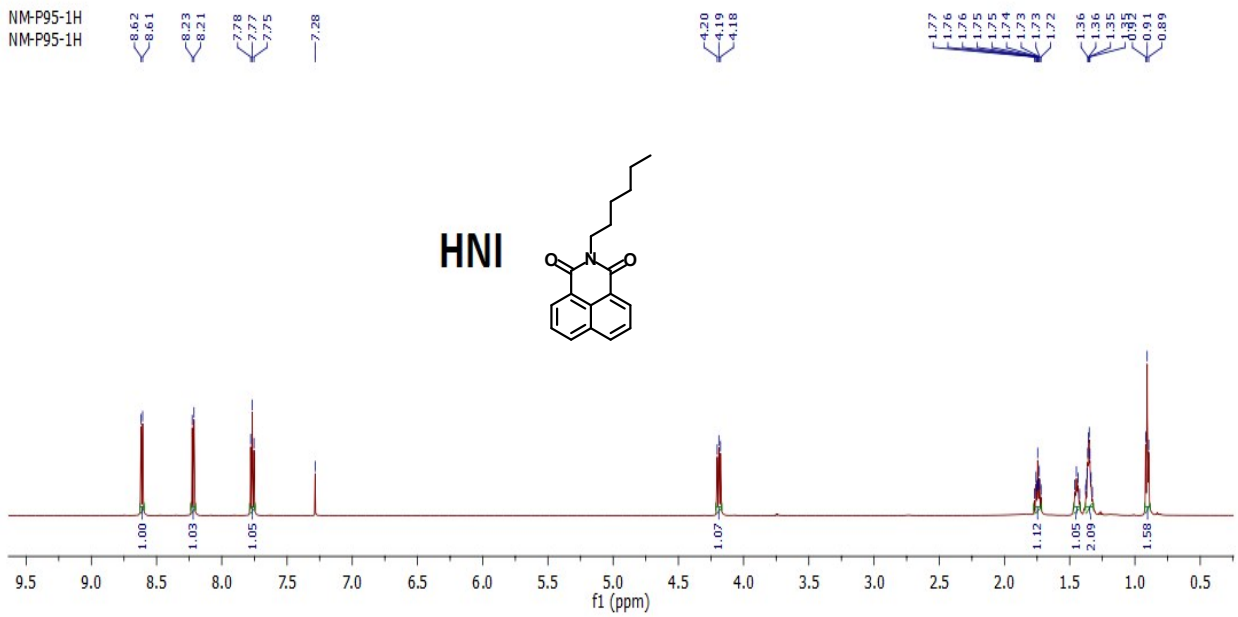

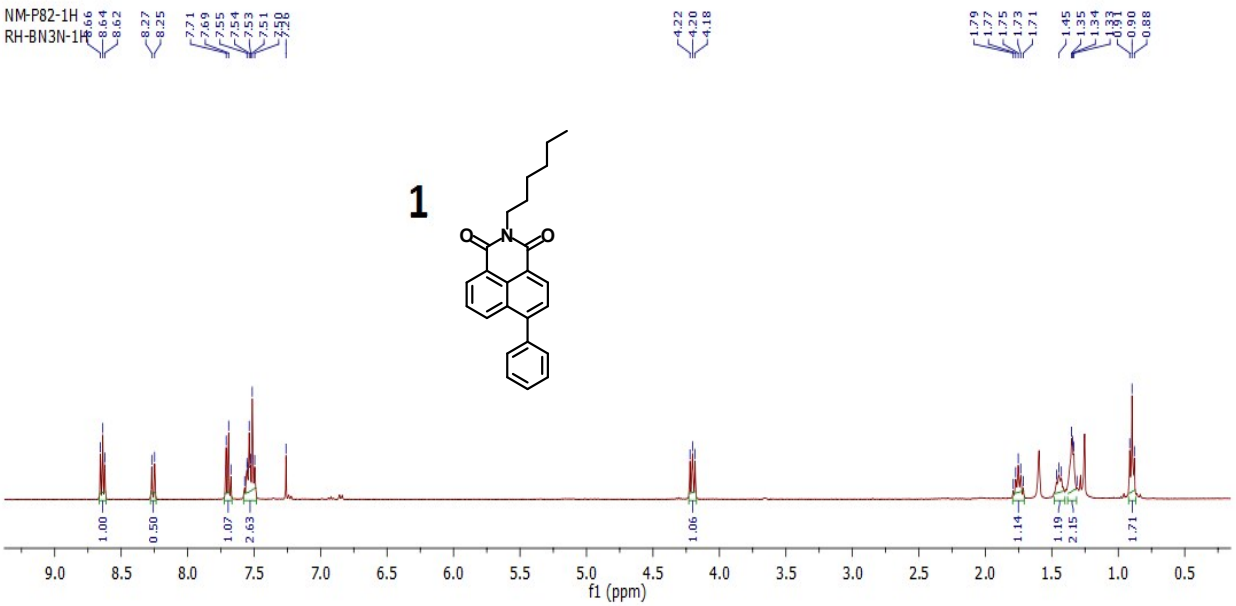
NM-P82-1H
RH-BN3N-1H
1
f1 (ppm)

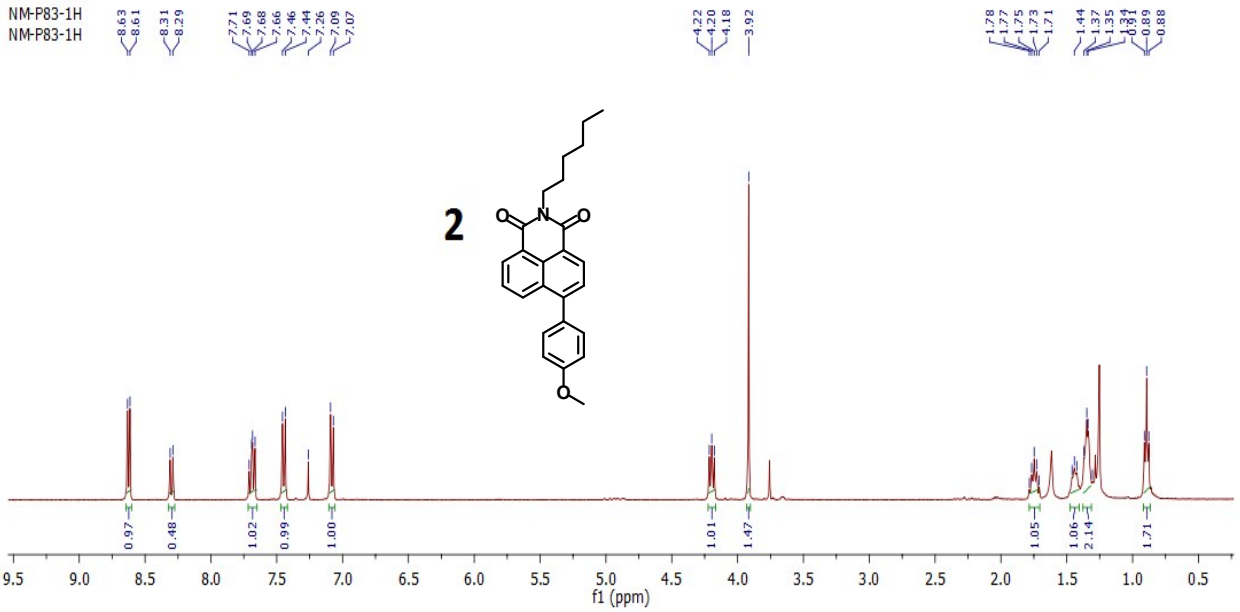
NM-P83-1H
NM-P83-1H
2
f1 (ppm)

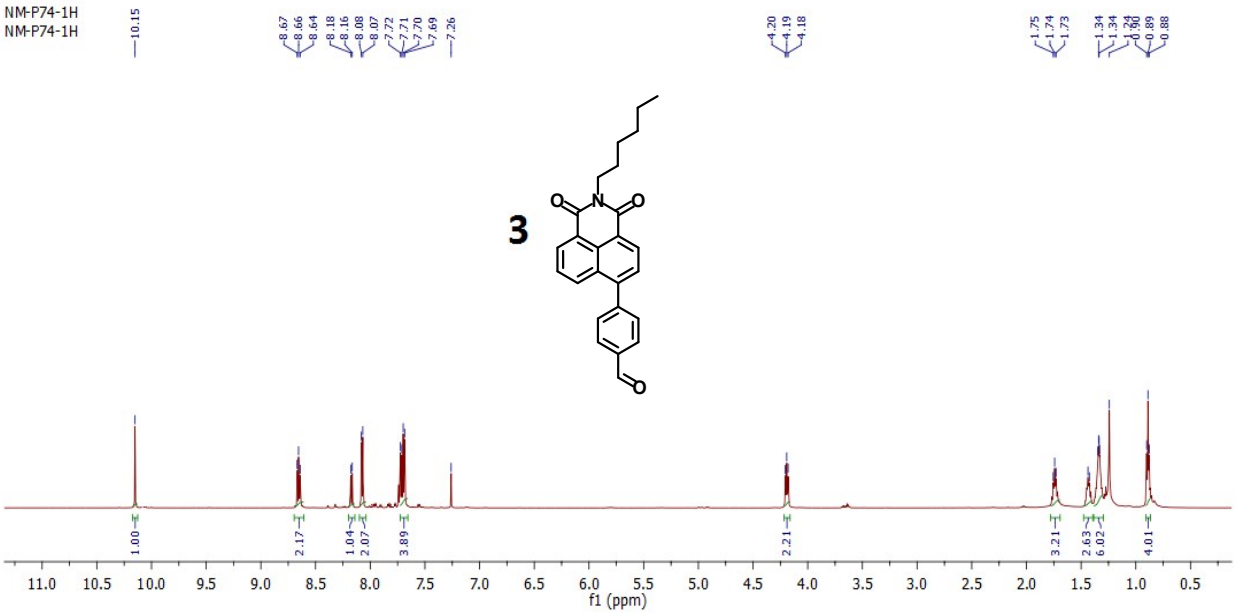
NM-P74-1H
NM-P74-1H
3
f1 (ppm)

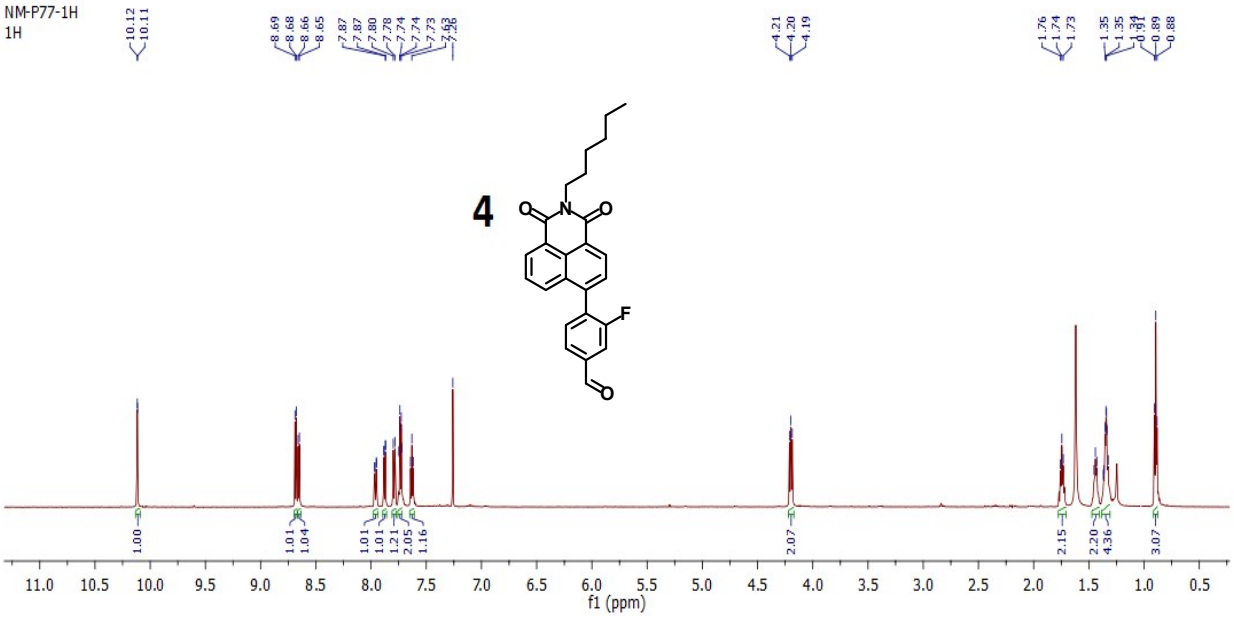
NM-P77-1H
1H
4
F
f1 (ppm)

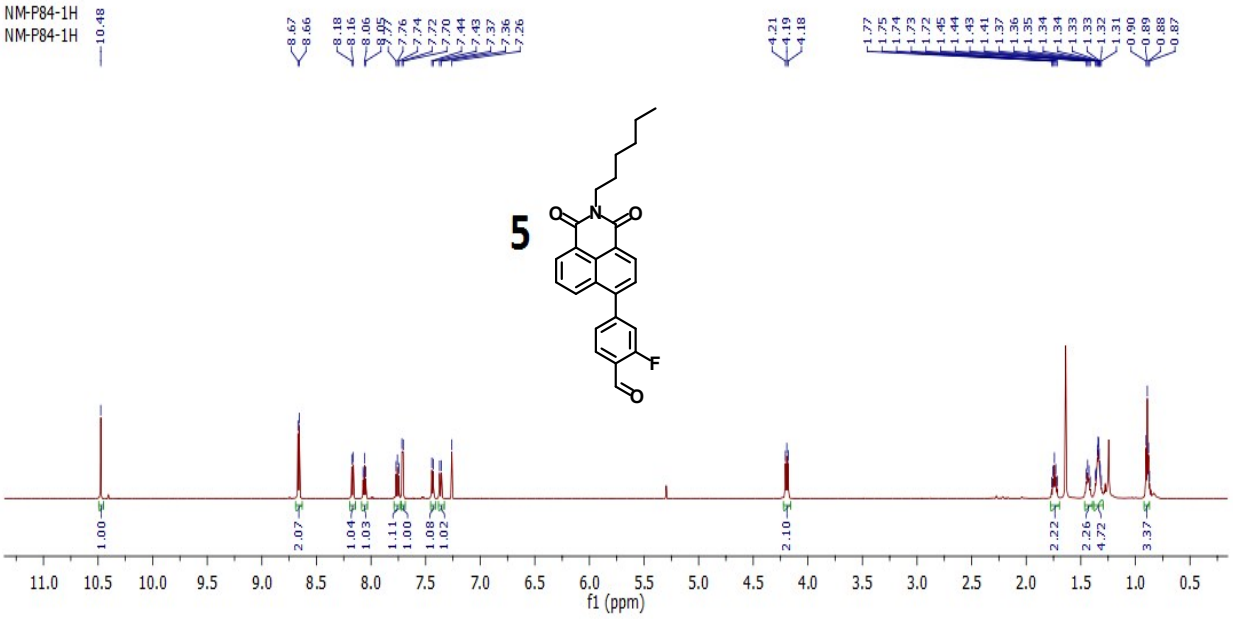
NM-P84-1H
NM-P84-1H
5
f1 (ppm)

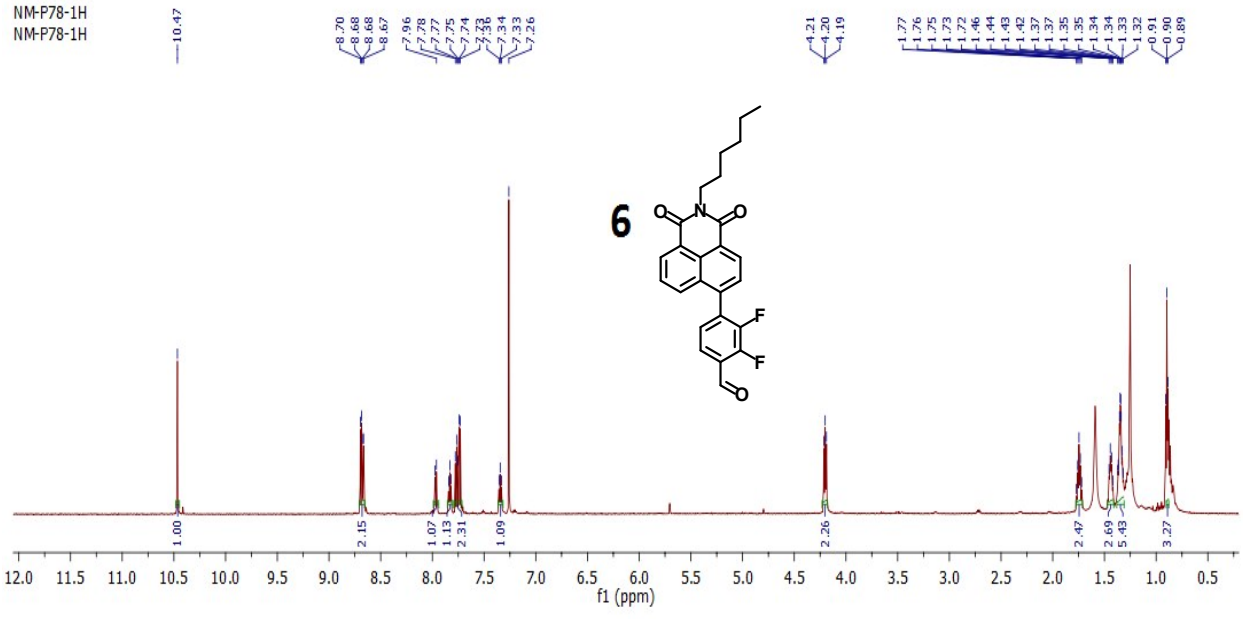
NM-P78-1H
NM-P78-1H
6
f1 (ppm)

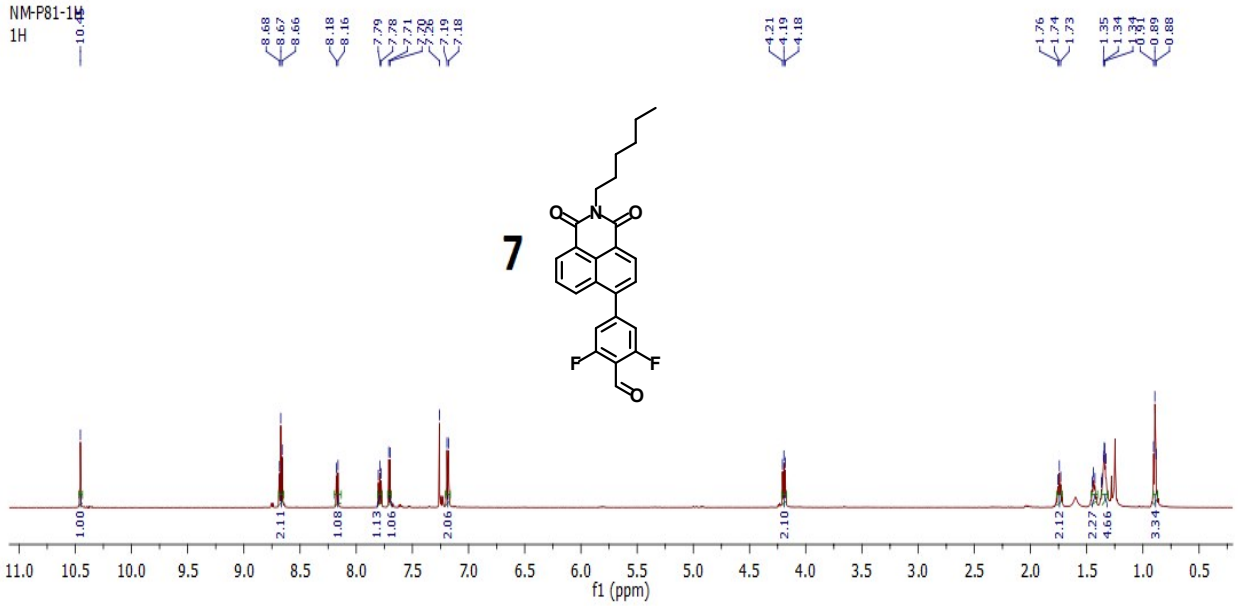
NM-P81-1H
1H
7
f1 (ppm)

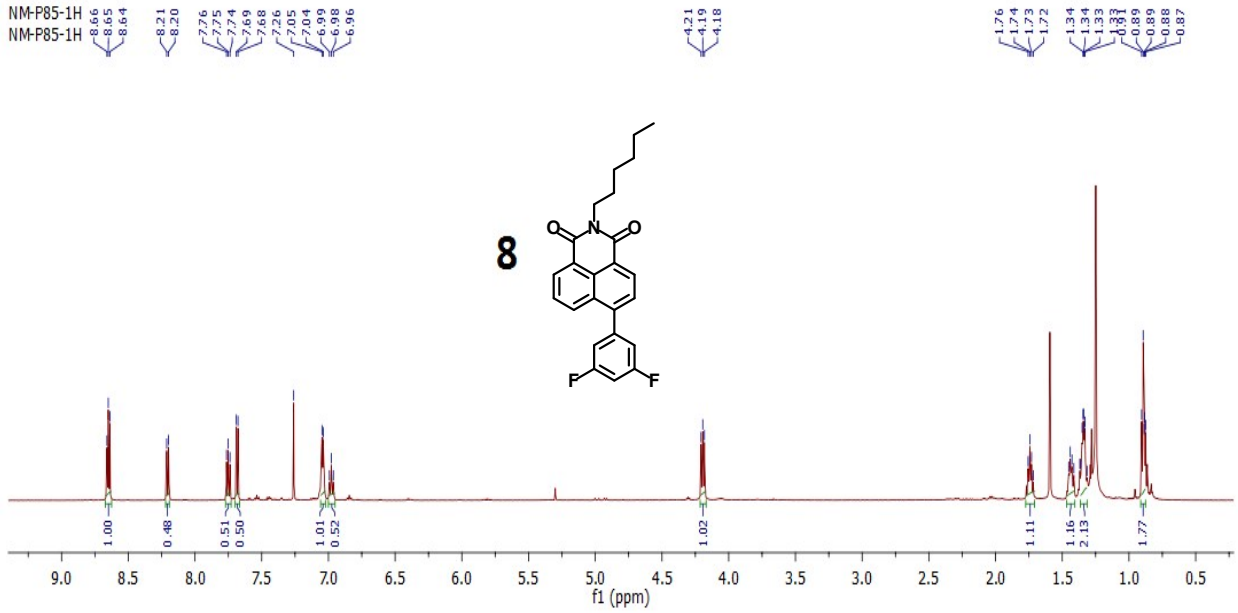
NM-P85-1H
NM-P85-1H
8
f1 (ppm)

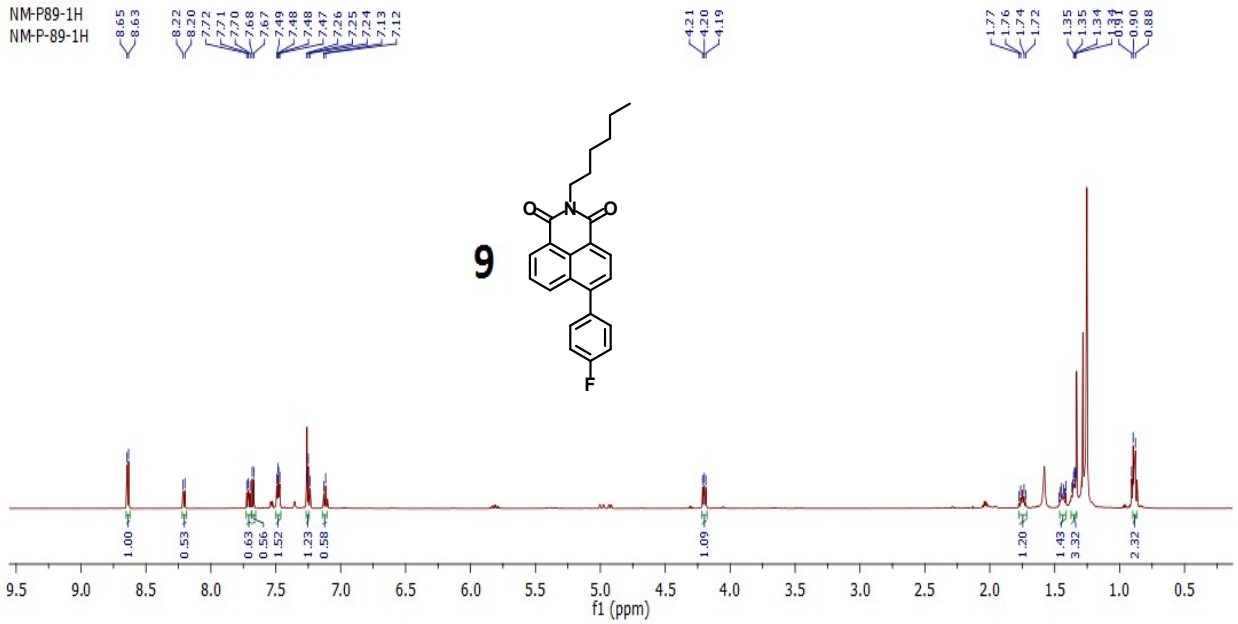
NM-P89-1H
NM-P-89-1H
9
F
f1 (ppm)

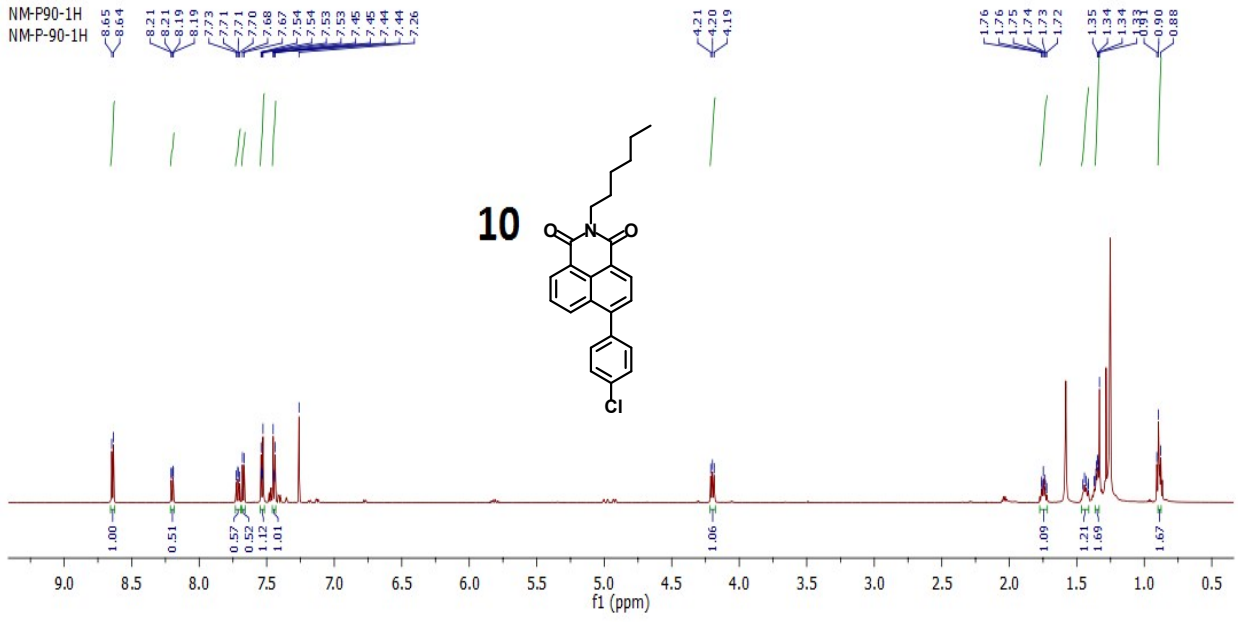
NM-P90-1H
NM-P-90-1H
10
Cl
f1 (ppm)

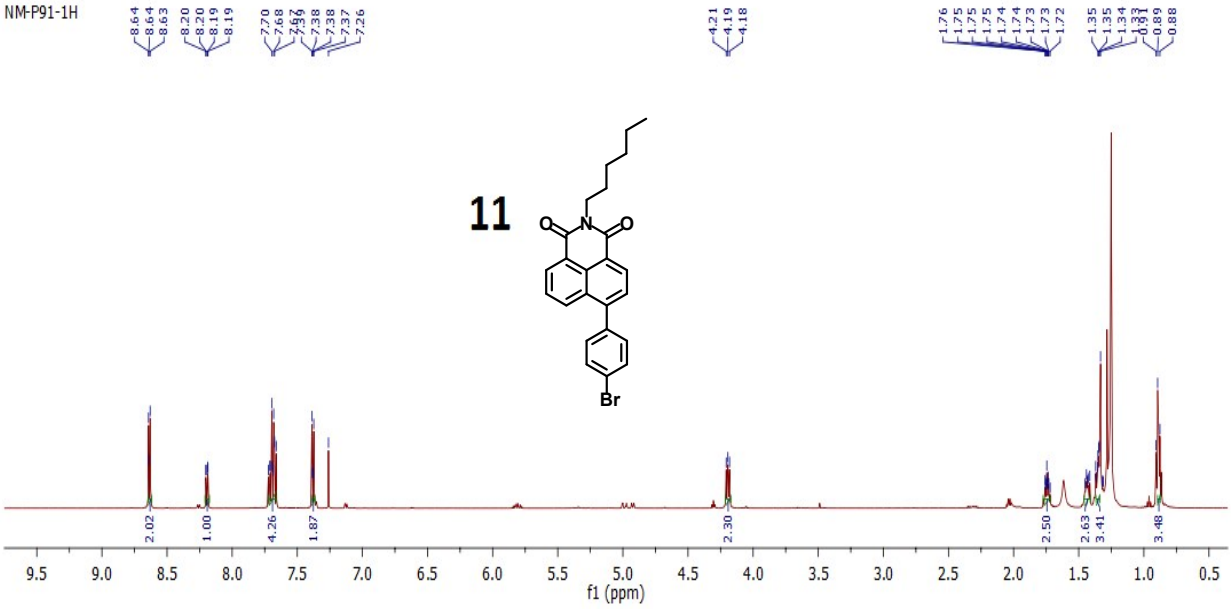
NM-P91-1H
11
Br
f1 (ppm)

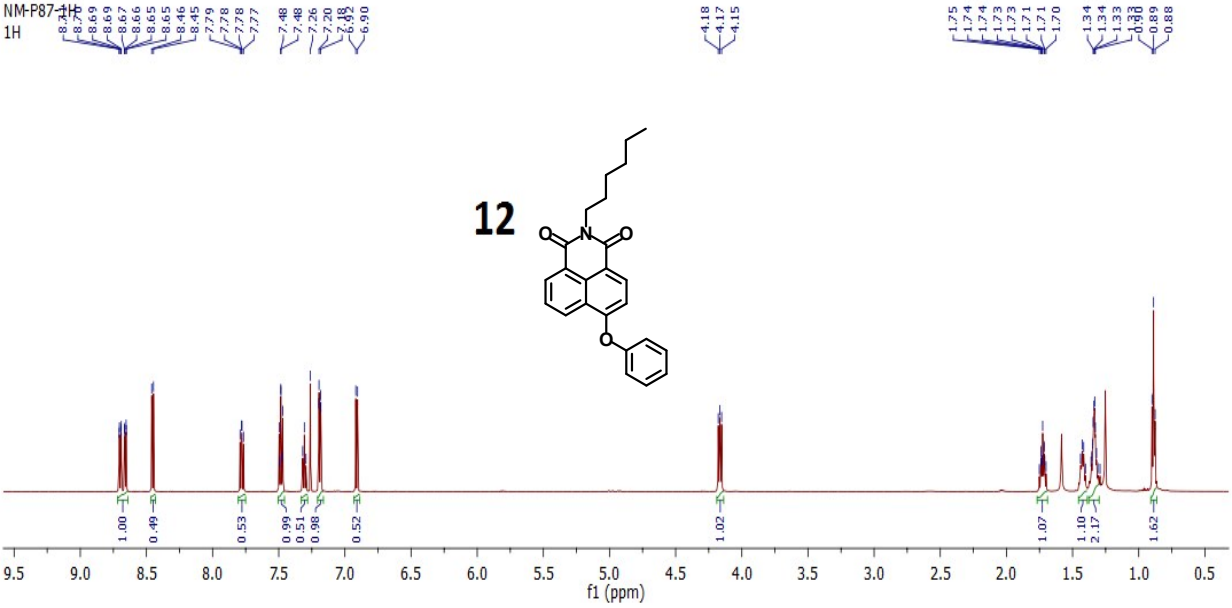
NM-P87-1H
1H
12
f1 (ppm)

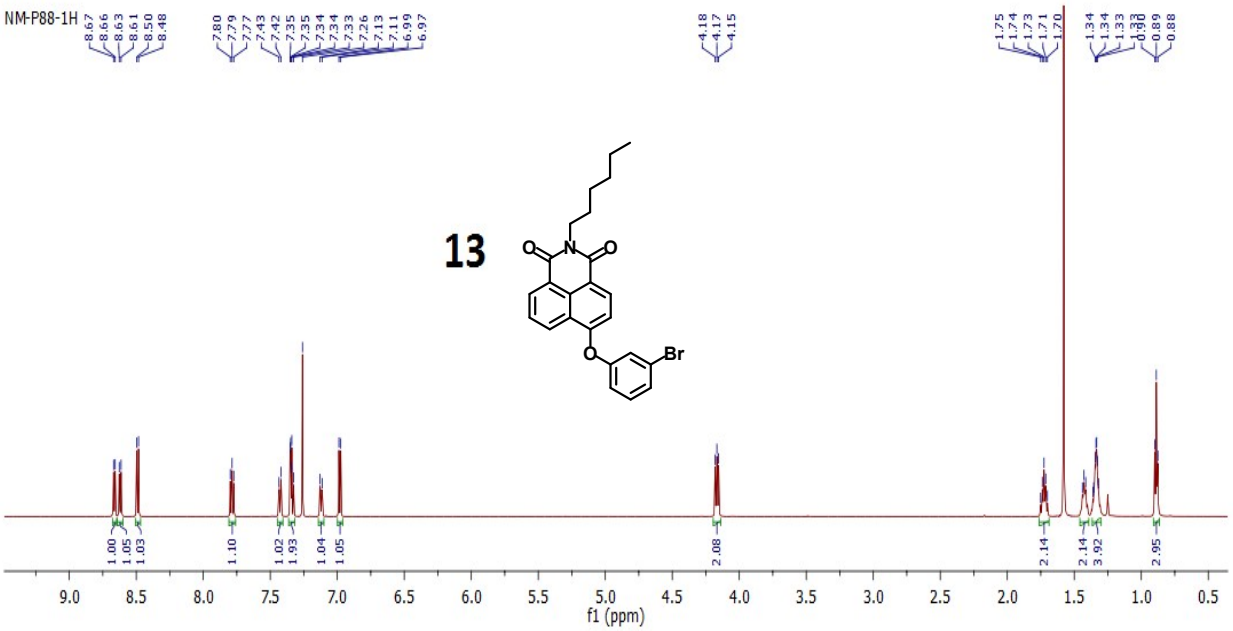
NM-P88-1H
13
Br
f1 (ppm)

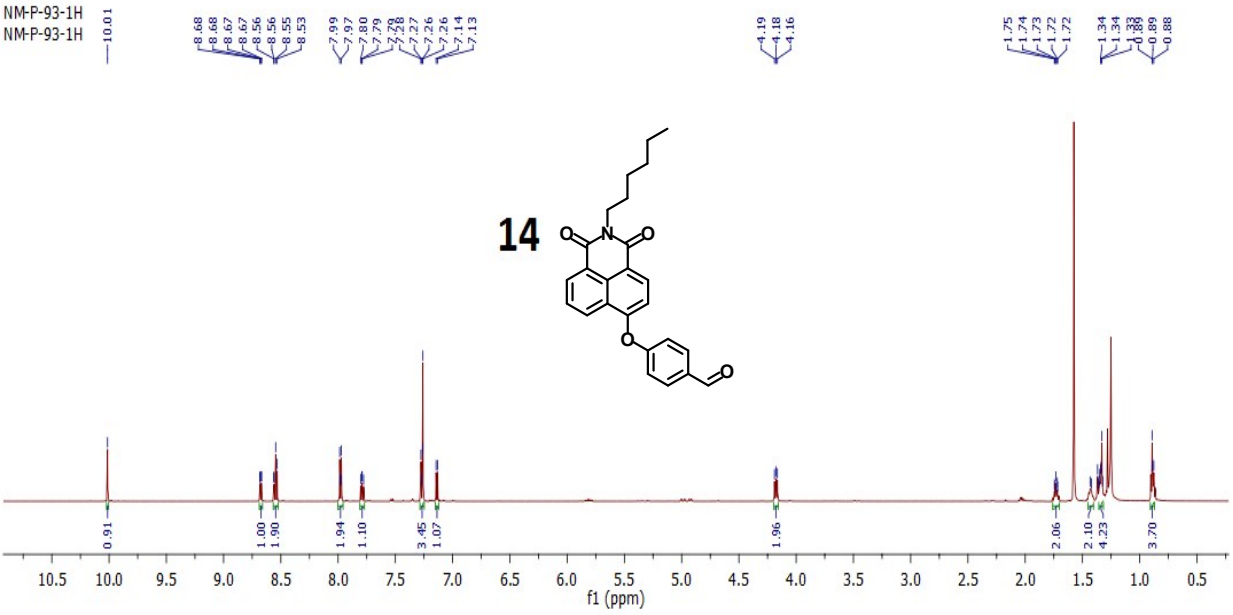
NM-P-93-1H
NM-P-93-1H
14
f1 (ppm)

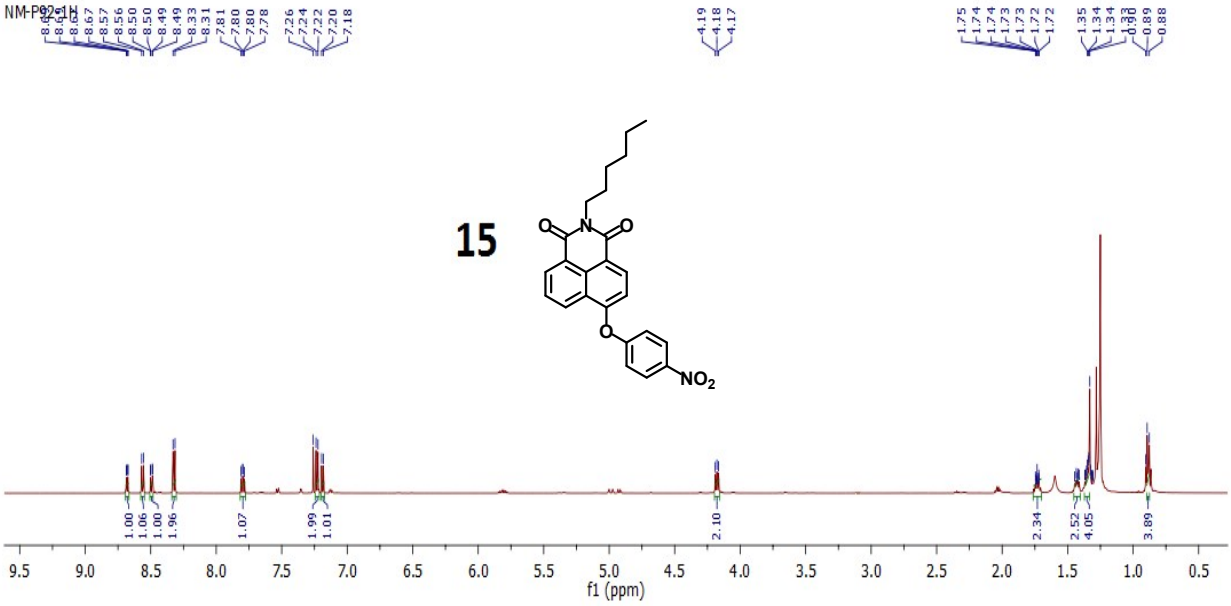
NM-P02-1H
15
NO2
1.00
1.06
1.00
1.96
1.07
1.99
1.01
2.10
2.34
2.52
4.05
3.89
f1 (ppm)

^{13}C NMR Spectra

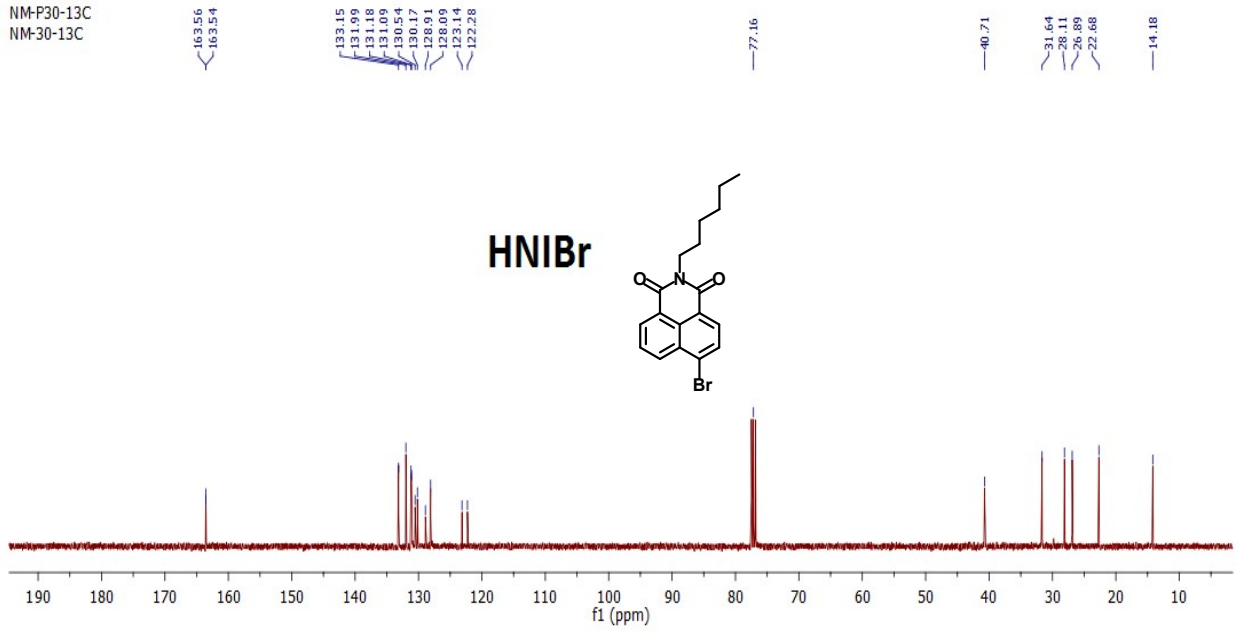

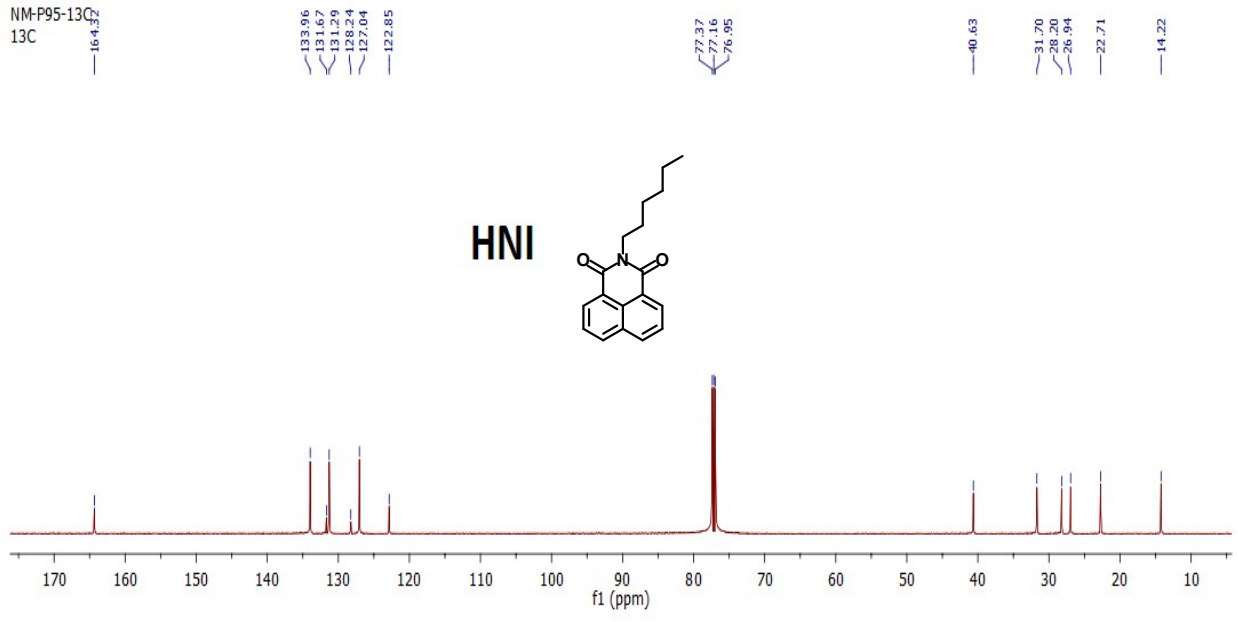

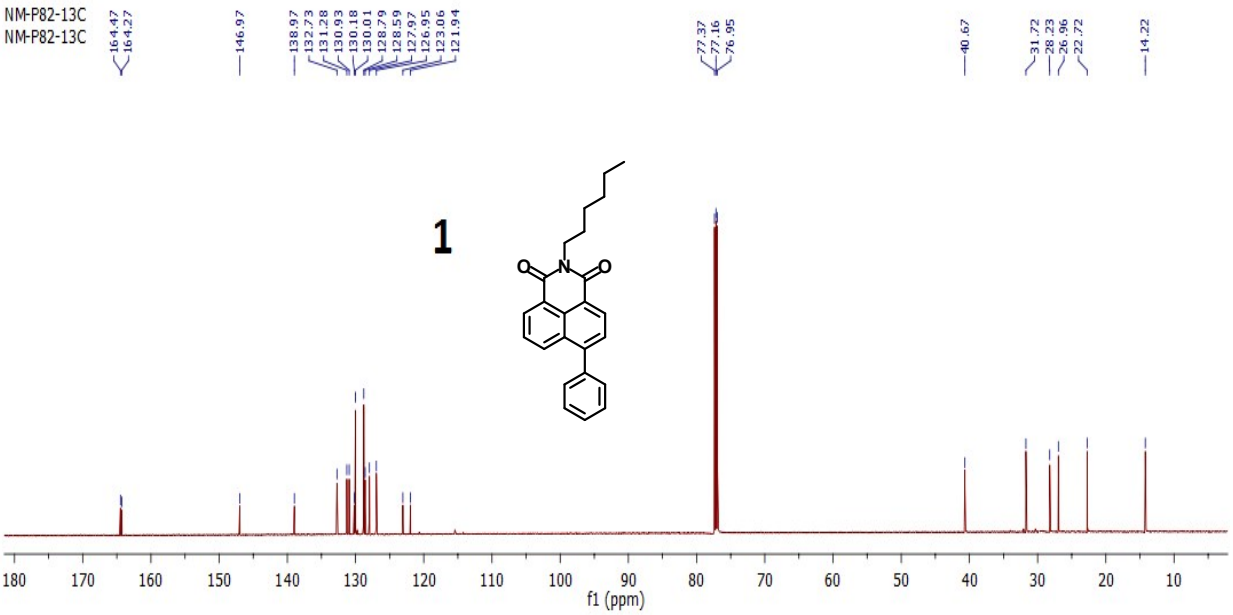
NM-P82-13C
NM-P82-13C
164.47
164.27
146.97
138.97
132.73
131.28
130.93
130.18
130.01
128.79
128.59
127.97
126.95
123.06
121.94
77.37
77.16
76.95
40.67
31.72
28.23
26.96
22.72
14.22
1
O
N
O
180
170
160
150
140
130
120
110
100
90
80
70
60
50
40
30
20
10
f1 (ppm)

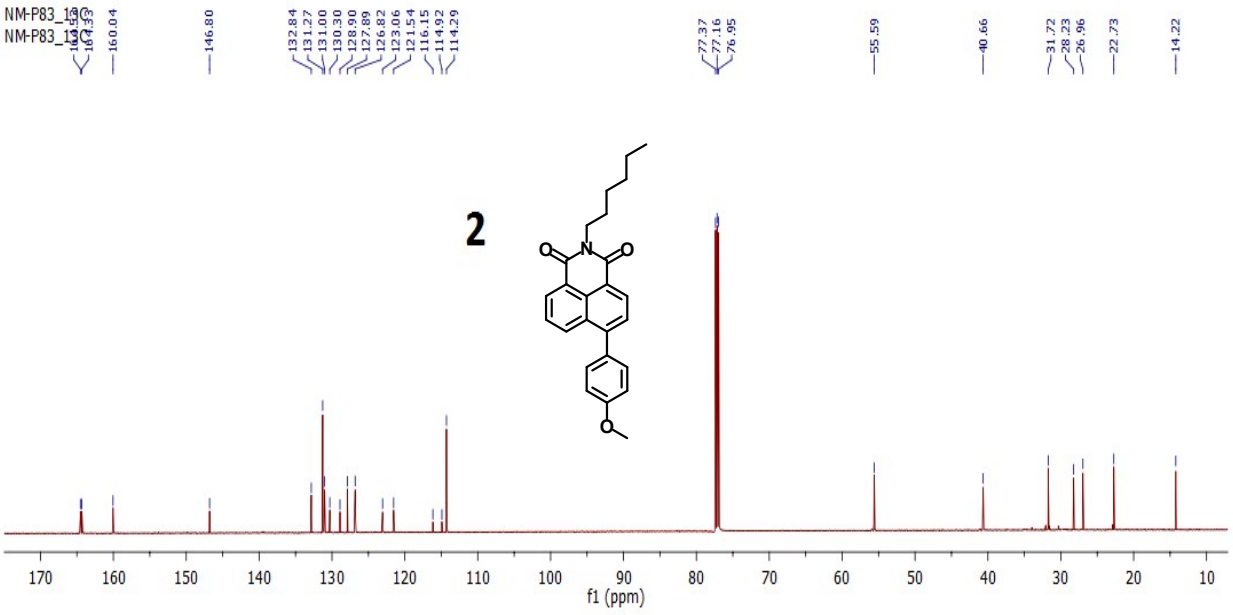
NM-P83_13C
NM-P83_13C
160.04
146.80
132.84
131.27
131.00
130.30
128.90
127.89
126.82
123.06
121.54
116.15
114.92
114.29
77.37
77.16
76.95
55.59
40.66
31.72
28.23
26.96
22.73
14.22
2
O
N
O
O
170
160
150
140
130
120
110
100
90
80
70
60
50
40
30
20
10
f1 (ppm)

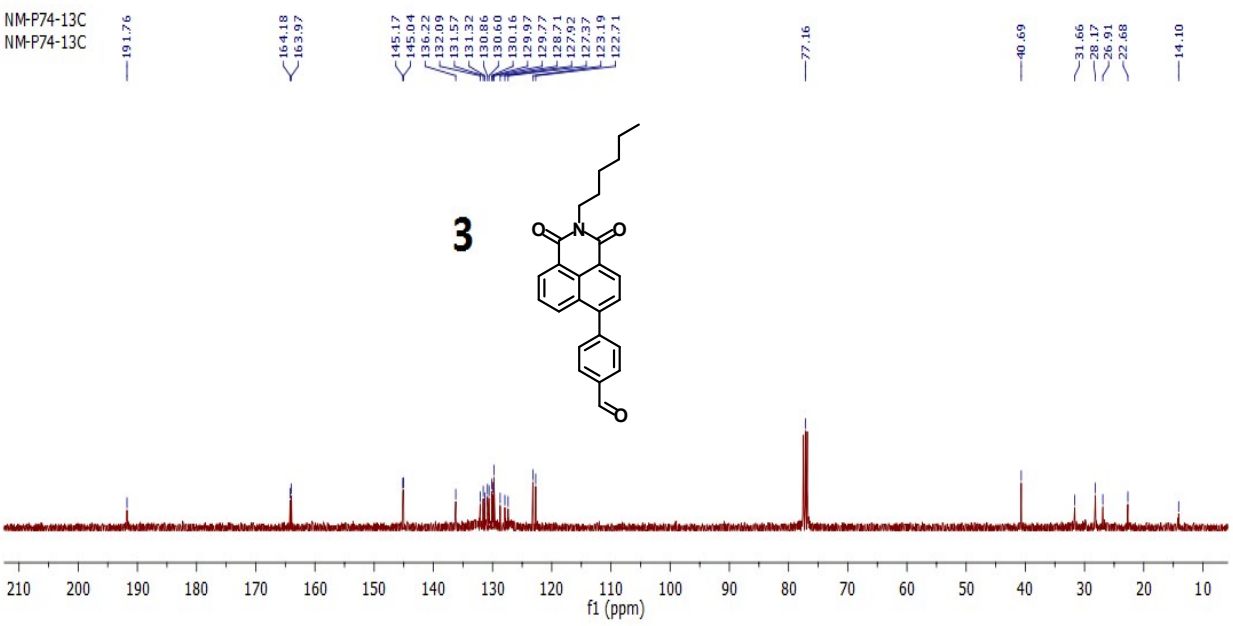
NM-P74-13C
NM-P74-13C
191.76
164.18
163.97
145.17
145.04
136.22
132.09
131.57
131.32
130.86
130.60
130.16
129.97
129.77
128.71
127.92
127.37
123.19
122.71
77.16
40.69
31.66
28.17
26.91
22.68
14.10
3
O
N
O
O
210 200 190 180 170 160 150 140 130 120 110 100 90 80 70 60 50 40 30 20 10
f1 (ppm)

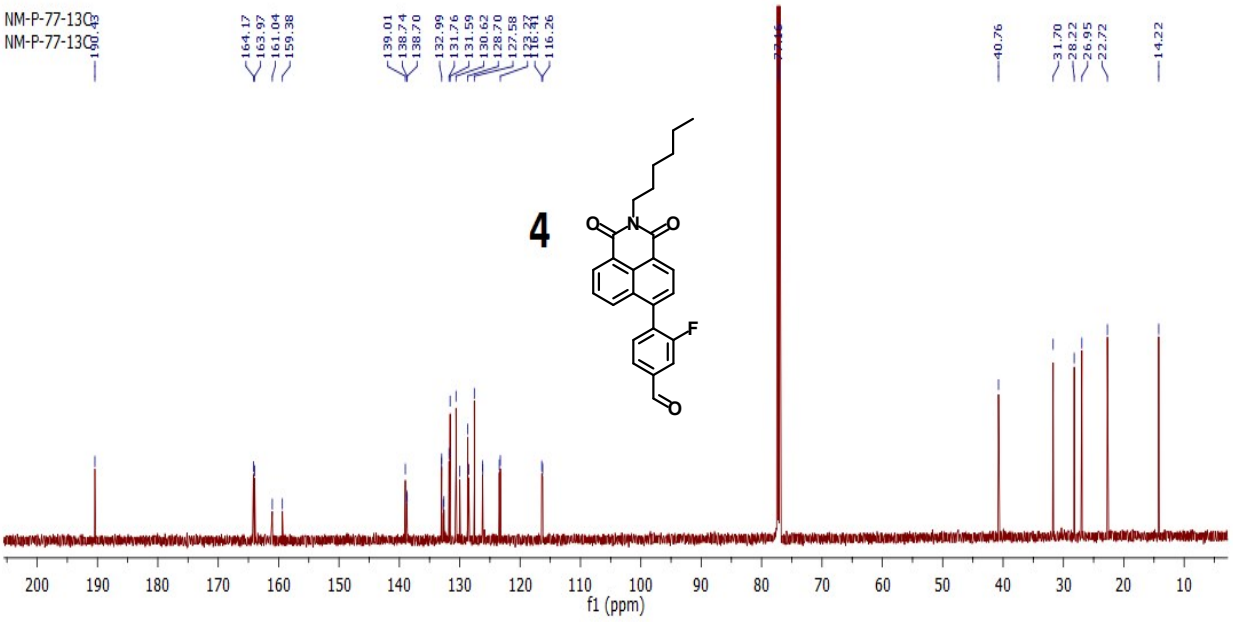
NM-P-77-13C
NM-P-77-13C
190.43
164.17
163.97
161.04
159.38
139.01
138.74
138.70
132.99
131.76
131.59
130.62
128.70
127.58
123.37
123.11
116.41
116.26
77.16
40.76
31.70
28.22
26.95
22.72
14.22
4
O
N
O
F
O
200 190 180 170 160 150 140 130 120 110 100 90 80 70 60 50 40 30 20 10
f1 (ppm)

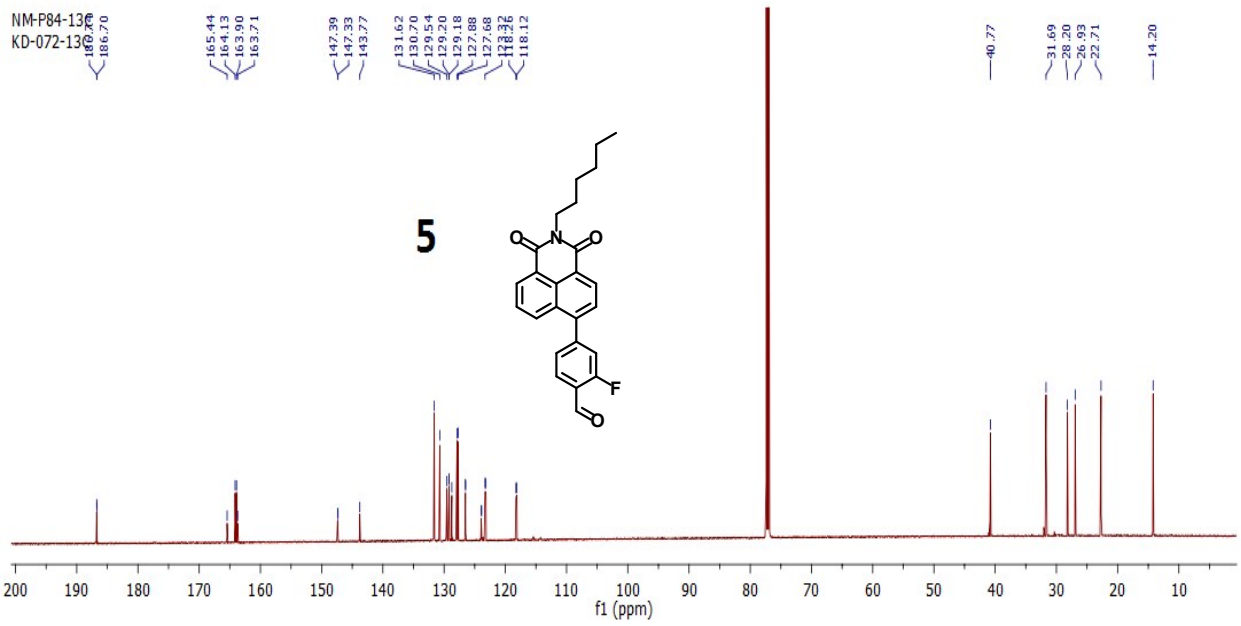
NM-P84-13C
KD-072-13C
186.70
165.44
164.13
163.90
163.71
147.39
147.33
143.77
131.62
130.70
129.54
129.20
129.18
127.88
127.68
118.12
40.77
31.69
28.20
26.93
22.71
14.20
5
F
O
200 190 180 170 160 150 140 130 120 110 100 90 80 70 60 50 40 30 20 10
f1 (ppm)

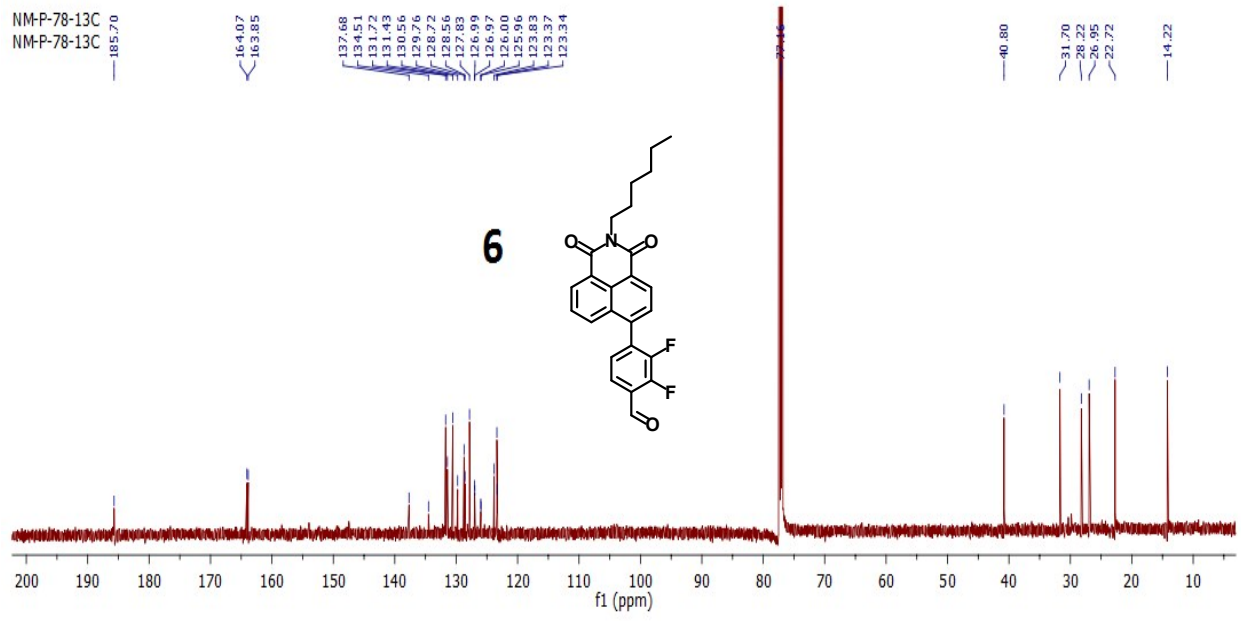
NM-P-78-13C
NM-P-78-13C
185.70
164.07
163.85
137.68
134.51
131.72
131.43
130.56
129.76
128.72
128.56
127.83
126.99
126.97
126.00
125.96
123.83
123.37
123.34
40.80
31.70
28.22
26.95
22.72
14.22
6
F
F
O
200 190 180 170 160 150 140 130 120 110 100 90 80 70 60 50 40 30 20 10
f1 (ppm)

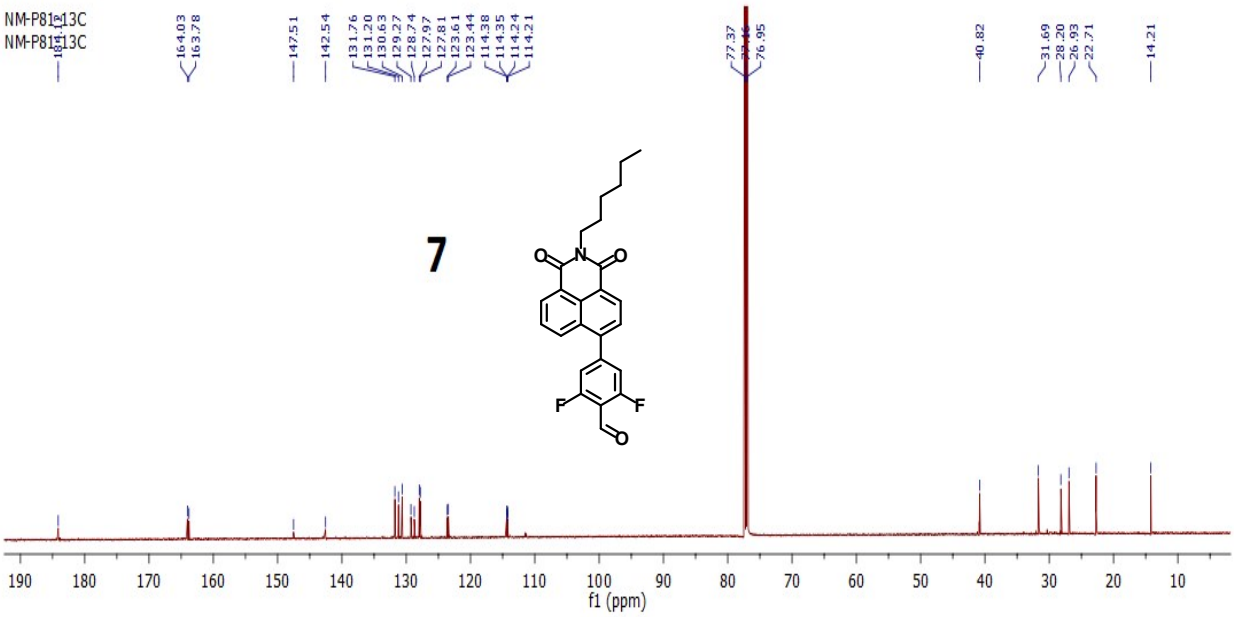
NM-P81-13C
NM-P81-13C
164.03
163.78
147.51
142.54
131.76
131.20
130.63
129.27
128.74
127.97
127.81
123.61
123.44
114.38
114.35
114.24
114.21
77.37
76.95
40.82
31.69
28.20
26.93
22.71
14.21
7
F
F
O
O
O
N
190
180
170
160
150
140
130
120
110
100
90
80
70
60
50
40
30
20
10
f1 (ppm)

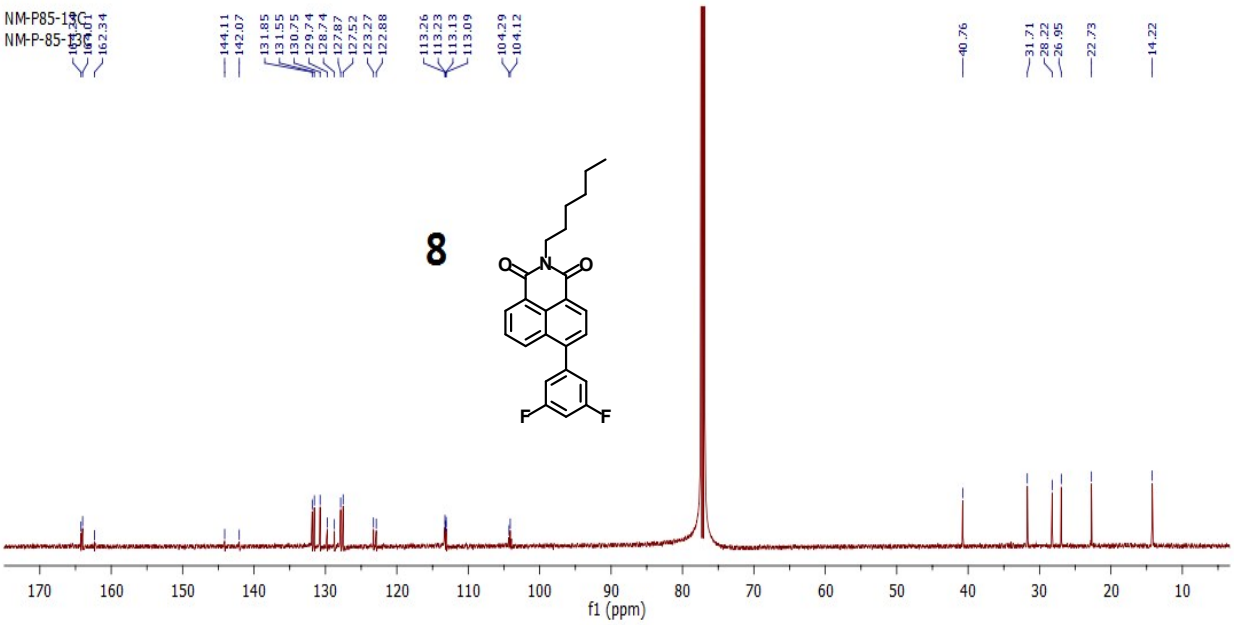
NM-P85-13C
NM-P-85-13C
162.34
144.11
142.07
131.85
131.55
130.75
129.74
128.74
127.87
127.52
123.27
122.88
113.26
113.23
113.13
113.09
104.29
104.12
40.76
31.71
28.22
26.95
22.73
14.22
8
F
F
O
O
O
N
170
160
150
140
130
120
110
100
90
80
70
60
50
40
30
20
10
f1 (ppm)

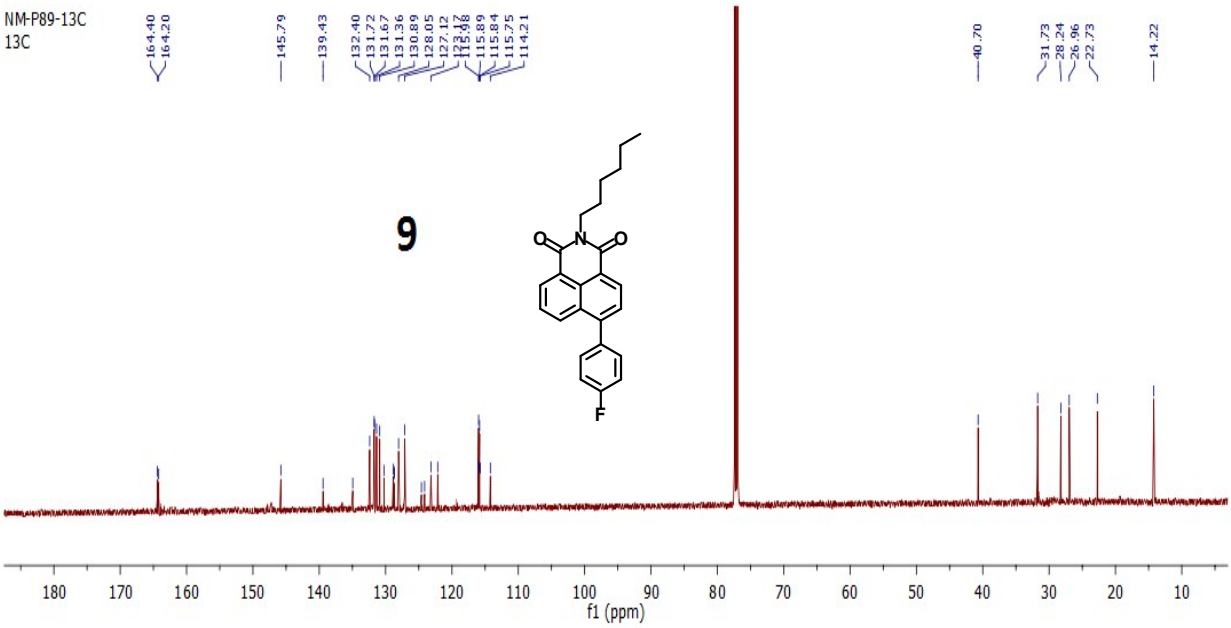
NM-P89-13C
13C
164.40
164.20
145.79
139.43
132.40
131.72
131.67
131.36
130.89
128.05
127.12
115.89
115.84
115.75
114.21
40.70
31.73
28.24
26.96
22.73
14.22
9
F
180
170
160
150
140
130
120
110
100
90
80
70
60
50
40
30
20
10
f1 (ppm)

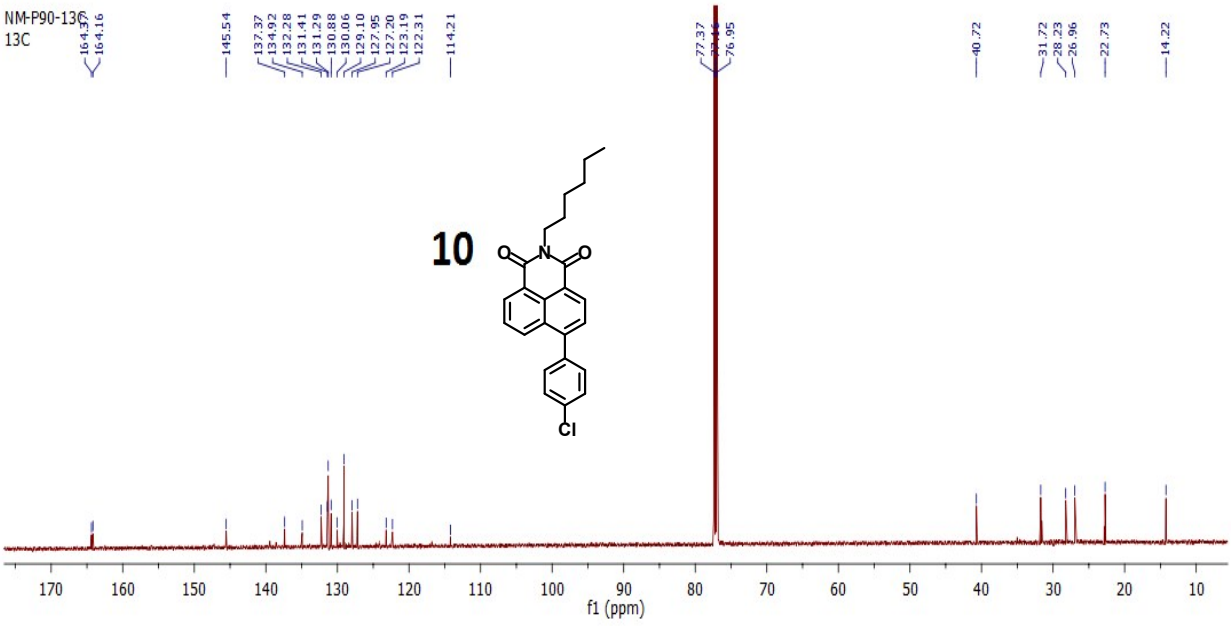
NM-P90-13C
13C
164.16
145.54
137.37
134.92
132.28
131.41
131.29
130.88
130.06
129.10
127.95
127.20
123.19
122.31
114.21
77.37
76.95
40.72
31.72
28.23
26.96
22.73
14.22
10
Cl
170
160
150
140
130
120
110
100
90
80
70
60
50
40
30
20
10
f1 (ppm)

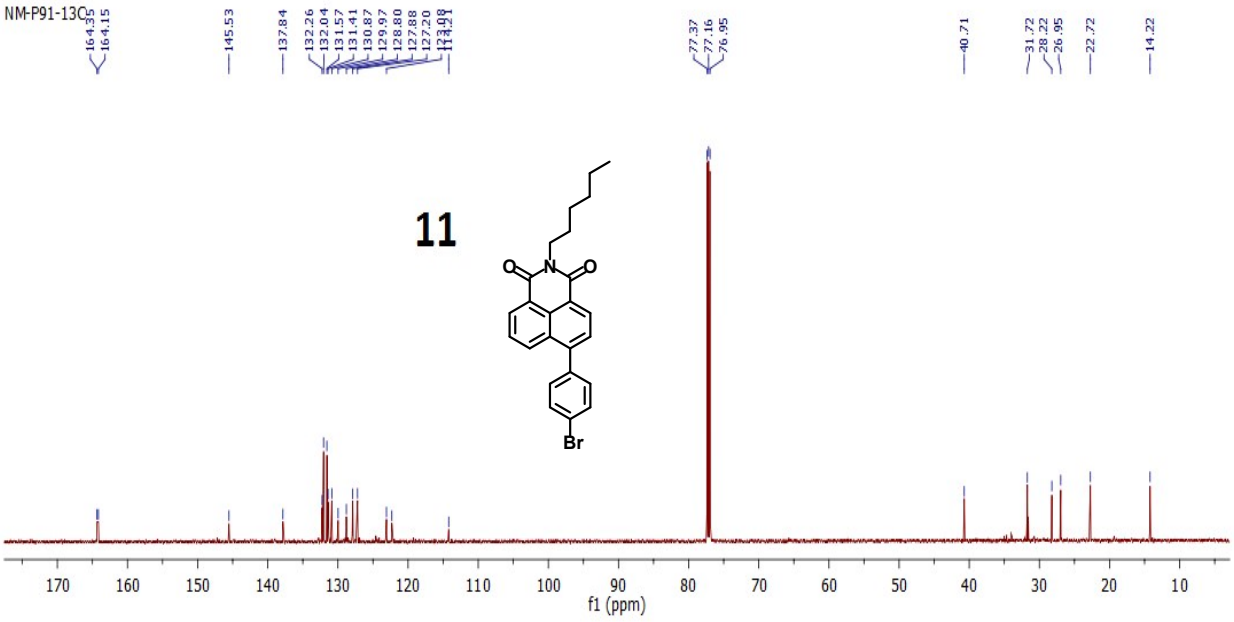
NM-P91-13C
164.35
164.15
145.53
137.84
132.26
132.04
131.57
131.41
130.87
129.97
128.80
127.88
127.20
123.08
114.21
77.37
77.16
76.95
40.71
31.72
28.22
26.95
22.72
14.22
11
Br
170
160
150
140
130
120
110
100
90
80
70
60
50
40
30
20
10
f1 (ppm)

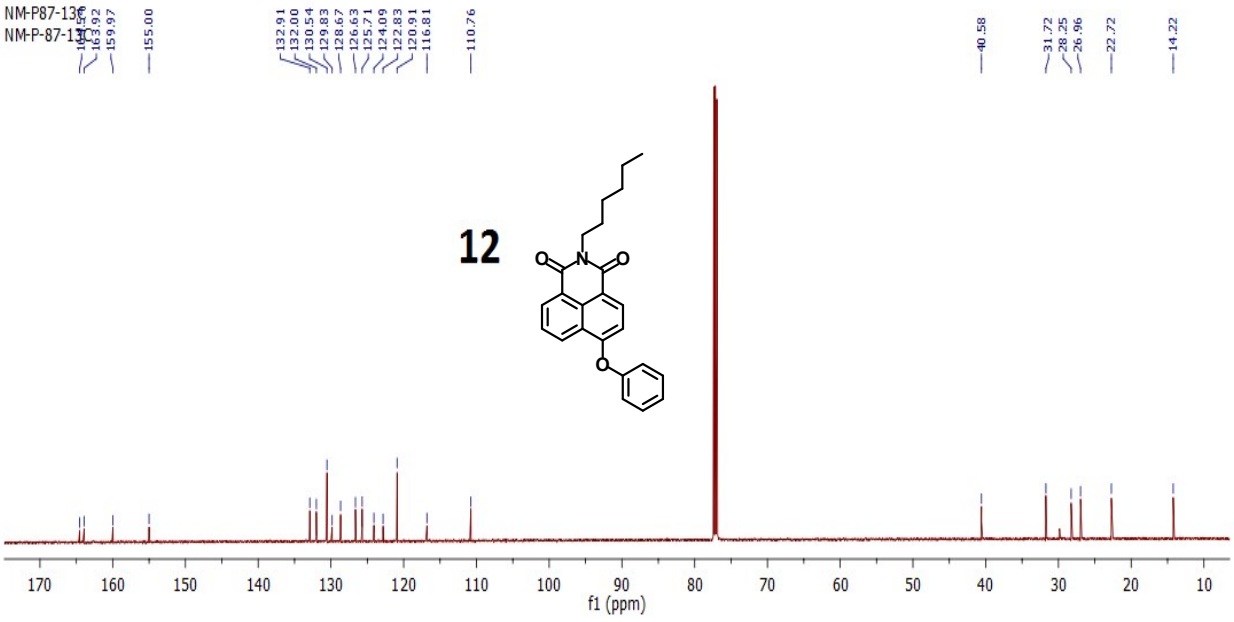
NM-P87-13C
NM-P-87-13C
164.54
163.92
159.97
155.00
132.91
132.00
130.54
129.83
128.67
126.63
125.71
124.09
122.83
120.91
116.81
110.76
40.58
31.72
28.25
26.96
22.72
14.22
12
O
170
160
150
140
130
120
110
100
90
80
70
60
50
40
30
20
10
f1 (ppm)

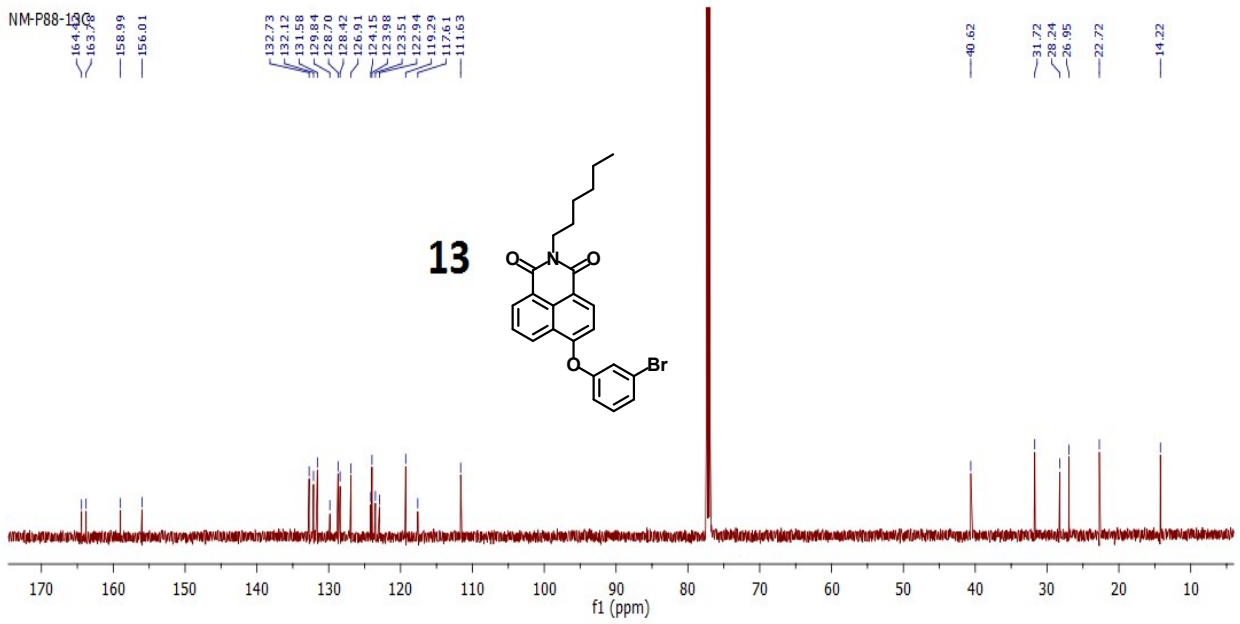
NM-P88-13C
164.44
163.78
158.99
156.01
132.73
132.12
131.58
129.84
128.70
128.42
126.91
124.15
123.98
123.51
122.94
119.29
117.61
111.63
40.62
31.72
28.24
26.95
22.72
14.22
13
Br
170
160
150
140
130
120
110
100
90
80
70
60
50
40
30
20
10
f1 (ppm)

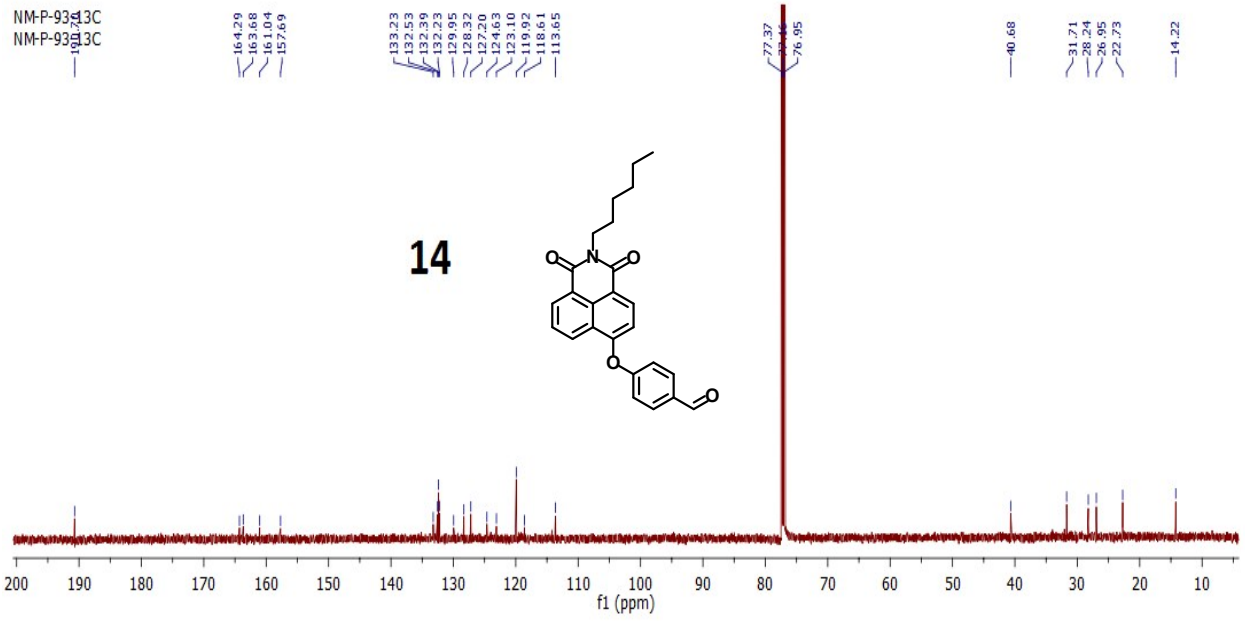
NM-P-93-13C
NM-P-93-13C
164.29
163.68
161.04
157.69
133.23
132.53
132.39
132.23
129.95
128.32
127.20
124.63
123.10
119.92
118.61
113.65
77.37
76.95
40.68
31.71
28.24
26.95
22.73
14.22
14
200
190
180
170
160
150
140
130
120
110
100
90
80
70
60
50
40
30
20
10
f1 (ppm)

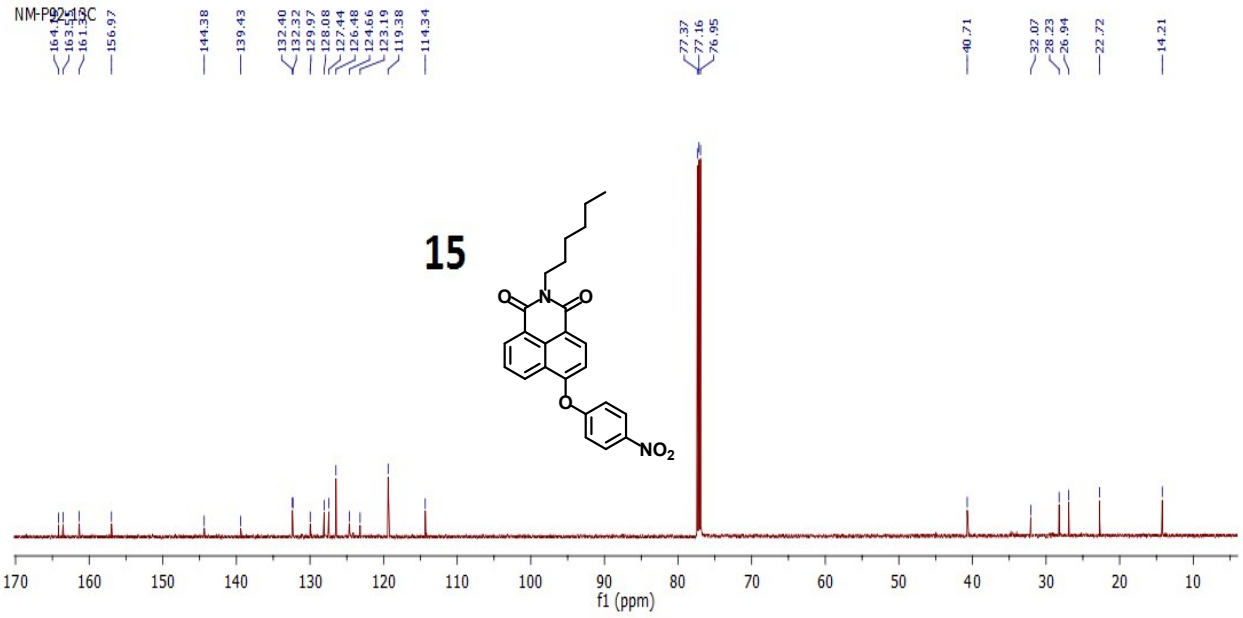
NM-P92-13C
164.82
163.51
161.32
156.97
144.38
139.43
132.40
132.32
129.97
128.08
127.44
126.48
124.66
123.19
119.38
114.34
77.37
77.16
76.95
40.71
32.07
28.23
26.94
22.72
14.21
15
O
N
O
O
NO2
170
160
150
140
130
120
110
100
90
80
70
60
50
40
30
20
10
f1 (ppm)

^{19}F NMR Spectra

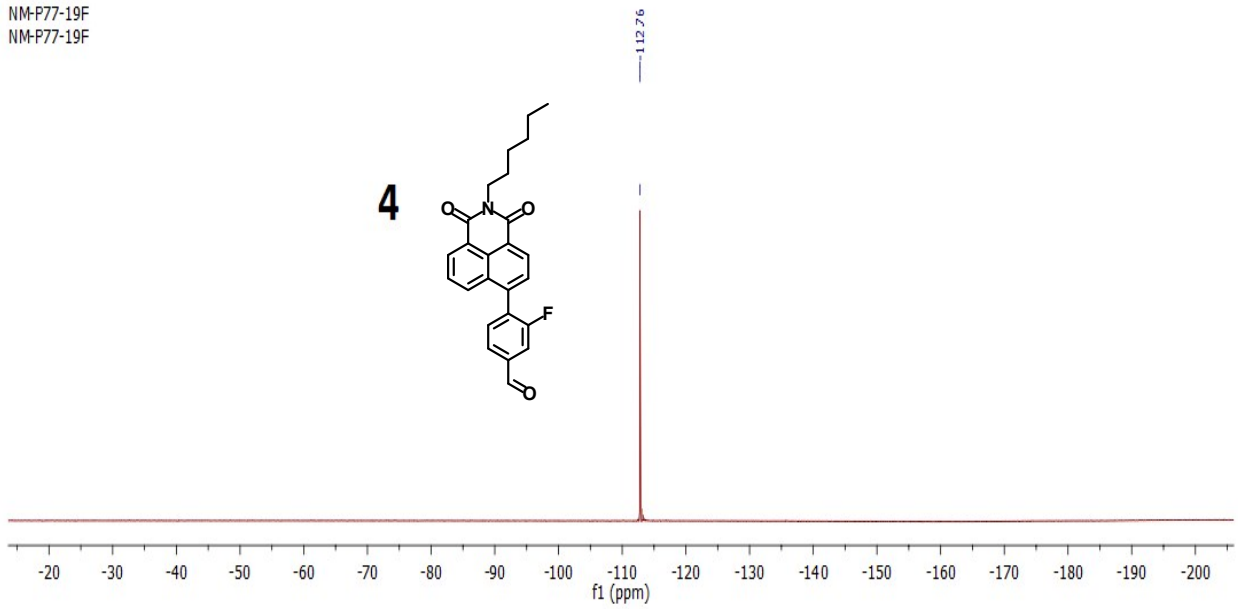

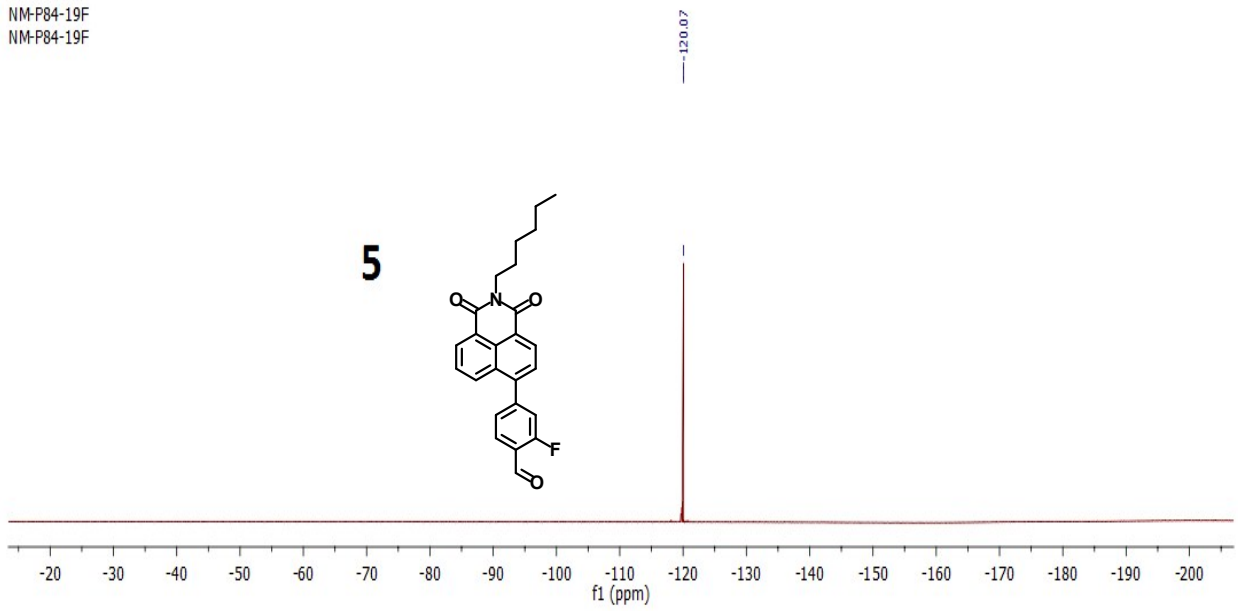

NM-P78-19F
NM-P78-19F

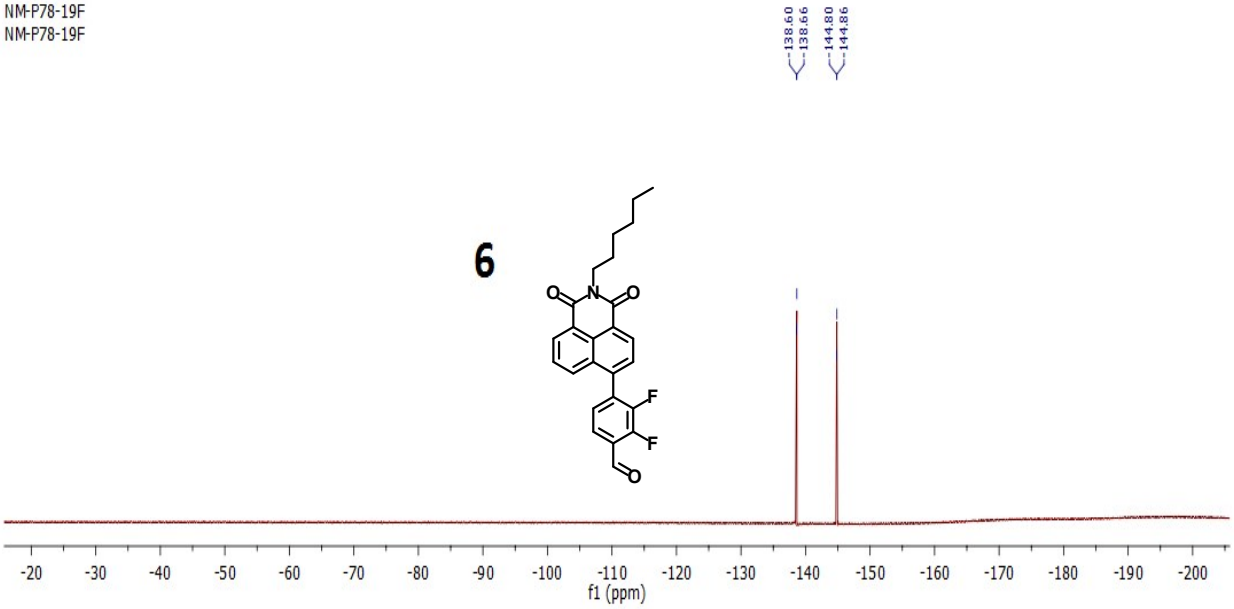

NM-P81-19F
NM-P81-19F

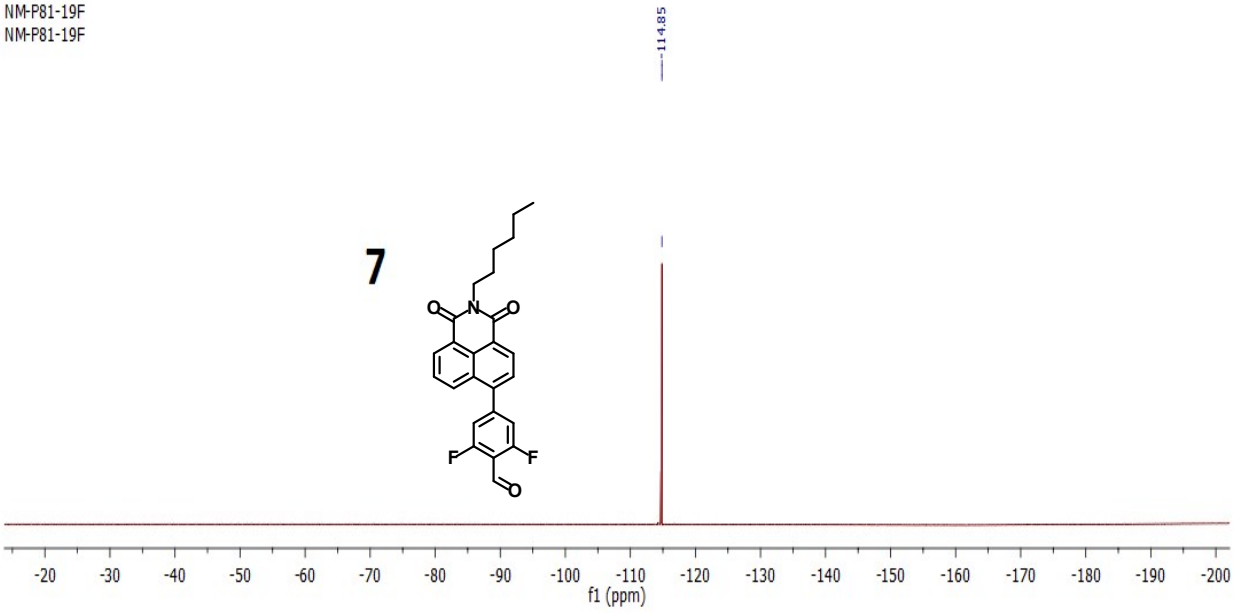

NM-P85-19F
NM-P85-19F

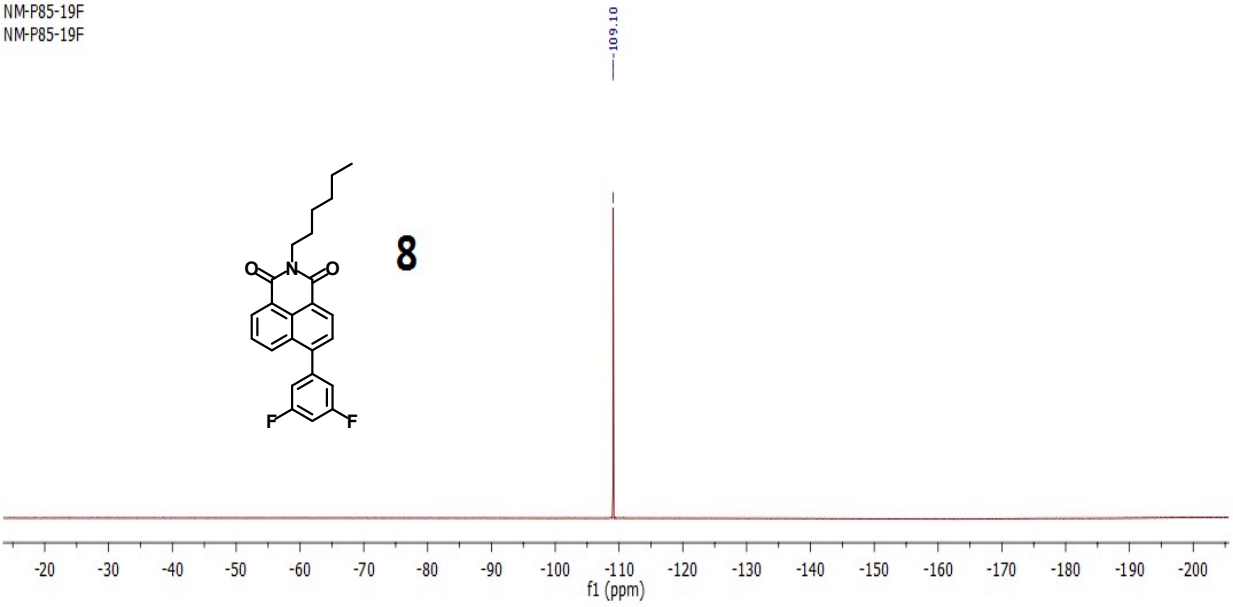

NM-P89-19F
NM-P89-19F

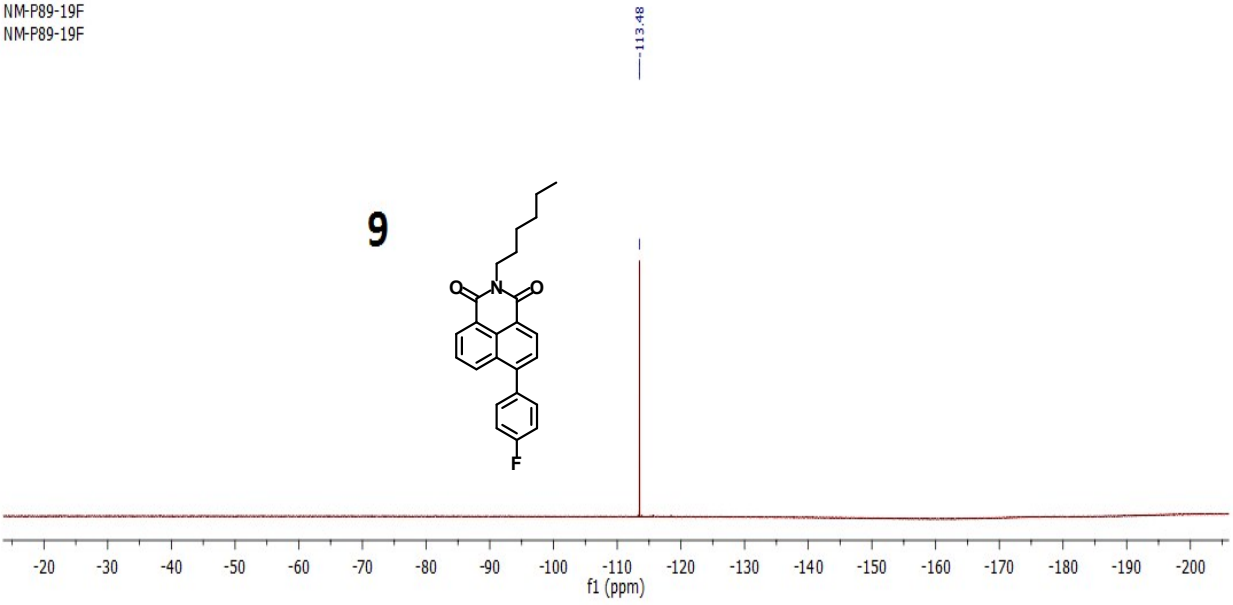

Mass Spectra

Sample Name	**Position**	**Instrument Name**	**User Name**
Inj Vol	**InjPosition**	**SampleType**	**IRM Calibration Status**
Data Filename	**ACQ Method**	**Comment**	**Acquired Time**

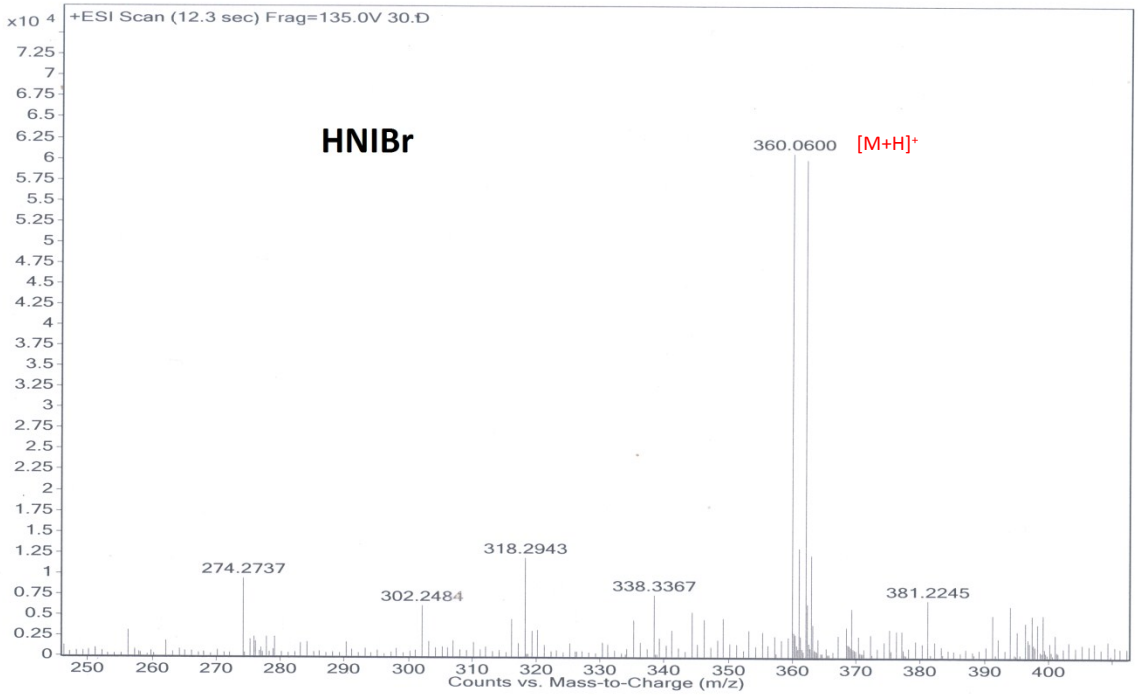

Sample Name	PM-95	**Position**	Vial 1	**Instrument Name**	Instrument 1	**User Name**	
Inj Vol	-1	**InjPosition**		**SampleType**	Sample	**IRM Calibration Status**	All Ions Missed
Data Filename	PM-95.d	**ACQ Method**		**Comment**		**Acquired Time**	1/17/2018 3:37:47 PM

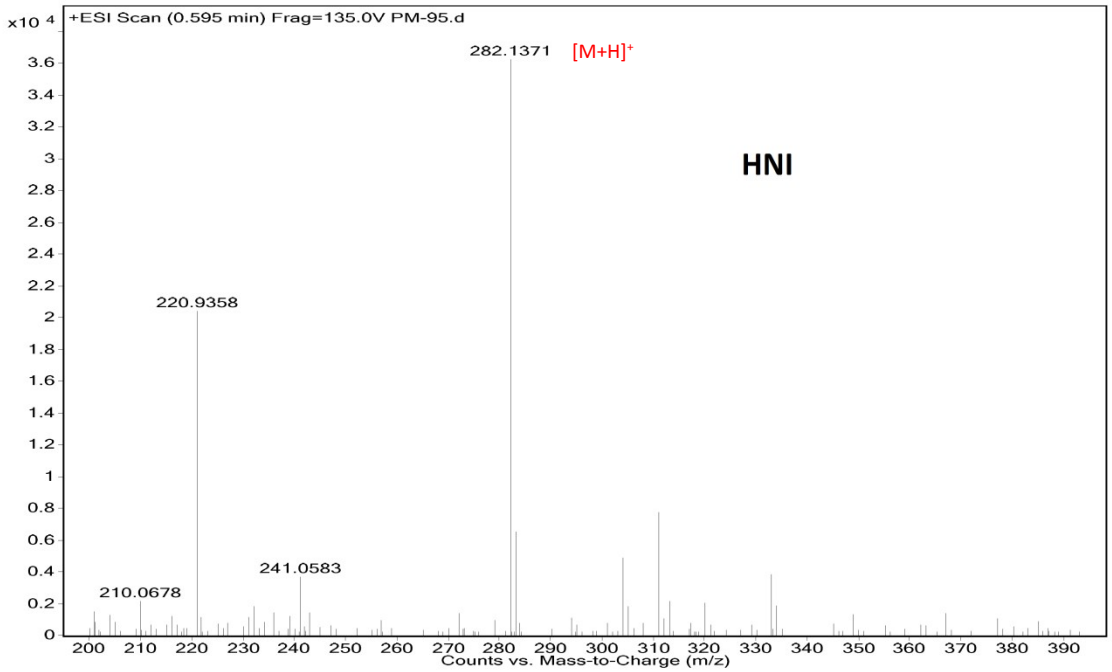

Sample Name	Unavailable	**Position**	Unavailable	**Instrument Name**	Unavailable	**User Name**	Unavailable
Inj Vol	Unavailable	**InjPosition**	Unavailable	**SampleType**	Unavailable	**IRM Calibration Status**	Some Ions Missed
Data Filename	P82.d	**ACQ Method**		**Comment**	Sample information is unavailable	**Acquired Time**	Unavailable

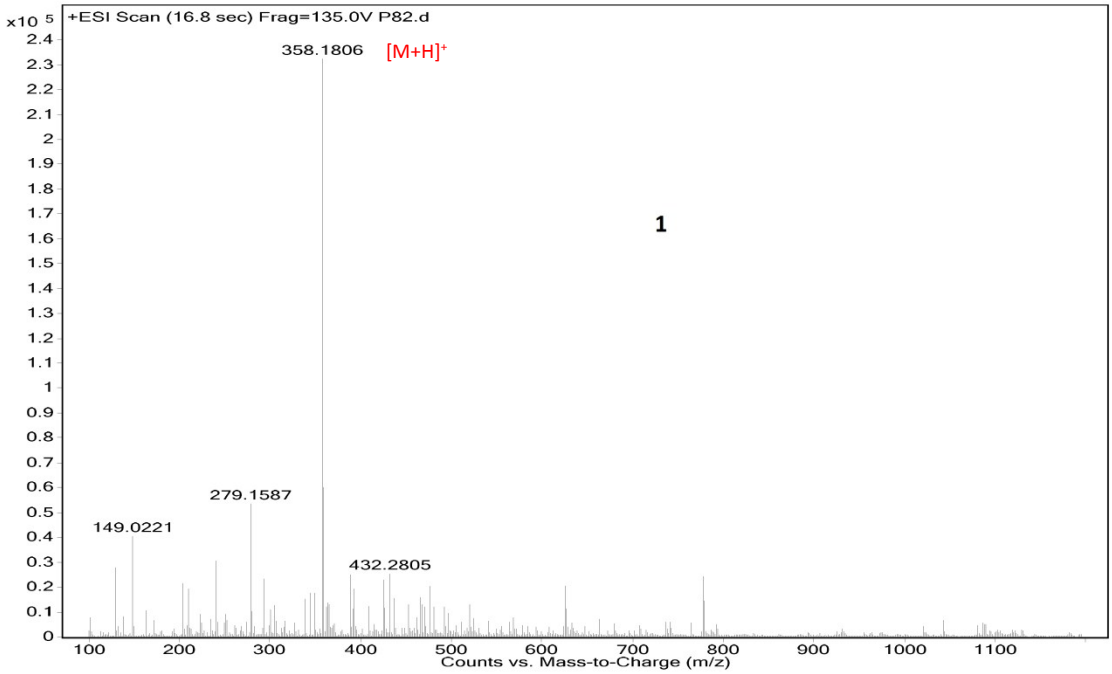

Sample Name	Unavailable	**Position**	Unavailable	**Instrument Name**	Unavailable	**User Name**	Unavailable
Inj Vol	Unavailable	**InjPosition**	Unavailable	**SampleType**	Unavailable	**IRM Calibration Status**	Some Ions Missed
Data Filename	P83.d	**ACQ Method**		**Comment**	Sample information is unavailable	**Acquired Time**	Unavailable

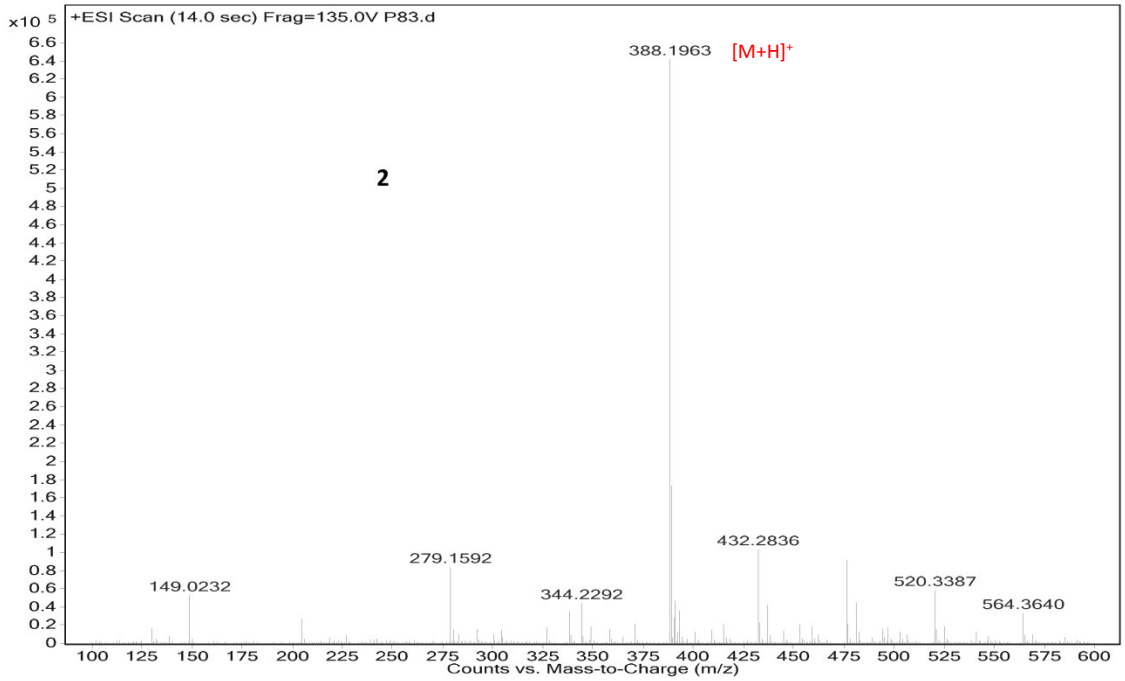

Sample Name	Unavailable	**Position**	Unavailable	**Instrument Name**	Unavailable	**User Name**	Unavailable
Inj Vol	Unavailable	**InjPosition**	Unavailable	**SampleType**	Unavailable	**IRM Calibration Status**	All Ions Missed
Data Filename	P74-1.d	**ACQ Method**		**Comment**	Sample information is unavailable	**Acquired Time**	Unavailable

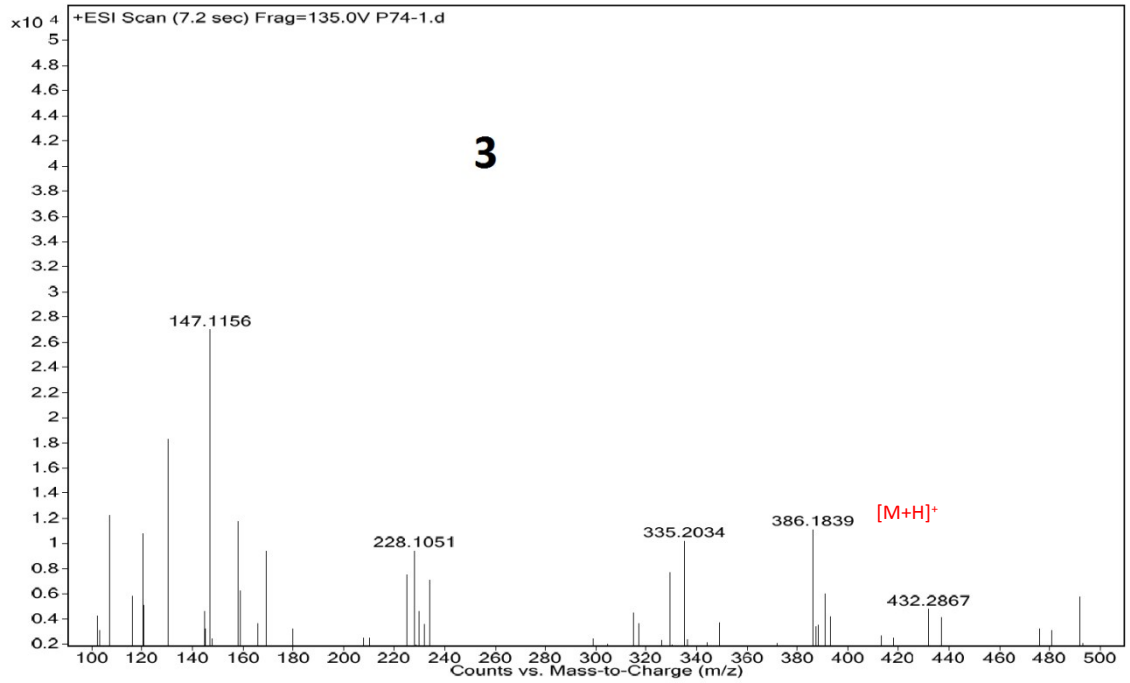

Sample Name	**Position**	**Instrument Name**	**User Name**
Inj Vol	**InjPosition**	**SampleType**	**IRM Calibration Status**
Data Filename	**ACQ Method**	**Comment**	**Acquired Time**

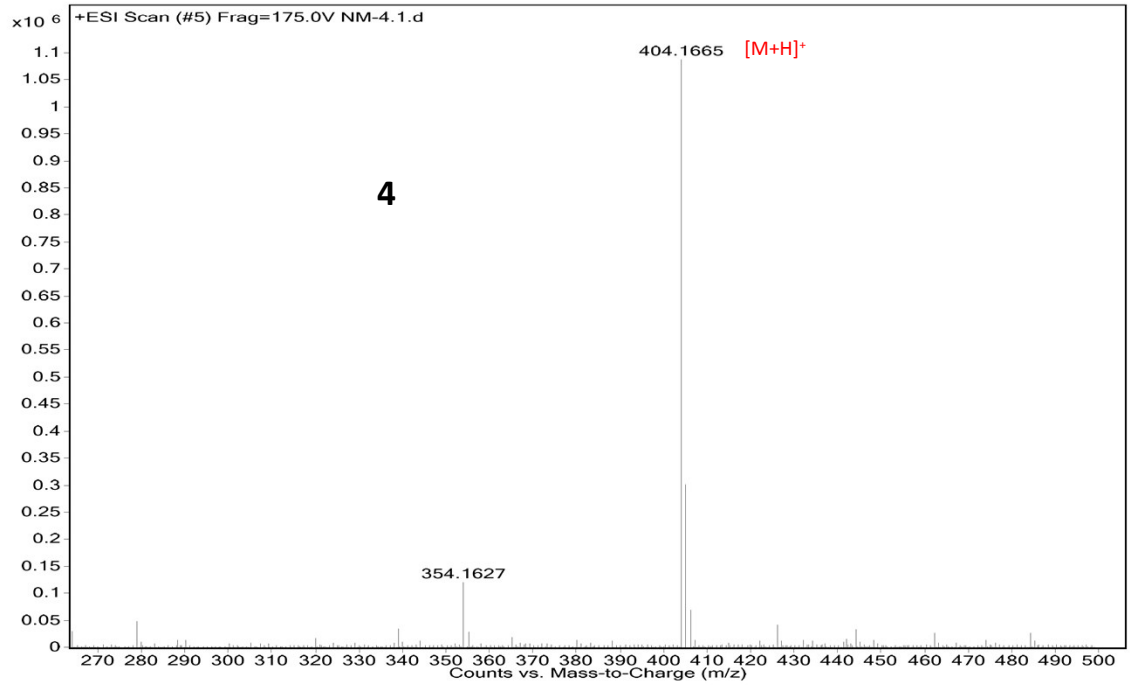

Sample Name	P84	**Position**	Vial 1	**Instrument Name**	Instrument 1	**User Name**	
Inj Vol	0	**InjPosition**		**SampleType**	Sample	**IRM Calibration Status**	Some Ions Missed
Data Filename	P84.d	**ACQ Method**		**Comment**		**Acquired Time**	8/7/2017 3:52:15 PM

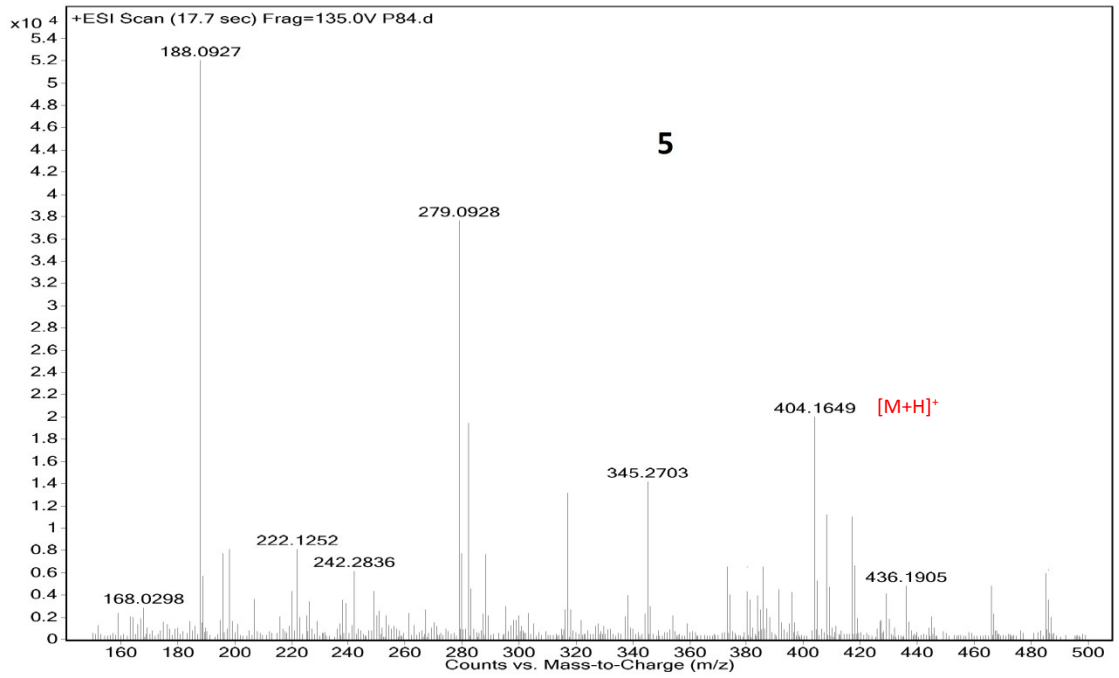

Sample Name	P-78	**Position**	Vial 1	**Instrument Name**	Instrument 1	**User Name**	
Inj Vol	0	**InjPosition**		**SampleType**	Sample	**IRM Calibration Status**	All Ions Missed
Data Filename	P-78.d	**ACQ Method**		**Comment**		**Acquired Time**	6/5/2017 12:02:28 PM

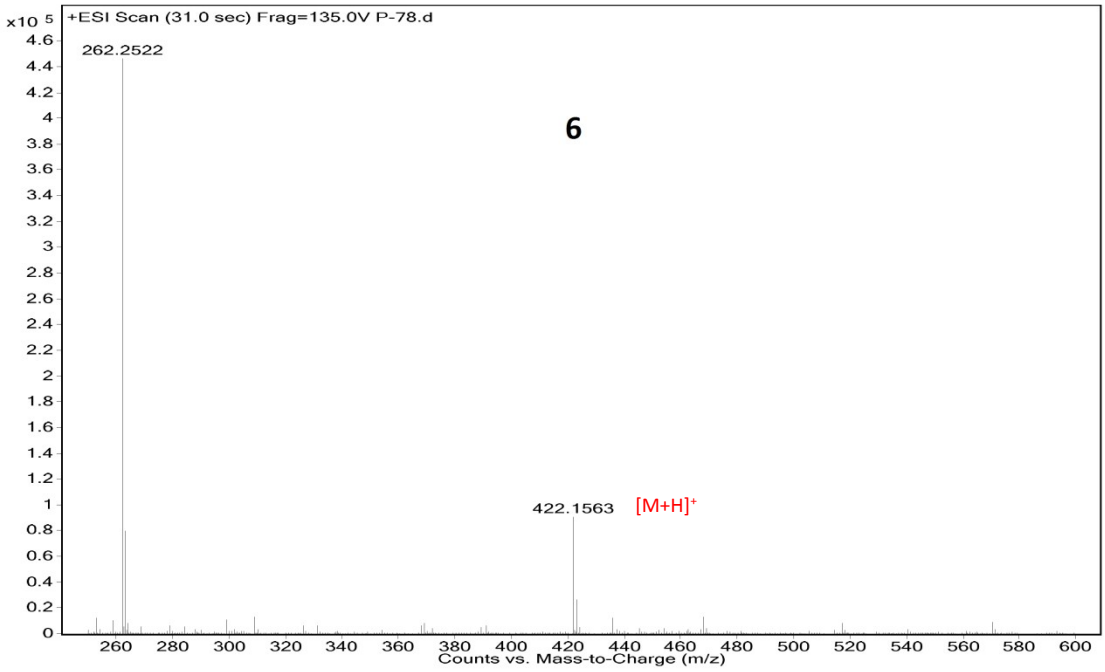

Sample Name	**Position**	**Instrument Name**	**User Name**
Inj Vol	**InjPosition**	**SampleType**	**IRM Calibration Status**
Data Filename	**ACQ Method**	**Comment**	**Acquired Time**

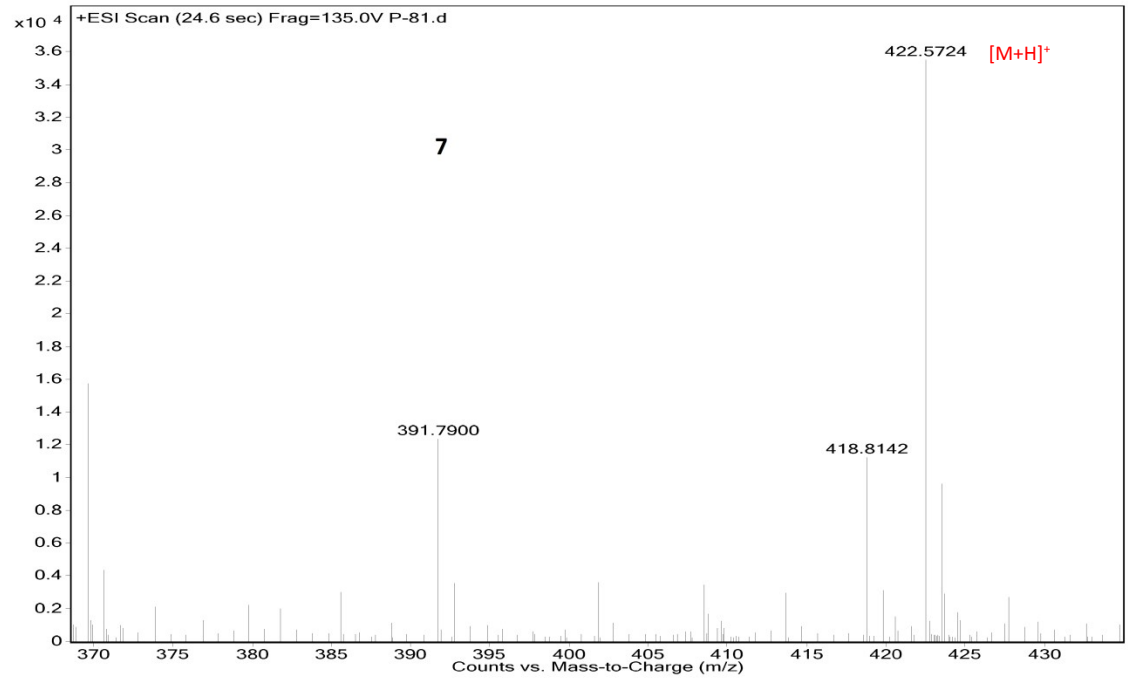

Sample Name	P85	**Position**	Vial 1	**Instrument Name**	Instrument 1	**User Name**	
Inj Vol	0	**InjPosition**		**SampleType**	Sample	**IRM Calibration Status**	Some Ions Missed
Data Filename	P85.d	**ACQ Method**		**Comment**		**Acquired Time**	8/7/2017 3:54:17 PM

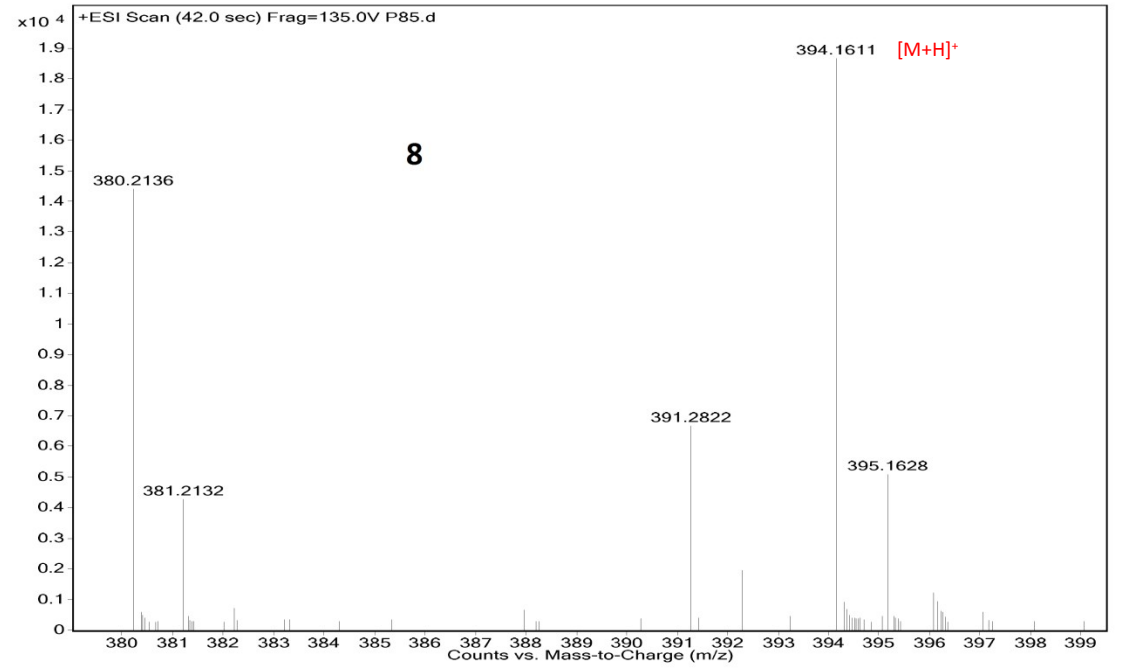

Sample Name	Unavailable	**Position**	Unavailable	**Instrument Name**	Unavailable	**User Name**	Unavailable
Inj Vol	Unavailable	**InjPosition**	Unavailable	**SampleType**	Unavailable	**IRM Calibration Status**	Some Ions Missed
Data Filename	P-89.d	**ACQ Method**		**Comment**	Sample information is unavailable	**Acquired Time**	Unavailable

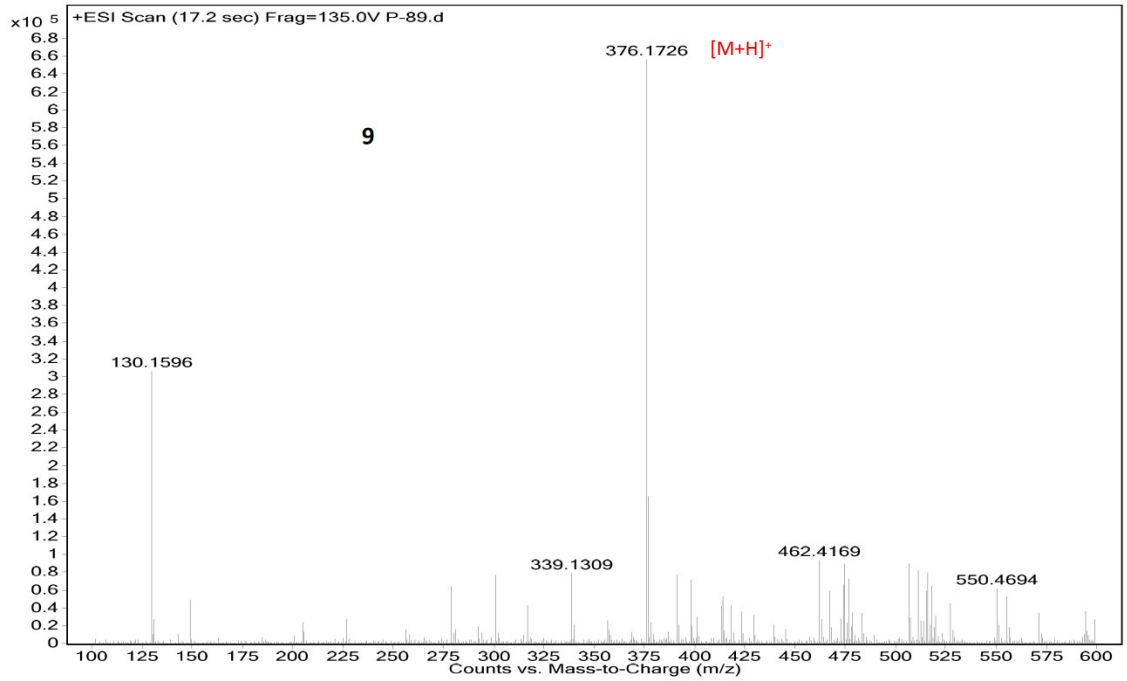

Sample Name	Unavailable	**Position**	Unavailable	**Instrument Name**	Unavailable	**User Name**	Unavailable
Inj Vol	Unavailable	**InjPosition**	Unavailable	**SampleType**	Unavailable	**IRM Calibration Status**	Some Ions Missed
Data Filename	P-90.d	**ACQ Method**		**Comment**	Sample information is unavailable	**Acquired Time**	Unavailable

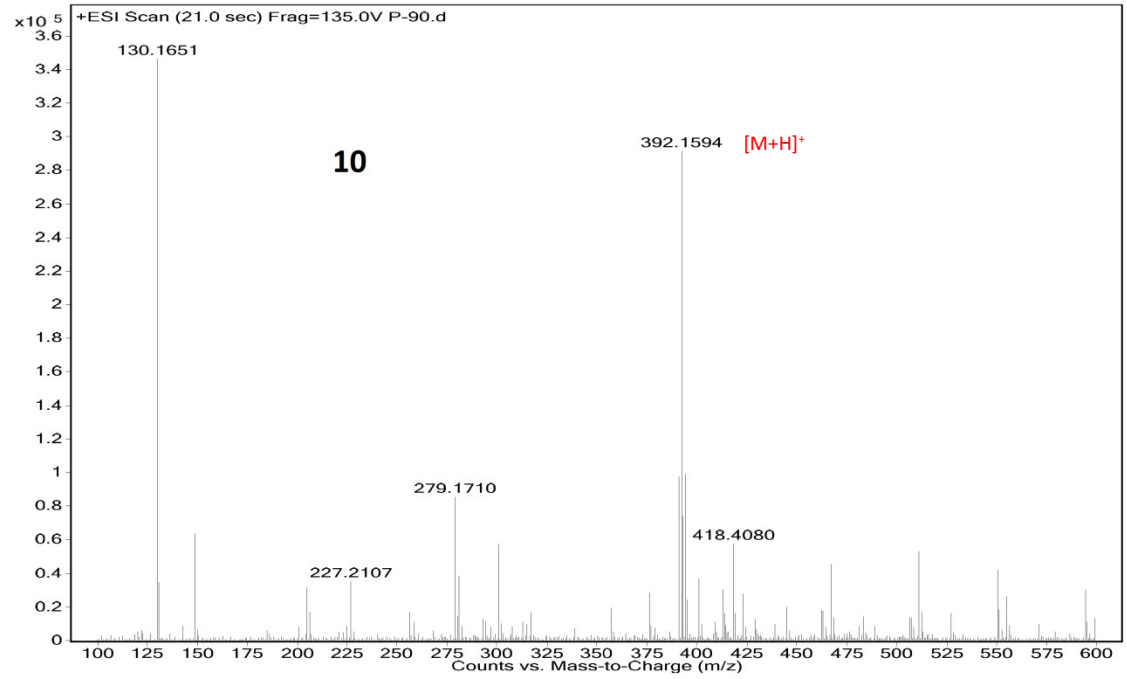

Sample Name	Unavailable	**Position**	Unavailable	**Instrument Name**	Unavailable	**User Name**	Unavailable
Inj Vol	Unavailable	**InjPosition**	Unavailable	**SampleType**	Unavailable	**IRM Calibration Status**	Some Ions Missed
Data Filename	P-91.d	**ACQ Method**		**Comment**	Sample information is unavailable	**Acquired Time**	Unavailable

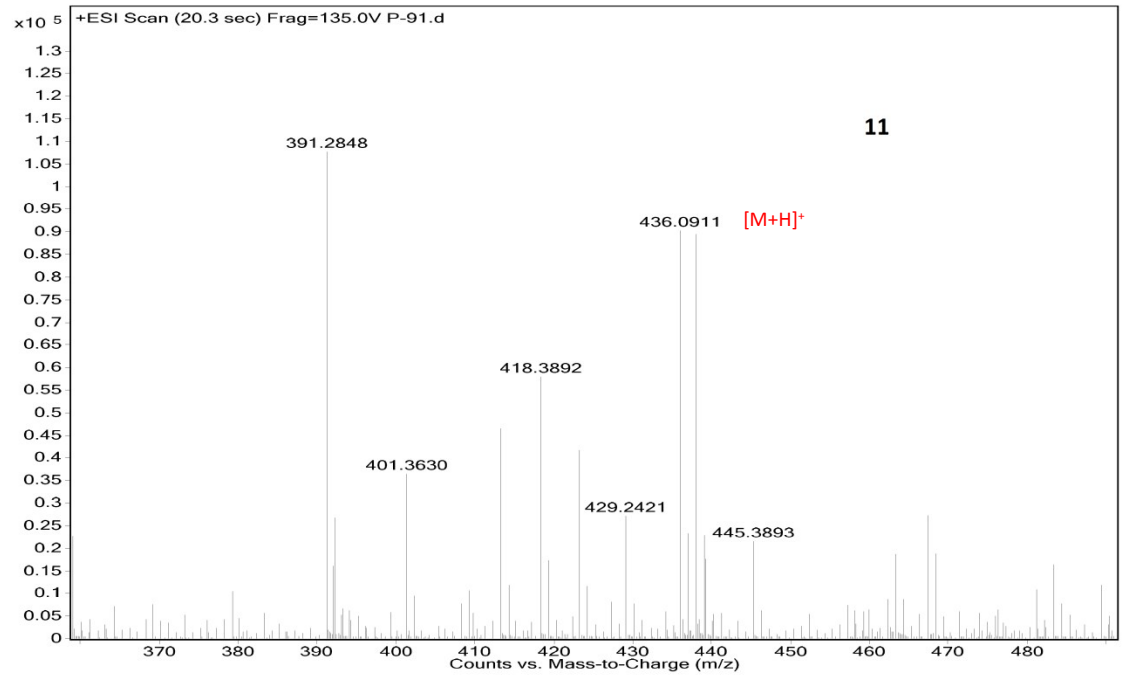

Sample Name	Unavailable	**Position**	Unavailable	**Instrument Name**	Unavailable	**User Name**	Unavailable
Inj Vol	Unavailable	**InjPosition**	Unavailable	**SampleType**	Unavailable	**IRM Calibration Status**	All Ions Missed
Data Filename	P87.d	**ACQ Method**		**Comment**	Sample information is unavailable	**Acquired Time**	Unavailable

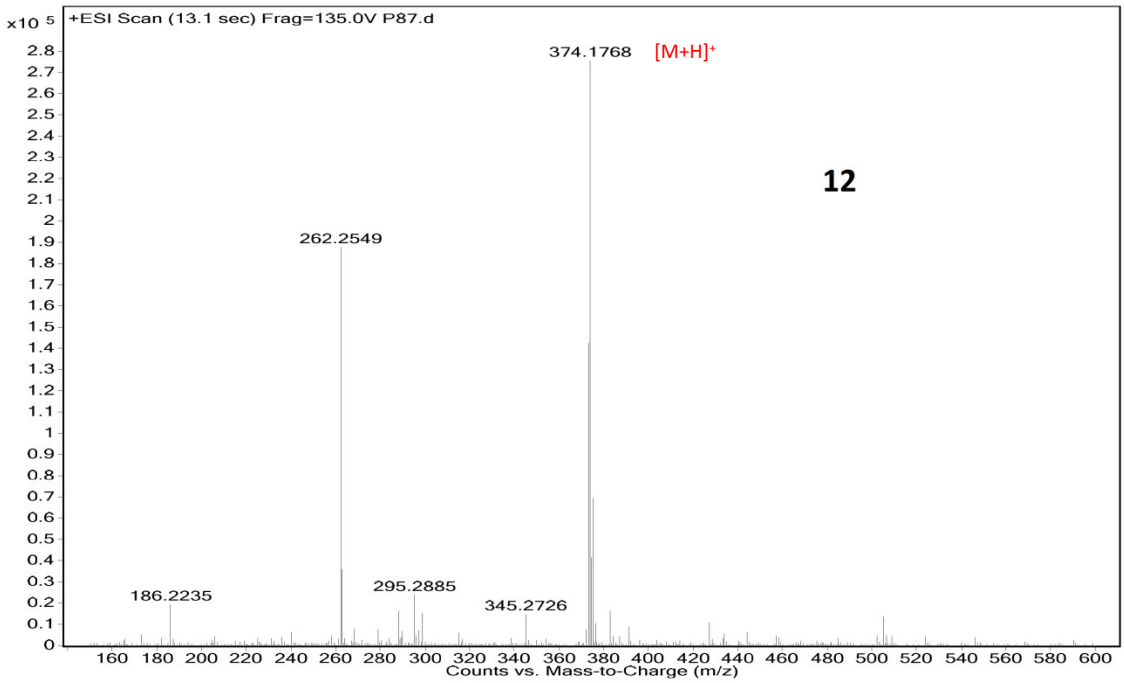

Sample Name	Unavailable	**Position**	Unavailable	**Instrument Name**	Unavailable	**User Name**	Unavailable
Inj Vol	Unavailable	**InjPosition**	Unavailable	**SampleType**	Unavailable	**IRM Calibration Status**	All Ions Missed
Data Filename	P88.d	**ACQ Method**		**Comment**	Sample information is unavailable	**Acquired Time**	Unavailable

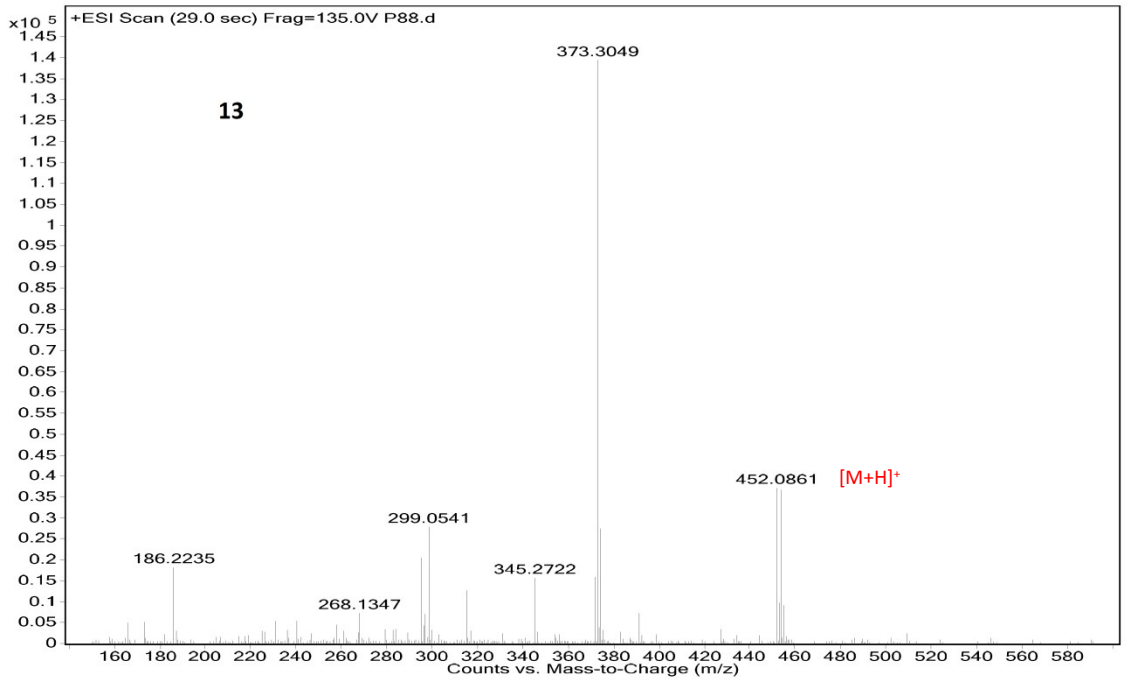

Sample Name	P93-1	**Position**	Vial 1	**Instrument Name**	Instrument 1	**User Name**	
Inj Vol	0	**InjPosition**		**SampleType**	Sample	**IRM Calibration Status**	Success
Data Filename	P93-1.d	**ACQ Method**		**Comment**		**Acquired Time**	10/9/2017 5:36:13 PM

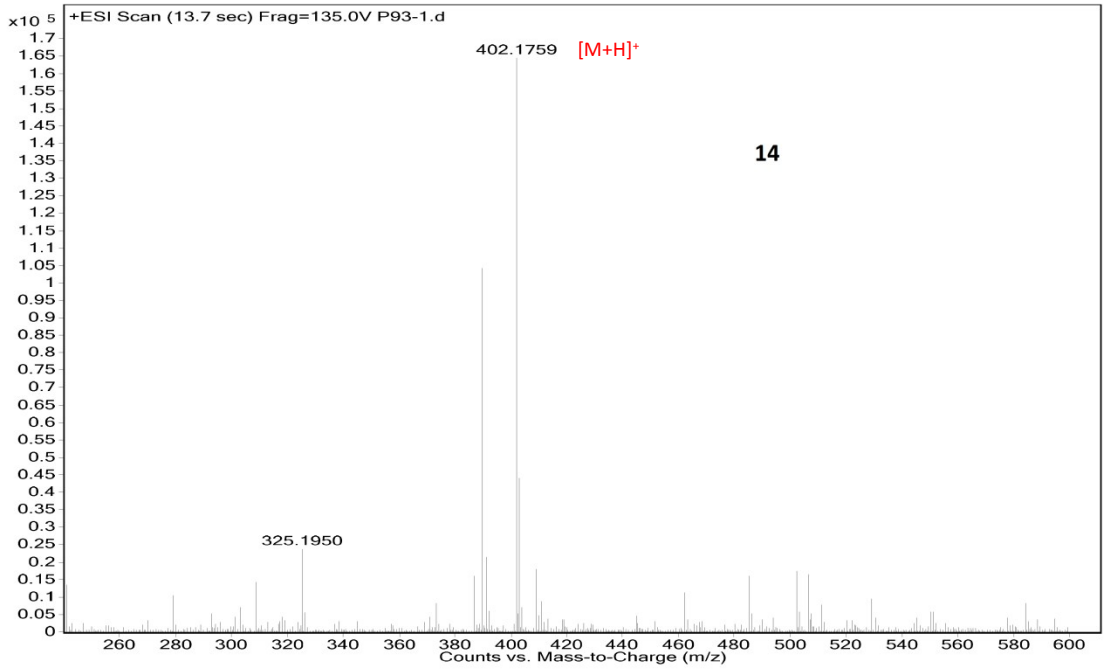

Sample Name	P92	**Position**	Vial 1	**Instrument Name**	Instrument 1	**User Name**	
Inj Vol	0	**InjPosition**		**SampleType**	Sample	**IRM Calibration Status**	Success
Data Filename	P92.d	**ACQ Method**		**Comment**		**Acquired Time**	10/9/2017 5:32:54 PM

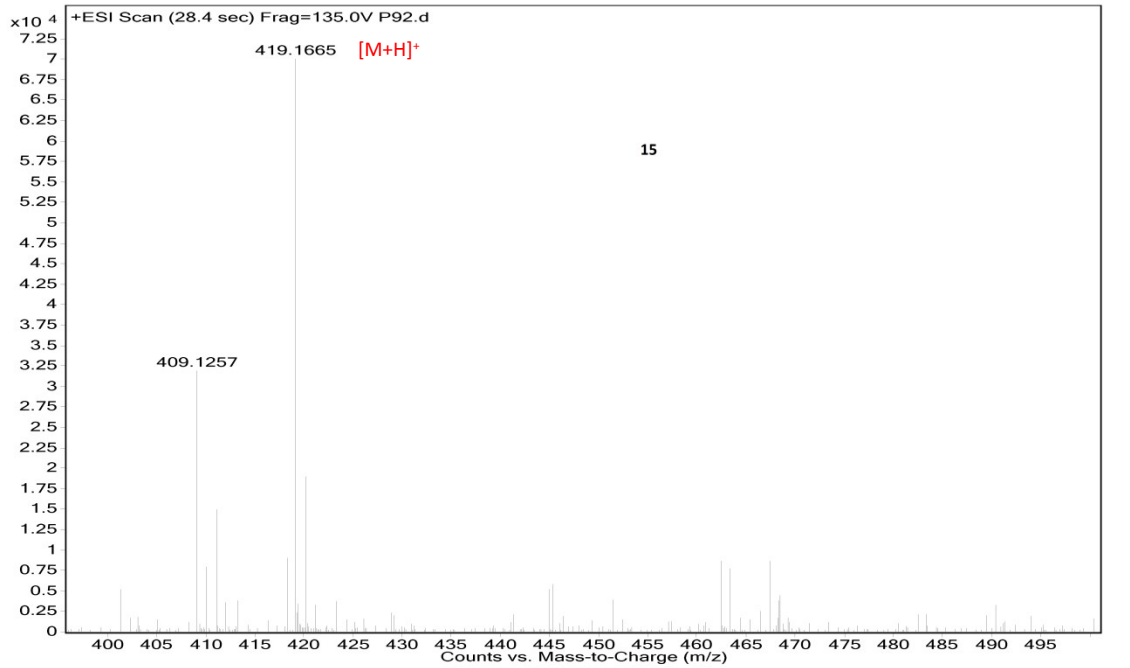

IR Spectra

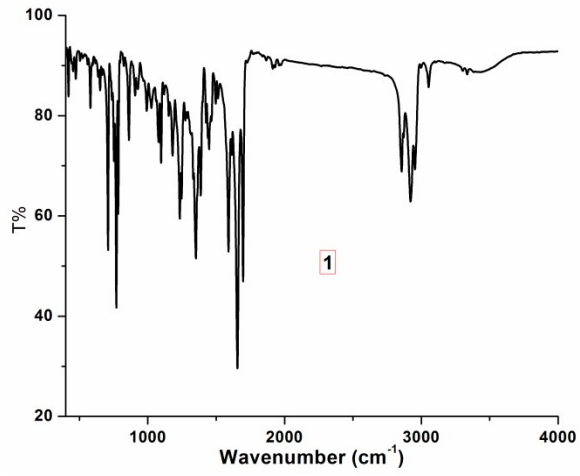
T%
Wavenumber (cm-1)
1

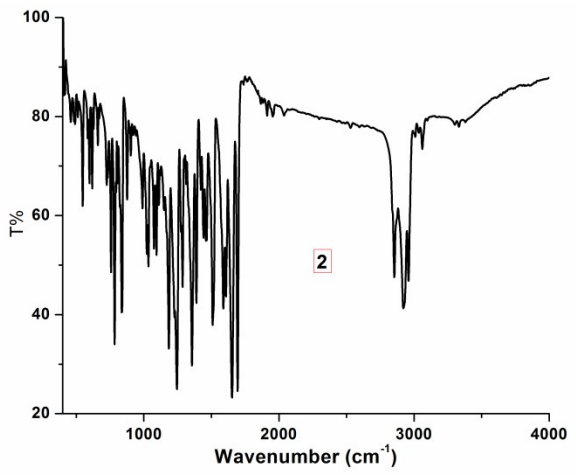
T%
Wavenumber (cm-1)
2

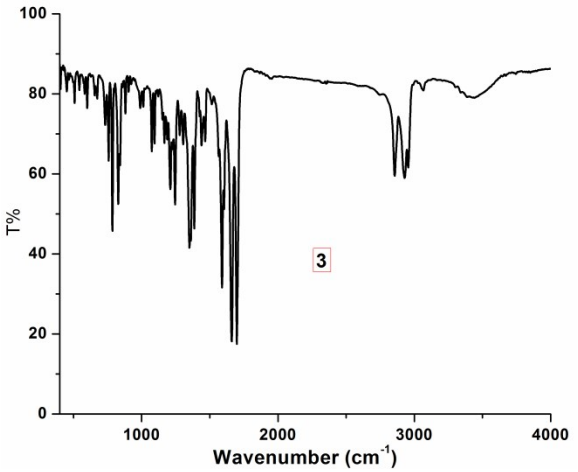
T%
Wavenumber (cm-1)
3

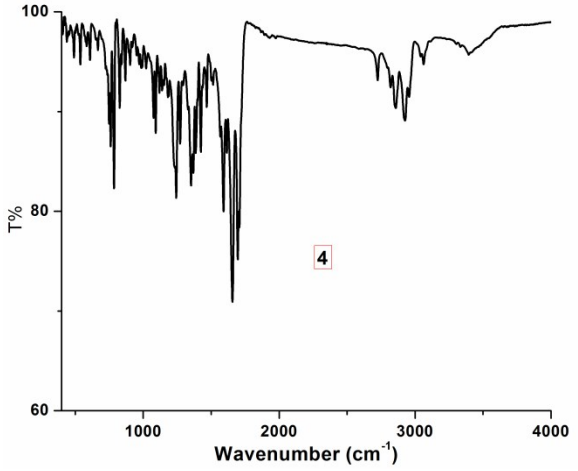
T%
Wavenumber (cm-1)
4

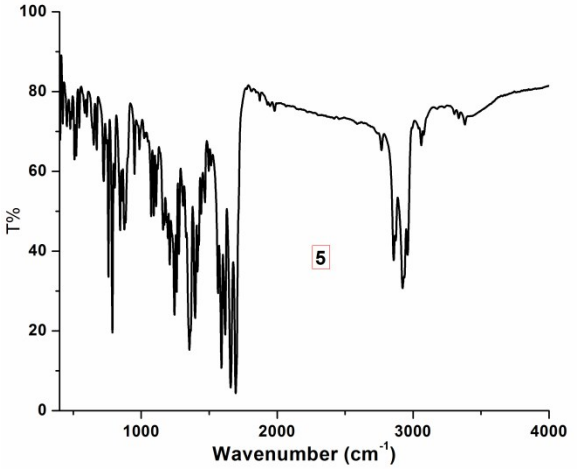
T%
Wavenumber (cm-1)
5

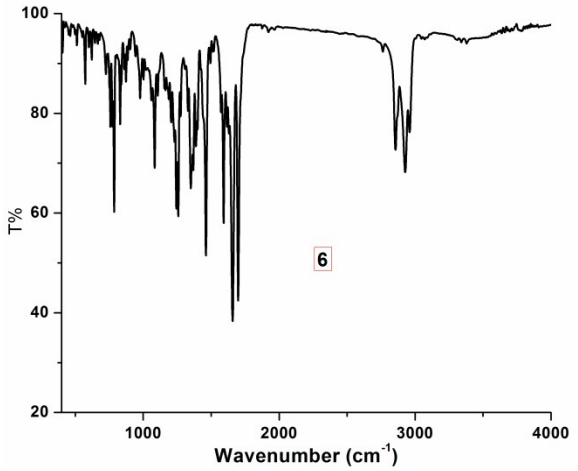
T%
Wavenumber (cm-1)
6

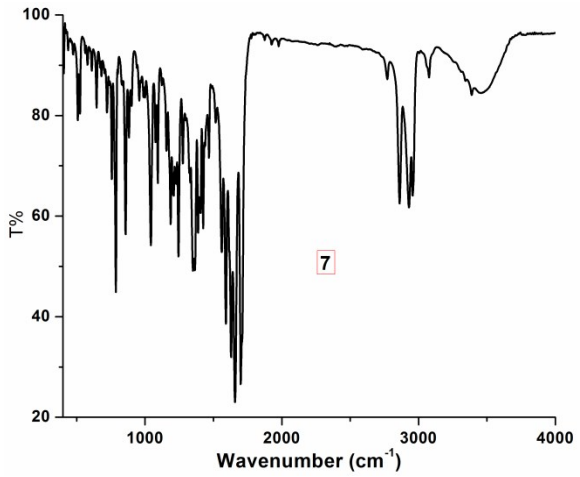
T%
Wavenumber (cm-1)
7

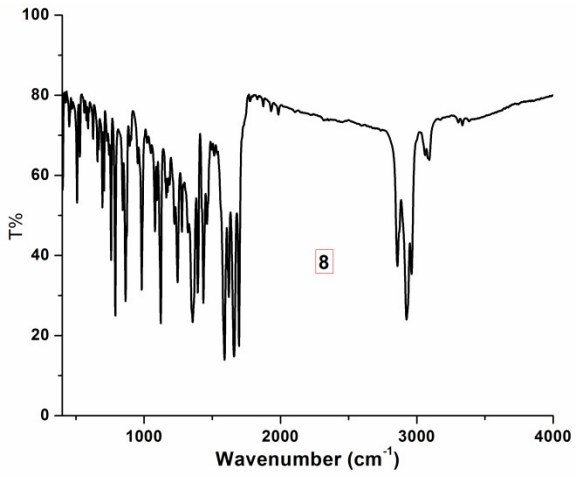
T%
Wavenumber (cm-1)
8

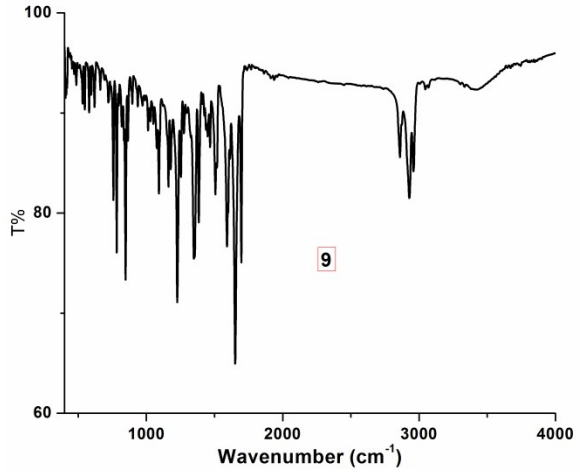
T%
Wavenumber (cm-1)
9

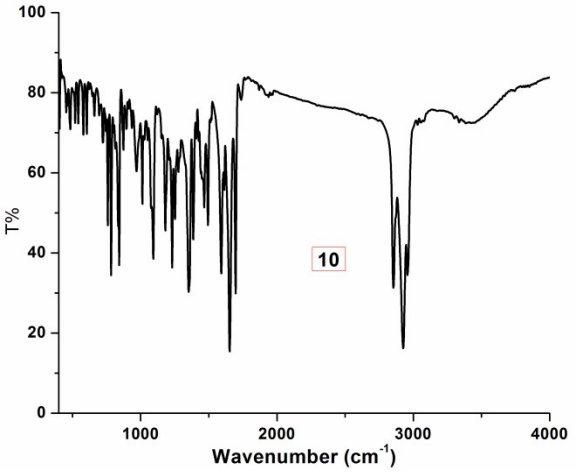
T%
Wavenumber (cm-1)
10

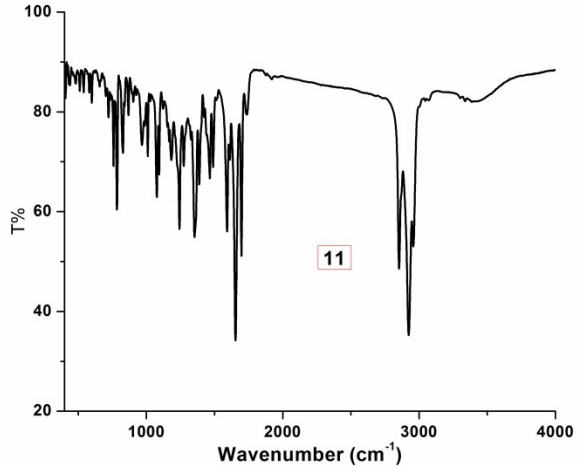
T%
Wavenumber (cm-1)
11

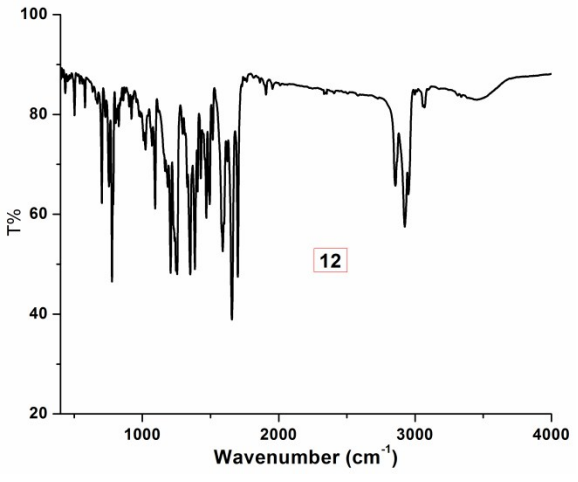
T%
Wavenumber (cm-1)
12

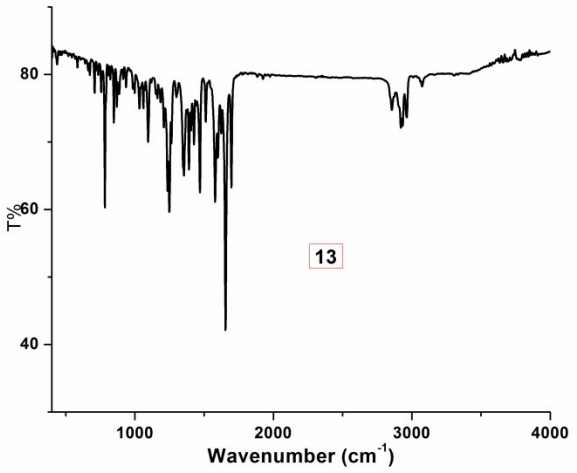
T%
80
60
40
13
1000
2000
3000
4000
Wavenumber (cm-1)

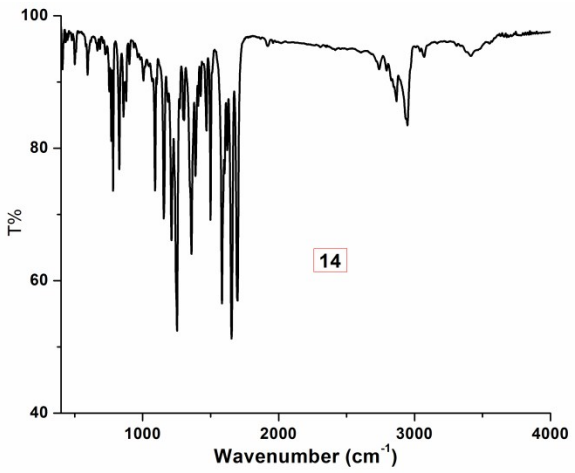
T%
100
80
60
40
14
1000
2000
3000
4000
Wavenumber (cm-1)

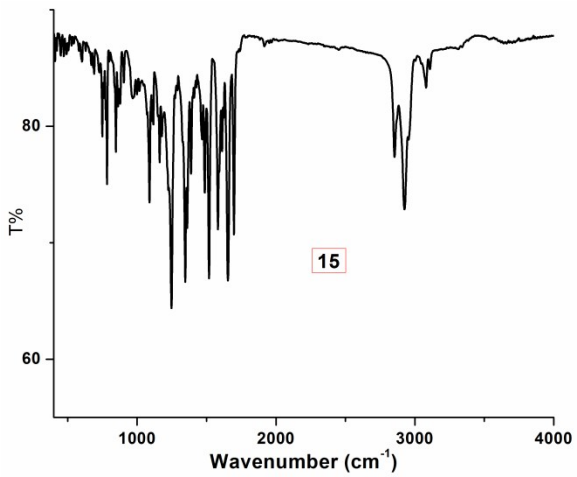
T%
80
60
15
1000
2000
3000
4000
Wavenumber (cm-1)

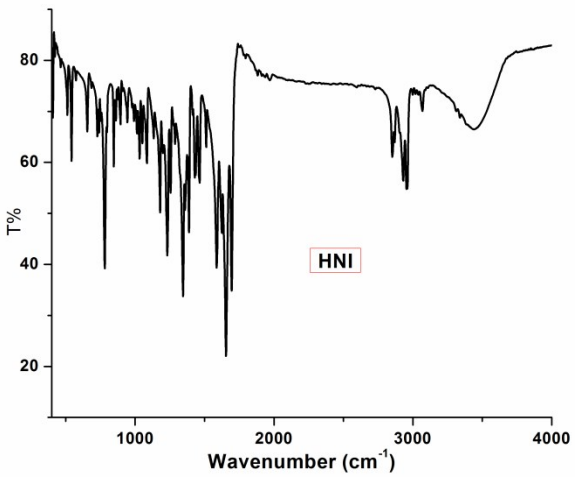
T%
80
60
40
20
HNI
1000
2000
3000
4000
Wavenumber (cm-1)

References

(1) Becke, A. D. *J. Chem. Phys.* **1993**, *98*, 5648.

(2) Frisch, M. J.; Trucks, G. W.; Schlegel, H. B.; Scuseria, G. E.; Robb, M. A.; Cheeseman, J. R.; Scalmani, G.; Barone, V.; Mennucci, B.; Petersson, G. A.; Nakatsuji, H.; Caricato, M.; Li, X.; Hratchian, H. P.; Izmaylov, A. F.; Bloino, J.; Zheng, G.; Sonnenberg, J. L.; Hada, M.; Ehara, M.; Toyota, K.; Fukuda, R.; Hasegawa, J.; Ishida, M.; Nakajima, T.; Honda, Y.; Kitao, O.; Nakai, H.; Vreven, T.; Montgomery, J. A.; Jr., Peralta, J. E.; Ogliaro, F.; Bearpark, M.; Heyd, J. J.; Brothers, E.; Kudin, K. N.; Staroverov, V. N.; Kobayashi, R.; Normand, J.; Raghavachari, K.; Rendell, A.; Burant, J. C.; Iyengar, S. S.; Tomasi, J.; Cossi, M.; Rega, N.; Millam, J. M.; Klene, M.; Knox, J. E.; Cross, J. B.; Bakken, V.; Adamo, C.; Jaramillo, J.; Gomperts, R.; Stratmann, R. E.; Yazyev, O.; Austin, A. J.; Cammi, R.; Pomelli, C.; Ochterski, J. W.; Martin, R. L.; Morokuma, K.; Zakrzewski, V. G.; Voth, G. A.; Salvador, P.; Dannenberg, J. J.; Dapprich, S.; Daniels, A. D.; Farkas, O.; Foresman, J. B.; Ortiz, J. V.; Cioslowski, J.; Fox, D. J. *Gaussian 09, Revision A.02, Gaussian, Inc., Wallingford CT*, **2009**.

(3) (a) Z. Chen, D. Wu, X. Han, Y. Nie, J. Yin, G.-A. Yu, S. H. Liu. (**2014**), CCDC 1014214: Experimental Crystal Structure Determination, Cambridge Crystallographic Data Centre. *http://dx.doi.org/10.5517/cc131cl3*. (b) Z. Chen, D. Wu, X. Han, Y. Nie, J. Yin, G.-A. Yu, S. H. Liu. *RSC Adv.* **2014**, *4*, 63985-63988.

(4) Sheldrick, G. M. SAINT and XPREP, 5.1 edn, Siemens Industrial Automation Inc., Madison, WI, **1995**.

(5) Sheldrick, G. M. SHELX97. Program for X-ray Crystal Structure Solution and Refinement, University of Göttingen, Germany, **1997**.